BUDAPEST UNIVERSITY OF TECHNOLOGY AND ECONOMICS
DEPARTMENT OF ORGANIC CHEMISTRY AND TECHNOLOGY
GEORGE A. OLAH DOCTORAL SCHOOL

Pharmaceutical applications of aqueous scaled-up electrospinning

Vizes oldat alapú méretnövelt elektrosztatikus szálképzés alkalmazása a gyógyszeriparban

Ph.D. thesis

Author: Panna Vass

Supervisor:
Dr. István Csontos
assistant professor

Co-supervisor:
Dr. Zsombor K. Nagy
associate professor

2020

Table of contents

Abbreviations

API – active pharmaceutical ingredient
C. butyricum – Clostridium butyricum
CD - cyclodextrin
CLS – classical least squares
CNM - clostridial nutrient medium
DES – drop electrospinning
DSC – differential scanning calorimetry
DNA - deoxyribonucleic acid
FDA – Food and Drug Administration (USA)
EDS – energy dispersive spectrometry
ES – electrostatic spinning/electrospinning
HP-β-CD - 2-hydroxypropyl-beta-cyclodextrin
HPLC – high-performance liquid chromatography
HSES – high-speed electrospinning
MCC – microcrystalline cellulose
MgSt – magnesium stearate
ONPG - o-nitrophenyl-β-D-galactopyranoside
PEO - polyethylene oxide
PVA – polyvinyl alcohol
PVP – polyvinyl pyrrolidone
PVPVA64 – vinylpyrrolidone-vinyl acetate 6:4 copolymer
RNA - ribonucleic acid
SBE-β-CD - sulfobutylether-β-cyclodextrin
SEM – scanning electron microscope
SNES – single needle electrospinning
TSA – tryptic soy agar
TSB – tryptic soy broth
XRPD – X-ray powder diffractometry
VOR - voriconazole

Thesis findings

1. A solid formulation of a model biopharmaceutical drug (β-galactosidase) was developed and produced by high-speed electrospinning for the first time. A fully aqueous polymeric solution was successfully electrospun with a 30 mL/h feeding rate, which is about 30x higher than the feeding rate usually attained with single-needle electrospinning. According to X-ray diffraction measurements, the mixture of polyvinyl alcohol, polyethylene oxide matrix, and β-galactosidase was in amorphous state in the fibers, whereas mannitol was crystalline (δ-polymorph). The presence of crystalline mannitol and the low water content enabled the grinding of the fibrous sample without secondary drying. The ground powder, mixed with tableting excipients, was successfully compressed into tablets. β-Galactosidase remained stable during each of the processing steps and for at least 1 year of storage at room temperature in the tablets. [I, II, IV, V, VIII, XVI]
2. A water-soluble cyclodextrin, 2-hydroxypropyl-beta-cyclodextrin (HP-β-CD) was used as a novel polymer-free matrix for the scaled-up electrospinning of a model protein-type drug. High feeding rate (400 mL/h which equals ~270 g solid product per hour) could be achieved this way. The new solid form was found suitable for grinding and tableting by direct compression. The model protein-type drug (β-galactosidase) remained stable during each of the processing steps (electrospinning, grinding, tableting) and for at least 6 months of storage at room temperature in the tablets. [VI, VIII, XVI]
3. An amorphous solid dispersion of a poorly soluble drug (voriconazole (VOR)) and a polymer-free matrix (SBE-β-CD) was electrospun with high production rate (~240 g/h) for the first time. This productivity is more than 12x higher than the highest aqueous electrospinning production rate reported so far. According to X-ray diffraction and differential scanning calorimetry, no traces of crystalline VOR were detectable in the fibers. Furthermore, Raman mapping and energy dispersive spectroscopy measurements showed a uniform distribution of amorphous VOR in the fibers. [III, VII, VIII, XX, XXI, XXII]
4. An intravenously injectable reconstitution powder dosage form was produced by electrospinning from an aqueous solution for the first time. High-speed electrospinning with a novel continuous (cyclone) collection was used to manufacture the innovative

formulation of the poorly water-soluble antifungal VOR with sulfobutylether-β-cyclodextrin (SBE-β-CD). This dosage form was compared to the freeze-dried, marketed product with the same composition, Vfend®. Reconstitution tests, carried out with the ground fibrous powder, showed complete dissolution resulting in a clear solution within 30 s (similarly to Vfend®). [III, VIII, XX, XXI, XXII]

5. Anaerobic bacteria-containing electrospun fibers were prepared with high production rate (~150 g/h) for the first time. Butyrate (an anti-inflammatory molecule) production capacity of the bacteria was retained after electrospinning. The fibers were pressed into tablets by direct compression after milling (by an oscillating mill) and mixing with tableting excipients. No significant decrease in bacterial viability was observed after either of the processing steps (milling and tableting). [VIII, IX, XVII, XVIII, XIX]
6. Long-term stability of a model anaerobic bacterium from the gut microbiome (*Clostridium butyricum*) incorporated into fibers of a water-soluble cyclodextrin matrix (HP-β-CD) was studied for the first time. Effect of the growth conditions of the bacteria and storage conditions of the fibers (temperature, presence of oxygen) on the viability of the bacteria in the fibers was investigated. High viability was preserved in the fibrous sample containing both spores and vegetative anaerobic bacteria after 12 months of storage at room temperature in the presence of oxygen. [IX, XVII, XVIII, XIX]

Új tudományos eredmények

1. Elsőként fejlesztettük ki és állítottuk elő egy modell biohatóanyag (β-galaktozidáz) szilárd formulációját nagysebességű elektrosztatikus szálképzéssel. Sikeresen szálképeztük a hatóanyag polimeres vizes oldatát 30 mL/h-ás adagolási sebességgel, ami nagyságrendileg 30x nagyobb, mint ami az egytűs elektrosztatikus szálképzéssel általában elérhető. Röntgendiffrakciós mérések alapján megállapítottuk, hogy a polivinil alkohol, a polietilén oxid mátrixalkotók és a β-galaktozidáz amorf, míg a mannit kristályos formában (δ-polimorf) volt jelen a szálakban. A kristályos mannit jelenléte és a szálak alacsony víztartalma lehetővé tette a szálak őrlését másodlagos szárítás nélkül. Az őrölt port tablettázási segédanyagokkal keverve sikeresen tablettáztuk. A β-galaktozidáz stabil maradt a feldolgozási lépések során és a tabletták stabilitása legalább 1 éves szobahőmérsékletű tárolása után is megfelelő. [I, II, IV, V, VIII, XVI]
2. Elsőként használtunk egy vízoldható ciklodextrint (2-hidroxipropil-β-ciklodextrin (HP-β-CD)), mint polimermentes mátrixot egy biohatóanyag esetén méretnövelt elektrosztatikus szálképzésére. Az alkalmazott adagolási sebesség 400 mL/h volt, ami hozzávetőlegesen 270 g szilárd terméknek felel meg óránként. Az új szilárd forma őrölhető és direkt préseléssel tablettázható volt. A modell fehérje-típusú hatóanyag (β-galaktozidáz) stabil maradt a feldolgozási lépések során (elektrosztatikus szálképzés, őrlés, tablettázás) és a tabletták legalább 6 hónapos szobahőmérsékletű tárolása után is megőrizték stabilitásukat. [VI, VIII, XVI]
3. Elsőként állítottuk elő elektrosztatikus szálképzéssel, a korábban publikált maximális termelést jelentősen (több mint 12x-esen) meghaladó termelékenységgel (~240 g/h), egy rossz vízoldhatóságú hatóanyag (vorikonazol (VOR)) és egy polimermentes mátrix (SBE-β-CD) amorf szilárd diszperzióját. Röntgendiffrakciós és differenciális pásztázó kaloriméteres mérések nem mutatták ki kristályos VOR jelenlétét a szálakban. Továbbá, Raman térképezéssel és energiadiszperzív spektroszkópiás méréssel bizonyítottuk, hogy az amorf VOR egyenletesen oszlik el a szálakban. [III, VII, VIII, XX, XXI, XXII]
4. Elsőként állítottunk elő egy intravénásan beadható rekonstitúciós por alapú gyógyszerformát vizes oldatból elektrosztatikus szálképzéssel. A nagysebességű elektrosztatikus szálképzést újfajta folyamatos (ciklonos) gyűjtéssel együtt sikeresen

alkalmaztuk a rossz vízoldhatóságú gombaellenes VOR szulfobutiléter-β-ciklodextrines (SBE-β-CD) innovatív gyógyszerformájának gyártására. Ezt a gyógyszerformát összehasonlítottuk a forgalomban lévő, ugyanolyan összetételű, fagyasztva szárítással előállított termékkel (Vfend®). A rekonstitúciós tesztek során az őrölt szálas por 30 s alatt teljesen feloldódott, egy tiszta oldatot eredményezve, hasonlóan a Vfend®-hez. [III, VIII, XX, XXI, XXII]

5. Elsőként valósítottuk meg elektrosztatikus szálképzéssel anaerob baktériumokat tartalmazó szálak nagy termelékenységű (~150 g/h) gyártását és direkt préselését, őrlést (oszcilláló őrlő) és homogenizálást követő tablettázással. A feldolgozási lépések (őrlés, tablettázás) nem csökkentették szignifikánsan a baktériumok életképességét. [VIII, IX, XVII, XVIII, XIX]
6. Vízoldható ciklodextrin mátrix (HP-β-CD) alapú szálakba ágyazott modell - a bél mikrobiomjából származó - anaerob baktérium törzs (*Clostridium butyricum*) hosszú távú stabilitásvizsgálatát elsőként valósítottuk meg. Vizsgáltuk a baktériumszaporítási körülmények és a szálképzett minták tárolási körülményeinek (hőmérséklet, oxigén jelenléte) hatását a szálakba ágyazott baktériumok életképességére. Az oxigén jelenlétében és szobahőmérsékleten tárolt, spórákat és vegetatív anaerob baktériumokat tartalmazó szálakban a sejtek 1 év után is nagymértékben megőrizték az életképességüket. [IX, XVII, XVIII, XIX]

1. Introduction

The biopharmaceutical industry has seen incredible growth in recent decades. The growing market and acceptance of biopharmaceuticals are accredited to their ability to treat previously untreatable diseases, resulting in huge market demand for biopharmaceuticals. However, the development of biopharmaceutical products is very challenging due to their limited physical and chemical stability in liquid form. To overcome this challenge, biopharmaceuticals are often dried to a solid form, which usually improves their stability significantly besides having additional benefits like reduced transportation costs, easier handling, and easier storage.

Currently, freeze drying and spray drying are the most widely used technologies to obtain solid biopharmaceutical formulations despite their disadvantages. Freeze drying is a highly energy- and time-intensive batch process that exposes biopharmaceuticals to freezing stresses, which can result in degradation. In contrast, spray drying is an economic continuous drying technology; however, the high drying gas temperatures used in the process can induce the denaturation of heat-sensitive proteins. Electrospinning (ES) is new and efficient continuous drying technology, which has been attracting increased interest in the preparation of solid biopharmaceutical formulations due to its ability to provide gentle drying at room temperature and provide nano- or microstructured solids. ES of biopharmaceuticals is usually carried out from aqueous solutions due to their sensitivity to most of the organic solvents and because they are already in an aqueous solution at the end of production. Aqueous ES, however, is considered challenging due to the relatively low volatility of water resulting in slower evaporation, which makes the productivity of the process reduced compared to the volatile organic solvents. For ES to be applied in the pharmaceutical industry, the production capacities of the technology need to reach the commercial needs.

Our objectives were to investigate a scaled-up fiber formation technology called high-speed electrospinning (HSES) to dry biopharmaceuticals at room temperature starting from aqueous polymeric and polymer-free solutions. It was intended to develop grindable fibers and convert them to tablets and to assess the effect of the downstream processing steps on the APIs. Long-term stability study of the biopharmaceuticals in the fibrous formulations and the scaled-up electrospinning of cyclodextrins to produce parenteral dosage forms was also planned to reveal the applicability of aqueous HSES in modern pharmaceutical technology.

2. Literature review

2.1 Current status of the biopharmaceutical industry

Biotechnology-derived medicinal products (proteins (including antibodies), nucleic acids (DNA, RNA or antisense oligonucleotides), living cells, vaccines, etc.) have enjoyed rapid expansion over the past decade and are currently one of the fastest-growing segments of the pharmaceutical industry market [1]. Biotech products accounted for 35% of all new Food and Drug Administration (FDA) approvals between 2000 and 2016 and at the end of 2016, more than 400 biologics were in Phase III trials [2]. The top 10 selling biopharmaceuticals together generated sales of $80.2 billion in 2017, which is almost 44% of total biopharmaceutical product revenues. Forty-five individual biopharmaceutical products recorded 'blockbuster' status sales (>$1 billion) in 2017. [1]. Biopharmaceuticals (covering biological medical products, biologicals, biologics) provide numerous benefits including high specificity and potency compared to small molecule drugs [3].

The most lucrative biopharmaceutical products are **proteins**. Sixty-two of the 71 genuinely new biopharmaceutical drugs that have come on the market between January 2014 and July 2018 were recombinant proteins. Monoclonal antibodies (mAbs) and insulins, the two most profitable types of proteins, generated $123+$22 billion in sales in 2017 [1]. Protein drugs have several advantages over small-molecule therapeutics. Proteins often serve a highly specific and complex set of functions that cannot be mimicked by simple chemical compounds. As the action of proteins is very specific, there is often less potential for protein therapeutics to disturb normal biological processes and cause adverse effects. Besides, the body naturally produces many of the proteins that are used as therapeutics, and therefore these molecules are often well tolerated and are less likely to induce immune responses. In addition, for diseases caused by a mutated or deleted gene, protein drugs can provide effective replacement treatment without the need for gene therapy, which is currently unavailable for most genetic disorders. Last, because proteins are unique in form and function, pharmaceutical companies are able to obtain far-reaching patent protection for these therapeutics, which makes proteins attractive from a financial perspective as well [4].

Since the start of the Human Microbiome Project in 2008, it has become evident that the **microbes** that live in the human body – called the microbiome – play critical roles in biological processes, including intestinal homeostasis, metabolism, and development of the immune system, among others [5]. Changes in the composition of the intestinal microbiota have been linked to diverse, complex diseases including inflammatory bowel disease,

metabolic diseases (diabetes, obesity), allergy, asthma, cancer, and neurologic and cardiovascular diseases [6]. Based on these links, numerous pharmaceutical companies started to focus on the development of microbiome therapeutics [7,8]. Even though there are no microbiome-based drug products on the market yet, the increasing interest in these therapies can be seen in the rising levels of both deal-making and investment over the last decade. Since 2015, more than $5.4 billion has been spent on acquisitions and partnerships in the therapeutic microbiome space. The FDA has also acknowledged the potential benefit offered by microbiome-based therapies and has stated a commitment to advancing the clinical science necessary to understand their safety and efficacy [9].

A key aspect of the therapeutic use of biopharmaceuticals like proteins, microbes, and other biologics is maintaining their activity during storage, transport, and administration. In liquid dosage forms, biopharmaceuticals often show instability due to being prone to physical and chemical degradation [10]. Therefore, the development of solid biopharmaceutical products that retain their initial activity can be a milestone in the commercialization of biopharmaceuticals. The elimination of water from the formulations improves the stability with additional benefits being reduced transportation costs and easier handling and storage [11]. However, biopharmaceuticals are usually very sensitive due to their structural complexity, and therefore, the selection of the best drying method capable of dehydrating the molecule without inducing degradation, producing a powder with adequate properties for oral downstream processing e.g. tableting, and in a cost-effective way, poses a great challenge. In addition, the choice of drying technology is strongly associated with the economics of drying and the intended route of drug delivery [12]. The next chapter discusses different technologies for the drying of biopharmaceuticals.

2.2 Drying of biopharmaceuticals

Several different techniques can be used to dry biopharmaceuticals and the choice of drying technology depends on several factors including the characteristics of the given biopharmaceutical, application of the product, economic considerations and productivity requirements. The most widely used technology is freeze drying followed by spray drying with electrospinning emerging as a viable alternative, even though no electrospun biopharmaceutical product has reached the market yet. Table 1 summarizes the main characteristics of these drying technologies, discussed in the following paragraphs. These technologies introduce varying stresses which will be discussed in this section. Figure 1 and Figure 2 attempt to depict and compare the characteristics of the three technologies that can affect the stability of biopharmaceuticals. The following paragraphs will also discuss the financial aspects of the technologies.

Table 1 Comparison of the main characteristics of freeze drying, spray drying and electrospinning

	Freeze drying	**Spray drying**	**Electrospinning**
Length of drying	Days/weeks	Seconds	Fraction of a second
Capital cost	Very high	Moderate	Moderate
Operating cost	High	Moderate	Low
Stresses	Freezing, dehydration	Shear, thermal, dehydration	Dehydration, shear
Production	Batch	Continuous	Continuous
Control of particle characteristics	No	Yes	Yes

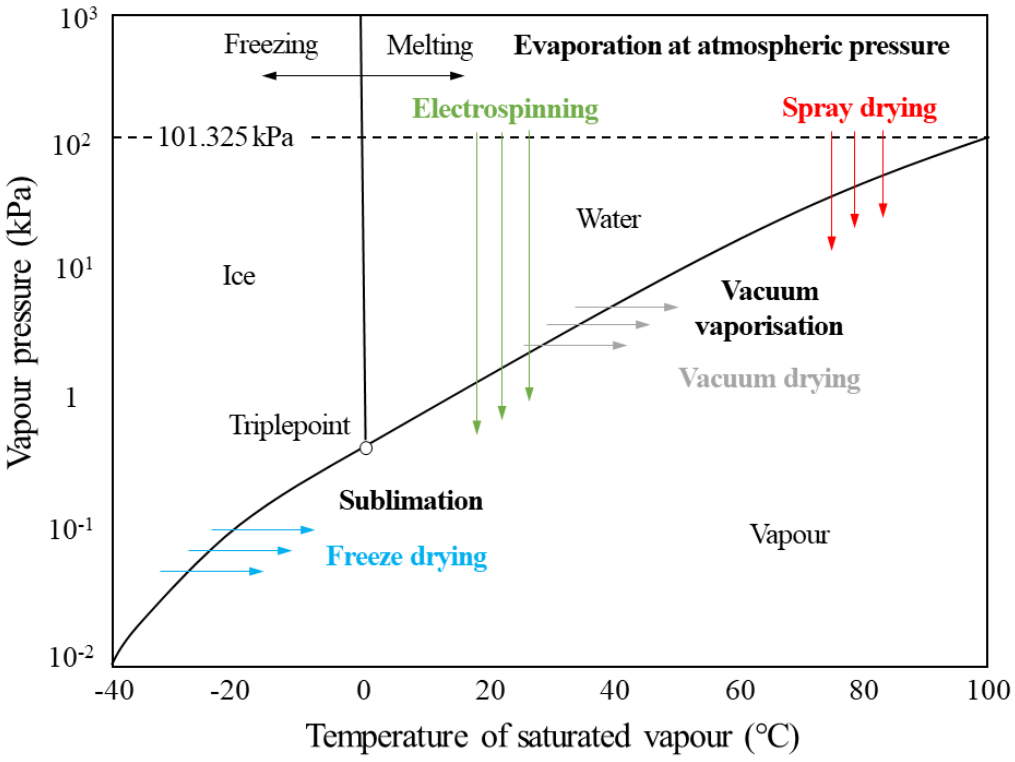

Figure 1 Phase diagram of water including different drying technologies: freeze drying, vacuum drying, spray drying, and electrospinning

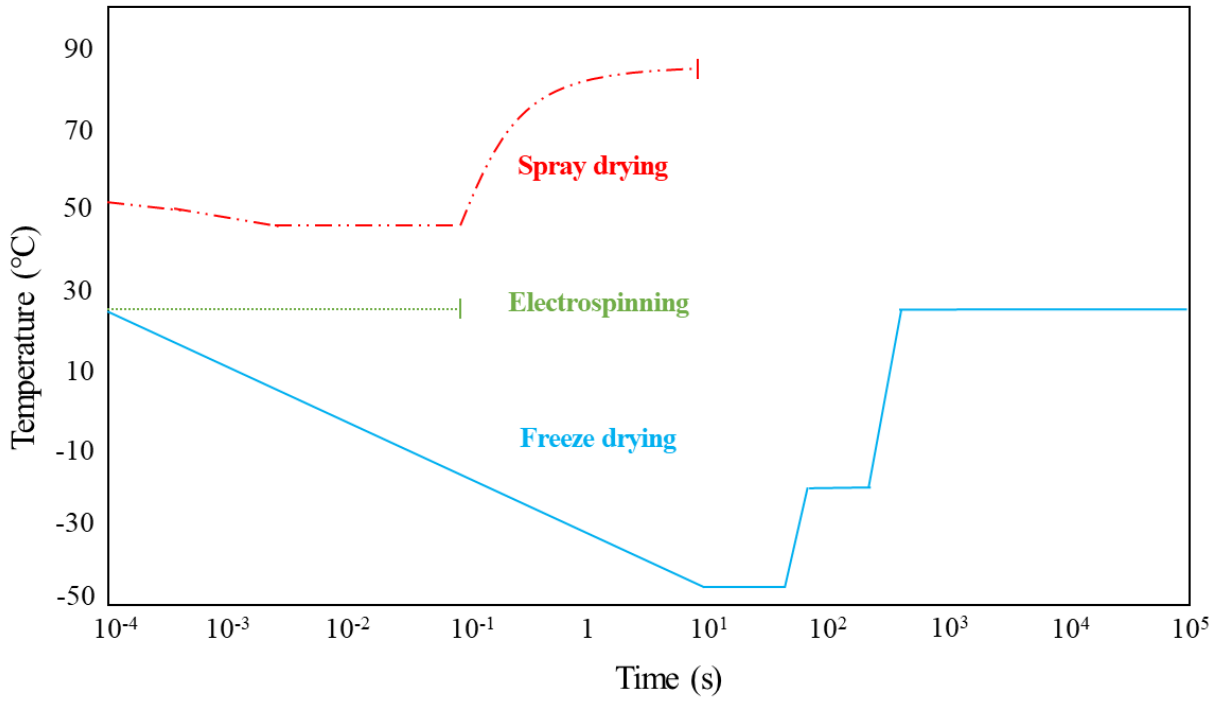

Figure 2 Comparison of product temperatures and drying times in freeze drying (—), spray drying (— ··), and electrospinning (···)

2.2.1 Freeze drying

Freeze drying (also known as lyophilization) is the most commonly used technology for the solid formulation of biopharmaceuticals and depicted in Figure 3. A traditional freeze drying cycle comprises three main stages: freezing, primary drying, and secondary drying [13]. During the freezing step, the product is cooled until it completely solidifies, and unbound water crystallizes. The cooling rate influences the type and size of the formed ice crystals and the pore structure. Rapid cooling results in smaller crystals, while if the rate of cooling is slow then larger ice crystals are formed [14]. The formation of larger ice crystals results in larger pores, which is believed to be responsible for an increased primary drying rate resulting in shorter drying times [15]. In the primary drying step heat and vacuum are applied in the chamber, which removes the crystalline ice in the product by sublimation. After primary drying, the product usually still contains about 10-20% of residual water which is reduced to 1-2% or less by secondary drying [16]. Secondary drying is carried out at a higher temperature compared to primary drying.

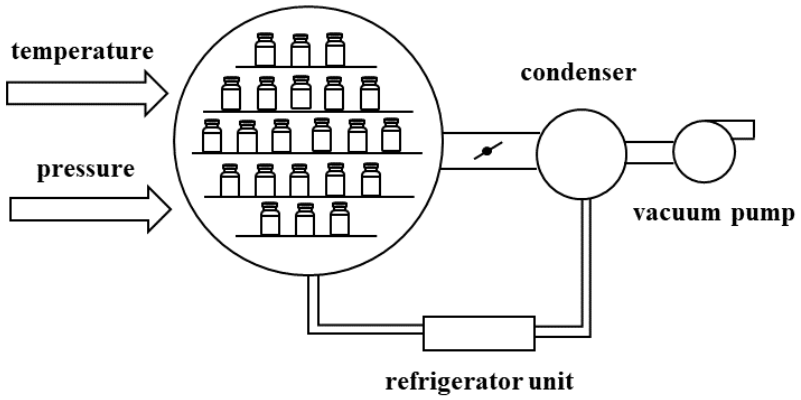

Technological aspects	Stresses
Takes days/weeks	Ice crystal formation (solid-liquid interfacial stress)
Very high capital cost	Change of ionic strength and pH
High operating cost	Phase separation
Batch production	Dehydration

Figure 3 The freeze drying technology and related aspects

More than 50% of biopharmaceuticals currently on the market are formulated using freeze drying despite its disadvantages [15]. Two major disadvantages are the energy- and time-consumption of the freeze drying process, which both are the highest among the dehydration technologies [17]. Freeze drying can take days or even weeks to finish, and as it is a batch process the yearly capacity of the technology can be suboptimal compared to other

technologies. Another drawback of freeze drying is the vial-to-vial heterogeneity, which results in poor control of product quality [18,19]. The huge industrial batch sizes are impractical for cycle development and therefore initial development steps are carried out in lab-scaled freeze-driers. The process then needs to be scaled up to pilot scale and finally to industrial scale. Differences in heat and mass transfer between each equipment scale require reoptimization and revalidation of these cycles. In addition, freeze drying processes are validated for a specified batch size and therefore revalidation is necessary each time the batch size is modified [20]. Freeze drying is recognized as the most expensive drying process due to the complex equipment and the cost of electricity used by the technology [21]. To reduce the limitations of the freeze drying batch processing, several research groups are working on the development of continuous freeze drying technologies. This is envisioned to reduce the drying time, improve productivity, better control and compliance through process analytical technology (PAT) application [20,22,23].

In addition, freeze drying of biopharmaceuticals in the absence of excipients often results in degradation, aggregation or precipitation due to the different freezing (formation of ice crystals and ice-water interface, ionic strength change, pH change, and phase separation) and dehydration stresses [24,25]. The most commonly used stabilizing excipients in freeze drying are sugars, sugar derivatives, surfactants, and polymers. Among the different sugars and sugar derivatives, disaccharides (trehalose, sucrose, and lactose) and mannitol seem to be the most effective and therefore the most frequently used stabilizers [24,26]. Generally, a carefully selected sugar excipient should adequately protect proteins from the freezing and drying stresses during the freeze drying process.

Figure 4A shows the typical product morphology after freeze drying. Generally, freeze-dried cakes are easily reconstituted and therefore freeze drying is a suitable technology for producing dried biopharmaceuticals for parenteral administration [27]. The technology lacks the opportunity to produce well-defined particles instead of cakes and therefore for oral administration applications freeze-dried cakes need further processing (e.g. milling, homogenization) before the material can be tableted or filled into capsules.

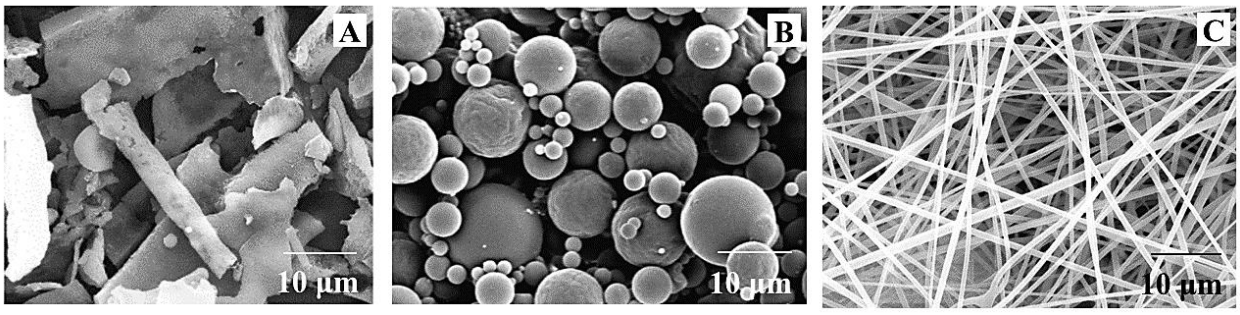

Figure 4 Scanning electron microscope images showing the typical morphologies of products of the different drying technologies: A) freeze-dried flake-like structures [28] B) spray-dried spherical particles [29] C) electrospun fiber structures

Due to strict regulations, technological advances are very slow in the pharmaceutical industry and therefore the long history and the industrial experience are the greatest advantages of freeze drying when considering drying method selection for a new biopharmaceutical formulation [30]. Other significant advantages are the capability to dry small batches, straightforward aseptic processing, limited product losses and the low drying temperature [31]. However, the high cost, freezing stresses, lack of control over powder properties, and long processing times make the technology less attractive for oral products and might facilitate the choice of alternative drying technologies like spray drying or electrospinning.

2.2.2 Spray drying

Spray drying is the preferred drying technology for many small molecules and especially for amorphous solid dispersions, but it has only been used sparingly for biopharmaceuticals due to concern over degradation by the high drying temperature employed [32]. Despite this, the technology is gaining popularity due to its particle engineering capabilities and relatively low cost. It produces dried particles by the atomization of the liquid feed into fine droplets (typically diameter <200 µm [28]), which are then dried by a hot gas stream. The fine liquid droplets have a large specific surface area and thus the solvent rapidly evaporates, and the dry powder is separated by a cyclone and collected in a product collector (Figure 5). The dehydration in spray drying happens in a matter of seconds, which makes spray drying a high throughput and economic technology. Spray drying is a continuous process allowing the large-scale production of dried biopharmaceuticals [27]. Both investment and operational costs of spray drying are significantly lower compared to freeze drying, although the generation of hot gas still consumes a substantial amount of energy [33]. It was estimated that spray drying is 4 to 7 times cheaper compared to freeze drying [34]. Another advantage of

spray drying is the ability to control the particle characteristics of the dried powder by varying the process parameters [35], and this makes spray drying an ideal choice for applications where particle characteristics are important. Spray drying is usually the selected technology for pulmonary and nasal delivery of biopharmaceuticals [30], but spray-dried powders usually also have good processability and can readily be tableted or filled into capsules (after mixing with excipients if needed). Figure 4b shows the typical spray dried product morphology (i.e. spheres).

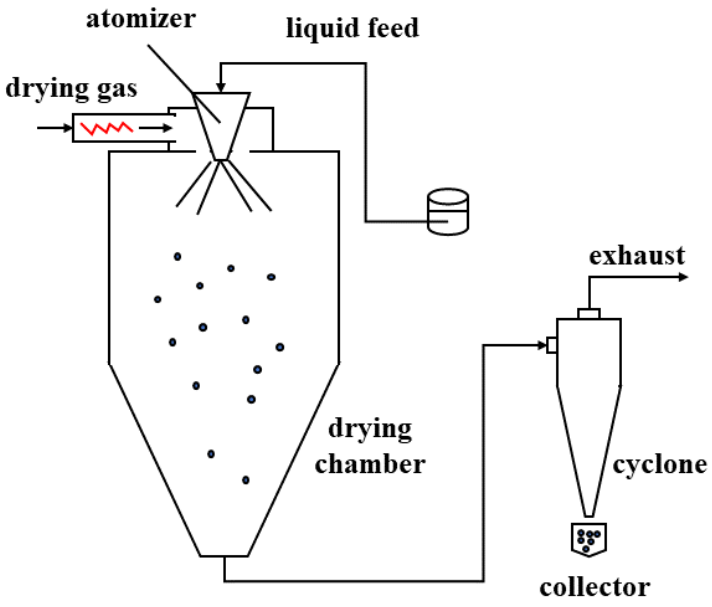

Technological aspects	Stresses
Takes seconds	Heat
Moderate capital cost	Shear
Moderate operating cost	Air-liquid interfacial
Continuous production	Dehydration

Figure 5 The spray drying technology and related aspects

Due to the concern that biopharmaceuticals may be thermally degraded during the process, spray drying is employed less frequently for the formulation of therapeutic biomolecules than freeze drying. Additionally, spray drying exposes biomolecules to shear, air-liquid interfacial and dehydration stresses [36]. Another limitation of the technology is that product recovery from benchtop spray dryers is generally around 50% or lower [37]. This requires working with larger amounts of the biological substance, which can be challenging especially in the early stages of development. However, recent developments of lab-scale spray driers have led to an increase in yields over 80% through the introduction of high-efficiency cyclones and the possibility to produce larger particles [38].

There are several different approaches to minimize thermal degradation of biopharmaceuticals during spray drying with the key focus being temperature and residence time. For instance, the outlet temperature of the drying gas is a key process parameter for the thermal degradation as this is the temperature at which the biopharmaceutical molecule spend the longest time [35]: if the outlet temperature is lower than the degradation temperature of the given biopharmaceutical then the material experiences less thermal degradation, however a too low outlet temperature can result in shorter shelf life due to increased residual water content. Therefore, the challenge is to optimize the outlet temperature to produce an adequately dry powder, yet not induce unacceptable degradation. Generally, spray drying of biopharmaceuticals is carried out well below 100 °C along with very low feeding rates (usually below 20 mL/min). Lower feeding rate is associated with decreased residual moisture content and higher yield [39]. The residence time of the molecule in the spray dryer is given by the drying chamber volume and the drying gas flow rate. The drying chamber volume is fixed by design and is therefore not adjustable. While it is possible to vary the drying gas flow rate to modify the drying time to reduce thermal degradation [40] this is typically not applied as it is preferable to run commercial spray dryers as maximum drying gas flow rate to maximize capacity.

In addition to optimizing the process parameters, the use of sugars and sugar derivatives to stabilize spray-dried biopharmaceutical formulations against dehydration and thermal stresses was adopted from the freeze drying literature. Essentially, during spray drying process development, usually the same disaccharides and sugar alcohols (trehalose, sucrose, and mannitol) are tested which had already been successfully applied for the freeze drying of the given biomolecule [36,38,41]. Surfactants are used extensively to minimize interfacial denaturation and aggregation since the atomization step in spray drying produces an extremely rapid and large expansion of the liquid-air surface [42].

Spray drying can be set up as an aseptic process to produce a sterile powder, however, this is not as straightforward as in case of freeze drying. Aseptic spray drying can be achieved by filtration of the liquid feed material, using HEPA filters on the atomizing and drying gas, sterilization of the nozzle and chamber walls and fast product collection. Sterilization of the equipment is usually carried out with a superheated steam. The main advantage offered by spray drying under aseptic conditions is avoiding the terminal sterilization that potentially denatures biopharmaceuticals [43,44]. Today, aseptic spray drying is used infrequently, but the emerging availability of the technology will probably help to extend the application of

spray drying to the clinical realm and ultimately to the commercial space for producing biopharmaceutical products [31]. The first biopharmaceutical product produced by aseptic spray drying was approved by the FDA in 2015 and this approval is considered as a vote of confidence for this enabling stabilization technology [45].

Although the application of spray drying for biopharmaceutical formulations currently is still limited in the pharmaceutical industry, the method provides such economic benefits that there is an evolving number of studies using the technology to dry different types of biopharmaceuticals [32,38,46,47]. The technology is fast, continuous and it can produce particles with controlled characteristics which makes the technology a great alternative to freeze drying for oral products.

2.2.3 Electrospinning

Freeze drying and spray drying are both currently applied in the pharmaceutical industry to produce dried biopharmaceuticals. However, as the biopharmaceutical market grows and the number of new, more sensitive biopharmaceuticals is continuously rising, there is an evolving need for gentle drying technologies that could enable the drying of biopharmaceuticals without causing degradation. Even though there is no biopharmaceutical drug on the market dried by electrospinning, this technology has been gaining considerable interest in the past decade. Due to its attractive characteristics, electrospinning has been shown by many studies to be a promising alternative to the currently used drying technologies for biopharmaceuticals [48-52].

Electrospinning (Figure 6) is a modern and efficient fiber production method which is based on the effect of high voltage on polymer solutions. First patents about electrospinning date back to 1902 [53,54], but substantial attention to the technology was provided only after the early 1990s [55-57]. Electrospinning produces dried particles by the electrical atomization of the liquid feed into ultra-fine (generally <10 μm [58]) fiber structures, which are then dried instantly (due to their high surface area) at room temperature. The basic technology is called single-needle electrospinning, the fiber-forming excipient (polymer or sugar) and the therapeutic agent are dissolved in a solvent and the solution is fed into a single spinneret at a constant controlled rate. High voltage is applied between the spinneret and the grounded metal collector, which causes the formation of a Taylor–cone first, and when the electrostatic forces overcome the surface tension a liquid jet erupts from the cone [59]. The unstable jet is splitting up into multiple jets drawn towards the grounded collector. During the process, the

jets get elongated attaining a fiber-like structure (Figure 4C), and the solvent evaporates instantaneously due to the high surface area as the fibers are often submicron-sized. The solid material is usually collected on a metal plate or cylinder (Figure 6). Electrospinning efficiency largely depends on the solution properties (typically viscosity, surface tension, and conductivity) [60]. Stable electrospinning is often only realized if the viscosity of the solution is high enough to produce the necessary polymer entanglements to form fibers and one of the most important factors which influence this aspect is the polymer concentration of the solution [61]. Electrospun fibrous materials need to be micronized (e.g. milling) before mixing with excipients, tableting or capsule filling [62].

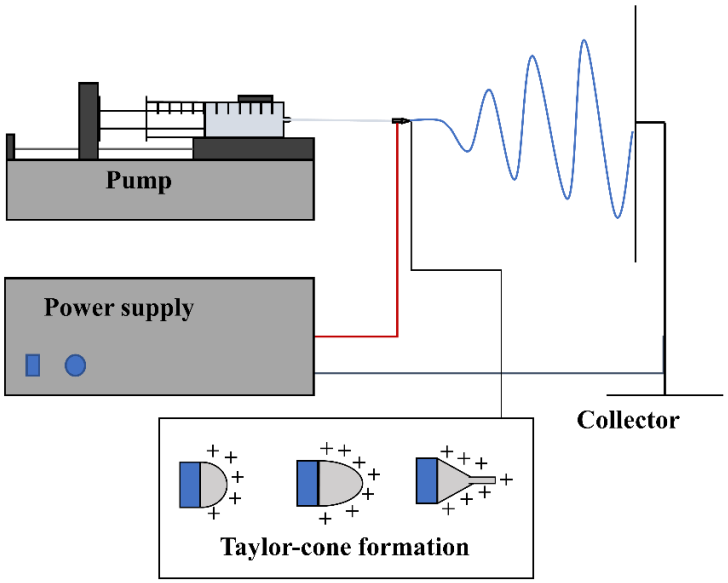

Technological aspects	Stresses
Takes about 0.1 second	Dehydration
Moderate capital cost	
Low operating cost	Air-liquid interface
Continuous production	

Figure 6 The electrospinning technology and related aspects

Drying (evaporation of the solvent) by electrospinning takes place extremely rapidly (about 0.1 s), making the technology the fastest dehydration method due to the extremely large specific surface area [63]. Electrospinning can be carried out at room temperature and atmospheric pressure, which makes very gentle drying possible (Figure 2). It is also a continuous process consuming very little energy resulting in an economically viable production alternative.

In case of biopharmaceuticals, water needs to be used as the solvent instead of the typically used organic solvents, and this results (similarly to spray drying) in lower productivity as evaporation is harder due to the high boiling point and evaporation enthalpy; in addition, the high surface tension of water also reduces the throughput. The use of surfactants, heated drying gas or the reduction of the amount of water in the solution can help to achieve a higher production rate of the solid product [27].

Electrospinning has the potential to be an alternative to freeze drying and spray drying due to its gentle drying conditions and short processing times (Figure 2). Over the recent years, numerous studies were published about the use of electrospinning for the solid formulation of different proteins [64], such as enzymes [50,65-67], hormones [68,69], a monoclonal antibody [70], proving that electrospinning provides gentle drying conditions for proteins despite the application of electric forces. Besides proteins, other biopharmaceuticals, like probiotics [71], vaccines [72], etc. have been successfully dried by the technology.

However, the exploration of different aspects of the technology like the scalability of aqueous electrospinning, downstream processability of the biopharmaceutical-containing fibers, and preparation of final dosage forms from the fibers had not yet been reported before this work was begun. This may be due, in part, to the fact that appropriate approaches for generating large quantities of fibers from aqueous solutions have not been described. A brief overview of the scaling-up possibilities can be read in the next section.

2.3 Scale-up of electrospinning

The laboratory-scale electrospinning device with a single needle has rather low productivity of 0.01-2 g dry product per hour [48] which does not satisfy the needs of the pharmaceutical industry. Therefore, multiple attempts were made for the scale-up of the technology to reach production rates sufficiently high for industrial applications [49]. These attempts included the use of multiple needles [73,74], free surfaces (like coils [75,76], balls [77], or bubbles [78,79]), or rotating spinnerets [80,81]. Even though numerous scaled-up electrospinning technologies have been developed, there are only a handful of articles discussing the utilization of scaled-up electrospinning for drug formulation development. This section aims to cover these works.

In the context of pharmaceutical applications, only a few nozzle-based technologies have been investigated for scaled-up production so far. The Fluidnatek LE-100 and LE-500 manufactured by Bioinicia are GMP-certified scaled-up electrospinning/electrospraying machines which can be used for pharmaceutical applications [82]. The Fluidnatek machines employ multiple needles to increase process productivity, however, clogging of the tubes, the negative influence of the electric field interference, and the difficult cleaning can hinder the vast application of this technique. Electroblowing is one of the stationary nozzle methods which seemed to be appropriate to satisfy the pharmaceutical needs. Um et al. compared electrospinning and electroblowing using a hyaluronic acid-containing system [83]. Their results highlight the advantages of the applied air blow such as the faster solvent evaporation and the higher feeding rate. Publication of Balogh et al. confirmed the latter statement since five times higher flow rate was achieved with electroblowing compared to single-needle electrospinning [84]. In this work, the air-assisted method was successfully applied for preparing fibrous diclofenac sodium-cyclodextrin complex-based reconstitution injection. Even higher feeding rate was reached with electroblowing in the case of itraconazole-loaded samples [85]. In this work, the authors compared electroblowing to spray drying and they not only showed that increased productivity (50 g/h) is achievable using the air-assisted technology, but they also demonstrated that the prepared amorphous solid dispersion showed better stability than the spray-dried samples. El-Newehy et al. prepared polyvinyl alcohol, polyethylene oxide and metronidazole containing nanofibers by the Nanospider^{TM} technology for creating a controlled release system [86]. The API release of the fibers reached 84% within 2 hours and the fibrous samples showed remarkable antimicrobial activity against the investigated pathogens. Krogstad and Woodrow compared a single-needle apparatus and a

Nanospider™ equipment. The tenofovir-loaded polyvinyl alcohol fibers produced by the two technologies were found to have similar morphology and release profile and this proved the wire technique to be a possible way for scaled-up production of drug-loaded fibers in the case of non-volatile aqueous solutions. The productivity of the Nanospider™ technology was 7.6 g/h when using a single wire of 25 cm length [87]. In 2012, corona electrospinning was developed to minimize the free liquid surface and maximize the jet formation using a rotating ring as a spinneret. Multiple Taylor-cones are self-assembling at the edge of the rotating (~100 rpm) spinneret, and thus several polymer fibers jet at the same time. The achievable flow rate was 300 ml/h with PVP K30 as the fiber forming polymer and ethanol as solvent [88,89]. High-speed electrospinning improves productivity significantly by combining electrostatic [90] and high-speed rotational [91] jet generation and fiber elongation (Figure 6). In the first article where high-speed electrospinning was described a 75-fold productivity improvement was achieved by the scaled-up technology (from 6 g to about 450 g solid product per hour) [92]. The morphology and the dissolution properties of the produced fibrous mats showed similarity to the samples prepared by single-needle electrospinning. It has been shown that rational selection of the applied polymer can ensure the stability of the amorphous drug in the matrix which meets the strict requirements of the pharmaceutical industry [93]. The technology proved to be appropriate for the formation of a flubendazole containing electrospun product as well [94]. Both the drug-loaded nanofibers and the tablets filled with the fibers had outstanding dissolution properties. Moreover, *in vivo* tests proved that the bioavailability of the amorphous drug form found in the fibers was much higher than the crystalline API's.

As it was mentioned before, in the case of sensitive large molecules or living bacteria, the use of water instead of organic solvents is required to maintain the active form. Owing to the relatively high boiling point of aqueous solutions, the evaporation of the solvent requires more time. Thus, the productivity of the aqueous single-needle electrospinning process is reduced (0.02-0.5 g/h) compared to the volatile organic solvents. There have only been few attempts to increase the productivity by the scale-up of the electrospinning process using water-based solutions. Needleless electrospinning of polyvinyl alcohol-chitosan aqueous solution with a spinning cylinder spinneret was applied and 50 g/h productivity was achieved [95]. The fibers were collected on a rotating drum, however, during continuous operation evaporation of water from the free liquid surface can be notable [96]. Besides this, one article

mentions the use of high-speed electrospinning to form fibers from purely aqueous solutions to obtain protein-loaded fibers [66].

After reviewing the current literature, it seems clear that there is significant lack of knowledge about the scaled-up electrospinning of fibers starting from aqueous solutions. **Therefore, it would be essential to explore if it is possible to produce large amounts of fibers from water-based systems and characterize the products obtained. Such a technology should also be compared to other processes e.g. freeze drying to reveal its advantages.**

2.4 Downstream processing of the electrospun fibers

The majority of the publications related to electrospinning are focusing solely on how to manufacture fibers with appropriate characteristics, such as the desired diameter (small or large) or drug release (immediate or controlled). However, only a few articles present ways to convert the obtained fibers into applicable pharmaceutical formulations. This chapter is dedicated to showing the downstream processing options for the obtained fibers, and the possibilities for preparing final dosage forms.

2.4.1 Collection of the fibers

The conventional way of producing e.g. tablets from the electrospun material starts with the collection of the fibers, followed by milling, homogenization with excipients and finally the compression into tablets. The first step is always the collection of the prepared fibrous material. On industrial-scale electrospinning machines, which are nowadays mainly applied for non-pharmaceutical purposes, such as Nanospider^{TM}, a substrate web potentially made of cellulose, synthetics, fiberglass or foils with a width of 1-1.7 m is used for capturing the fibers. Similarly, Szabó et al. developed a continuous collector equipped with polypropylene (PP) collecting fleece and a doctor blade that removes the fibers (Figure 7) [97], but as it is not a closed system, the collection efficiency of this method can be low.

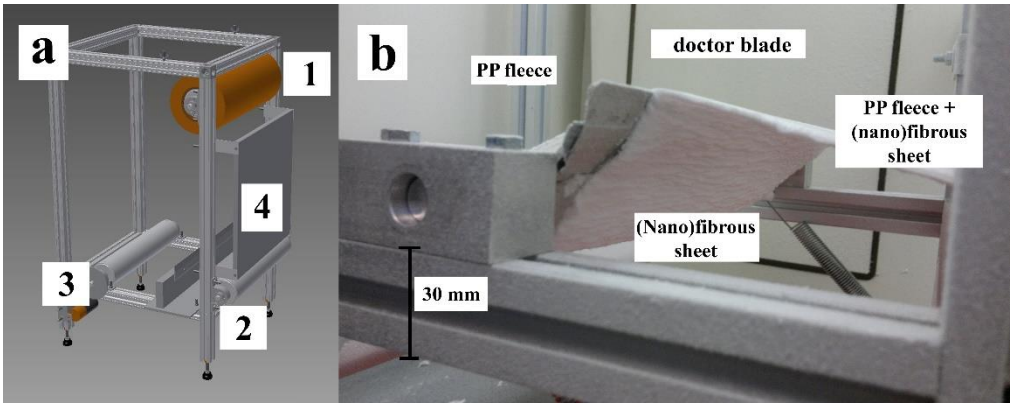

Figure 7 Equipment for collecting fibers: (a) a 3D image showing the whole equipment (b) an image showing the equipment during the collection of PVPVA64 fibers with the doctor blade removing it [97]

A similar type of collection, which is not yet suitable for scaled-up electrospinning, was developed by Balogh and co-workers in two recent publications [98,99]. The drug-loaded fibers are electrostatically deposited onto a pullulan film attached to a moving roll. This technology is not designed to produce tablets (however, it seems possible with minor modifications): the obtained sheet was cut into immediate-release orally dissolving webs.

After the literature review, it is apparent that the collection of electrospun fibers for pharmaceutical applications has not been studied extensively. **It would be important to develop collection methods with high collection efficiency that can be incorporated into continuous manufacturing lines.**

2.4.2 Grinding/milling of the fibers

Another great challenge in addition to process scalability is to achieve appropriate downstream processability of the electrospun fibers [62]. In this respect, the friability/grindability of the fibers and the properties (e.g. flowability) of the ground fibrous powder are also critical, however, not much information can be found about this subject in the literature. Presumably, the grindability of the electrospun sheets mainly depends on the type and the molecular weight of the applied polymer (the higher the molecular weight, the poorer the grindability), besides other factors like fiber diameter, residual moisture, and the plasticizer effect of the API. Microfibers obtained by high-speed rotary spinning technique (without voltage) have been ground via two methods. In the first case, a vibrating mill was applied for the micronization of PVP fibers after the first fine cutting, but the ground fibers possessed weak flowability [100]. In the other study, the mat was ground by means of a grinder equipped with knives [101]. SEM images proved the fragmented state of the fibers. Grinding of nanofibers prepared by high-speed ES has been performed by a hammer mill, a cutting mill and an oscillating sieve mill [62,102]. All the tested techniques could be successfully applied for the purpose. Grindability of fibers made of polyvinyl alcohol and polyethylene oxide could be enhanced by the addition of sugars or sugar derivatives such as glucose or mannitol to the ES solution [102]. However, before this work was started, no article could be found in which it was attempted to develop grindable, hence downstream processable electrospun formulations of biopharmaceuticals.

2.4.3 Conventional tablet formation

Tablets account for 80% of all formulations [103] due to their obvious advantages such as self-administration, accurate dosing, mechanical strength, and diversity. Despite this, only a few examples can be found in the literature where fibrous mats are processed into conventional tablets via the traditional process (milling followed by homogenization with excipients and compression) [62,100,101,104]. Generally, the properties of the prepared blends (particle size distribution, flowability) and tablets (hardness, friability, disintegration time, dissolution) were examined and published. When electrospun nanofibers containing PVPVA64 and itraconazole were investigated in terms of compression behavior [62], it was

shown that the fibrous material can take up a large percentage of tablet volume due to its low bulk density. In spite of the low bulk density and the relatively poor flowability, rotary tableting could be carried out and tablets with acceptable weight variation was obtained [104]. To process an electrospun fibrous sheet to tablets in a continuous manner also seems feasible, which could potentially be a really important feature, as a switch is expected from batch to continuous manufacturing in the near future [97]. Yet, no studies were found in the literature in which conversion of fibrous sheets containing biopharmaceuticals into an oral final dosage form (e.g. tablet or capsule) via the conventional way was attempted.

To summarize, it is of great interest to investigate if it is possible to develop biopharmaceutical-loaded grindable fibers and convert the ground fibers into tablets. Effects of the downstream processing steps on sensitive biopharmaceuticals should also be assessed.

2.4.4 Parenteral dosage forms from fibers

Parenteral administration, despite its numerous disadvantages (low patient compliance due to pain and discomfort, the need for sterile environment, local adverse reactions etc.), remains the main choice for drug delivery route in emergency situations, in intensive care, in case of low oral bioavailability of the drug, or when the rate of absorption and duration of the effect must be strictly controlled [105]. Parenteral delivery of biopharmaceuticals (especially proteins and peptides) is often unavoidable mainly to avoid biological barriers through which it is difficult for large molecules, like proteins to pass, and to achieve pharmacologic levels of circulating protein over a relatively short period of time [106]. However, both small molecule drugs and biopharmaceuticals have decreased stability in solution due to the higher reactivity in the liquid phase. This problem can be overcome by using reconstitution injections as this type of formulation combines the advantages of parenteral administration (efficient and immediate systemic delivery) and solid formulation (increased stability in solid form).

Electrospun parenteral drug delivery systems have not been studied extensively, as drug-loaded electrospun fibers are generally not suitable for parenteral delivery, as the molecular weight of most polymers applied as fiber matrices exceed the glomerular filtration limit (~40,000-60,000 Da). Lower molecular weight polymers (e.g. PVP K17, PVA 30,000) might be utilized in electrospun parenteral formulations, but electrospinnability of these polymers tend to be significantly worse compared to polymers with high molecular weight. Instead of polymers, Balogh et al. used 2-hydroxypropyl-β-cyclodextrin (HP-β-CD) as carrier and

solubilizer for diclofenac sodium, a drug with limited water solubility to prepare a reconstitution bolus injection by electrospinning [84]. However, when this work was started this was the only study in which a cyclodextrin-based parenteral formulation was developed by single-needle electrospinning, despite cyclodextrins having many advantageous properties. Cyclodextrins (CDs) are water-soluble oligosaccharides with low molecular weight, containing six (α-CD), seven (β-CD) or eight (γ-CD) α-D-glucopyranose units (Figure 8).

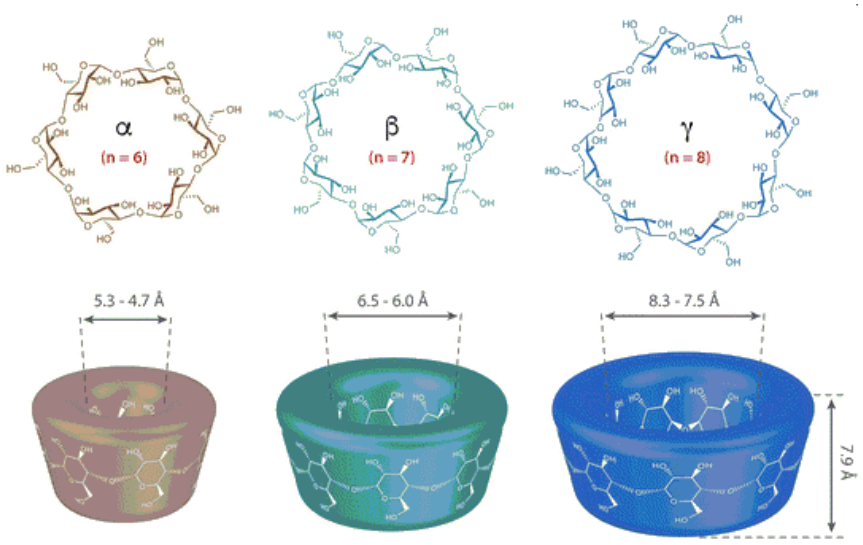

Figure 8 Chemical structure and dimensions for α-, β- and γ-cyclodextrins [107]

One of the most appealing characteristics of these cyclic molecules is that they have a relatively hydrophobic central cavity that readily forms a non-covalent host-guest inclusion complex with a lipophilic compound or moiety. The formed complex remains water-soluble due to the hydrophilic outer surface of the hosting CD molecule. This favorable feature can be utilized in pharmaceutical formulations. Nowadays, there are over 60 commercially available pharmaceutical products containing CDs as excipients. In addition, CDs are reported to act as stabilizers for biological drugs like peptides and proteins [108,109]. HP-β-CD and other cyclodextrins (CDs) have been successfully electrospun recently as CDs are capable of forming polymer-like supramolecular structures via intramolecular interactions [110-112]. Generally, high CD concentrations are required to generate strong and large associates in the solution (resulting in high solution viscosity), which can form fibers [84,113]. However, no article could be found in which cyclodextrin fibers were produced in a scaled-up manner.

The literature review revealed that electrospun cyclodextrin-based parenteral formulations have not been studied thoroughly yet. **Therefore, it would be important to investigate if it is possible to produce cyclodextrin fibers by a scaled-up electrospinning technology and to examine if these fibers can be used as parenteral drug dosage forms.**

2.5 Objectives

After surveying the current ‘state of the art’ related to biopharmaceuticals and electrospun materials, the main objectives of the experimental work could be set up:

- to investigate if it is possible to produce dried fibers in a scaled-up manner from aqueous polymeric and polymer-free systems at room temperature by high-speed electrospinning;
- to develop biopharmaceutical-containing grindable fibers and to produce solid oral formulations from the ground fibrous powder; in addition, to investigate if the downstream processing steps have a negative effect on the APIs;
- to develop an electrospun cyclodextrin-based parenteral formulation and to evaluate if large amounts of cyclodextrin fibers can be produced from aqueous solutions.
- to carry out a long-term stability study of the biopharmaceuticals in the fibers produced by scaled-up electrospinning;

3. Materials and methods

3.1 APIs

β-Galactosidase

β-Galactosidase, also called lactase, is a glycoside hydrolase enzyme that catalyzes the hydrolysis of lactose, the main carbohydrate in milk, into glucose and galactose through the breaking of a glycosidic bond. The enzyme is widely used as a drug for the treatment of lactose intolerance. It is estimated that about 70% of adults worldwide are not able to digest lactose due to the insufficient production of β-galactosidase, which brings on gastrointestinal symptoms when dairy products are consumed [114]. Powder of β-galactosidase (opti-lactase A-100; min. 100,000 FCC Unit/g) from *Aspergillus oryzae* was kindly provided by Optiferm GmbH (Oy-Mittelberg, Germany).

Voriconazole (VOR)

Formula: $C_{16}H_{14}F_3N_5O$

Molar mass: 349.311 g/mol

Appearance: odorless, white powder

Supplier: pure API - Sigma-Aldrich (Budapest, Hungary)

Vfend® - local pharmacy

Solubility: 0.0978 mg/mL [115]

Indication: antifungal

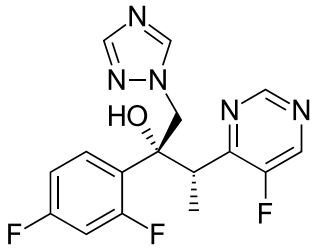

Clostridium butyricum

Clostridium butyricum are strictly anaerobic spore-forming bacteria commonly found in the human gastrointestinal tract [116]. *C. butyricum* has been shown to regulate gut homeostasis and anti-inflammatory response in inflammatory bowel disease by the production of butyrate, which makes it a good model for the research of microbiome-based therapeutics [117]. *C. butyricum* Prazmowski 1880 was obtained from the National Collection of Agricultural and Industrial Microorganisms (Budapest, Hungary).

3.2 Excipients

Table 2 List of electrospinning excipients

Chemical name	Brand name	Structure	Supplier	Characteristics
Polyvinyl alcohol (PVA)	Mowiol® 18-88	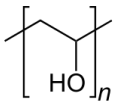	Sigma-Aldrich (Darmstadt, Germany)	86.7-88.7 mol% hydrolysis, M_w: 130 000
Polyethylene oxide (PEO)	POLYOX™	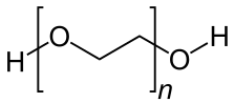	Colorcon (Dartford, UK)	M_w: 2 M
Mannitol	Mannogem EZ	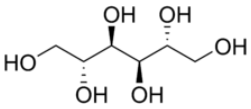	SPI Pharma, (Wilmington, DE, USA)	Nonhygroscopic, directly compressible
2-Hydroxypropyl-β-cyclodextrin (HP-β-CD)	Kleptose® HPB	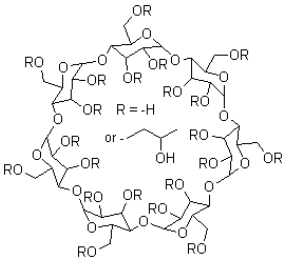	Roquette Pharma (Lestrem, France)	Molar substitution nominal value: 0.62
Sulfobutylether-β-cyclodextrin sodium (SBE-β-CD)	Dexolve™	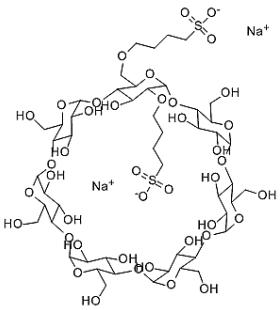	Cyclolab Cyclodextrin Research and Development Laboratory Ltd. (Budapest, Hungary)	Average degree of substitution: 6.5

Table 3 List of tableting excipients

Chemical name	Brand name	Supplier	Characteristics
Microcrystalline cellulose (MCC)	Vivapur® 200	JRS Pharma (Rosenberg, Germany)	Applied as a filler and binder in tablets, mean particle size = ~250 μm, bulk density 0.31-0.37 g/cm^3
Croscarmellose sodium	Ac-Di-Sol®	DuPont (Midland, MI, USA)	Applied as a disintegrant in tablets, bulk densit 0.53 g/cm^3
Mannitol	Pearlitol® 400DC	Roquette Pharma (Lestrem, France)	Used as a filler in tablets, mean particle size = ~360 μm, bulk density 0.68 g/cm^3
Silicium dioxide	Aerosil® 200	Evonik Industries (Essen, Germany)	Glidant in tablets with high specific surface area
Magnesium stearate (MgSt)	-	Hungaropharma Ltd. (Budapest, Hungary)	Water-insoluble lubricant, average particle size = ~10 μm
Cross-linked polyvinylpolypyrrolidone	Kollidon Cl	BASF (Ludwigshafen, Germany)	Applied as a disintegrant in tablets, particle size = 90-130 μm

3.3 Other materials

O-nitrophenyl-β-D-galactopyranoside (ONPG) - Carbosynth (Compton, UK)

Clostridial Nutrient Medium (CNM) - Merck KGaA (Darmstadt, Germany)

Tryptic Soy Broth (TSB) - Merck KGaA (Darmstadt, Germany)

Tryptic Soy Agar (TSA) - Merck KGaA (Darmstadt, Germany)

Columbia Blood Agar plates - Biolab Ltd. (Budapest, Hungary)

AnaeroGen™ 2.5 L (anaerobic gas generating sachets) - Diagon Ltd. (Budapest, Hungary)

3.4 Methods

3.4.1 Culturing of Clostridium butyricum

C. butyricum was grown in CNM at 37 °C under anaerobic conditions for 48 hours, which resulted in a mixture of spores and vegetative cells. *C. butyricum* was grown in TSB at 37 °C under anaerobic conditions for 24 hours, which resulted in exclusively vegetative bacteria. The cultures were centrifuged at 9,000 rpm for 10 minutes. The cells were then washed twice with phosphate buffered saline and resuspended in an appropriate volume of sterile water to obtain concentrations of bacteria from 10^7 to 10^8 colony-forming units CFU/mL.

3.4.2 Electrospinning techniques

The preparation of the solutions for all techniques was performed in the same way. The matrix and the API were added to purified water in a glass vial and the mixture was stirred with a magnetic stirrer until complete dissolution. (The one exception was *Clostridium butyricum*, where the matrix was dissolved in purified water, and the bacteria were added to this solution. The mixture was stirred on a magnetic stirrer until complete homogenization.) If needed, heating was applied to facilitate the dissolution.

3.4.2.1 Drop electrospinning (DES)

A drop of the solution (~ 20 µL) was placed on the tip of a metal needle (d = 5 mm) attached to high voltage (20 kV, Unitronik Ltd., Nagykanizsa, Hungary). Few milligrams of the product were collected on the collector placed above the needle (120 mm distance).

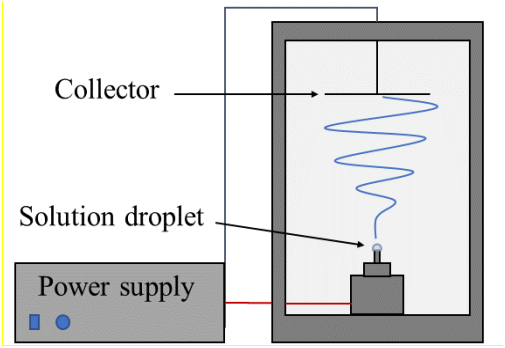

Figure 9 Schematic drawing of the drop electrospinning (DES) equipment

3.4.2.2 Laboratory-scale high-speed electrospinning

The lab-scale high-speed electrostatic spinning (HSES) setup (Figure 10) consists of a circular-shaped, stainless steel spinneret (d = 34 mm) connected to a high-speed motor. The disk-shaped spinneret was equipped with 8 equidistantly distributed orifices (d = 330 µm)

located in the side wall of the wheel. The solution was fed with a SEP-10 S Plus syringe pump (Viltechmeda Ltd., Vilnius, Lithuania). The rotational speed of the spinneret was fixed at 8,000 rpm. The applied voltage was 37 kV during the experiments using a high-voltage power supply (Unitronik Ltd., Nagykanizsa, Hungary). A vertical drying airflow (2 bar) and the electrostatic forces directed the fibers to the grounded metal collector covered with aluminum foil, which was placed at a fixed distance (35 cm) from the spinneret. The experiments were performed at room temperature (25 °C).

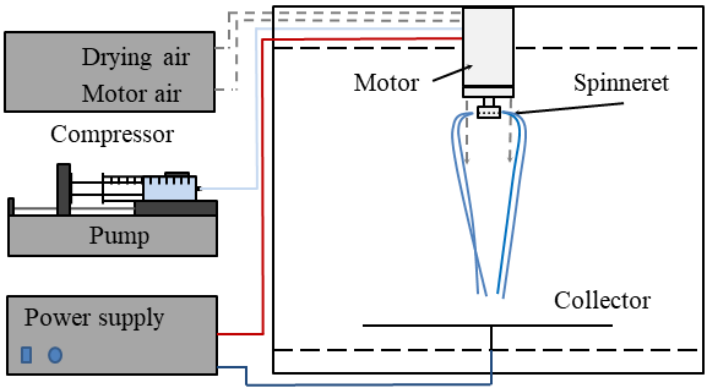

Figure 10 Schematic drawing of laboratory-scale high-speed electrospinning

3.4.2.3 Pilot-scale high-speed electrospinning

The pilot-scale HSES setup (Figure 11) consists of a stainless steel spinneret (d = 34 mm) connected to a high-speed motor. The disk-shaped spinneret was equipped with 36 equidistantly distributed orifices (d = 330 μm) located in the side wall of the wheel. The solution was fed with a SEP-10 S Plus syringe pump (Viltechmeda Ltd., Vilnius, Lithuania). The rotational speed of the spinneret was fixed at 40,000 rpm. The applied voltage was 40 kV during the experiments (Unitronik Ltd., Nagykanizsa, Hungary). The conical bottom of the drying chamber was grounded, and it acted as the counter electrode. Air knives were used to remove the dried material from the surface of the chamber and a constant airflow (120 m^3/h, room temperature) was applied to help the dried fibers to reach the cyclone. The produced fibrous material was collected by a cyclone. The experiments were performed at ambient temperature (25 °C).

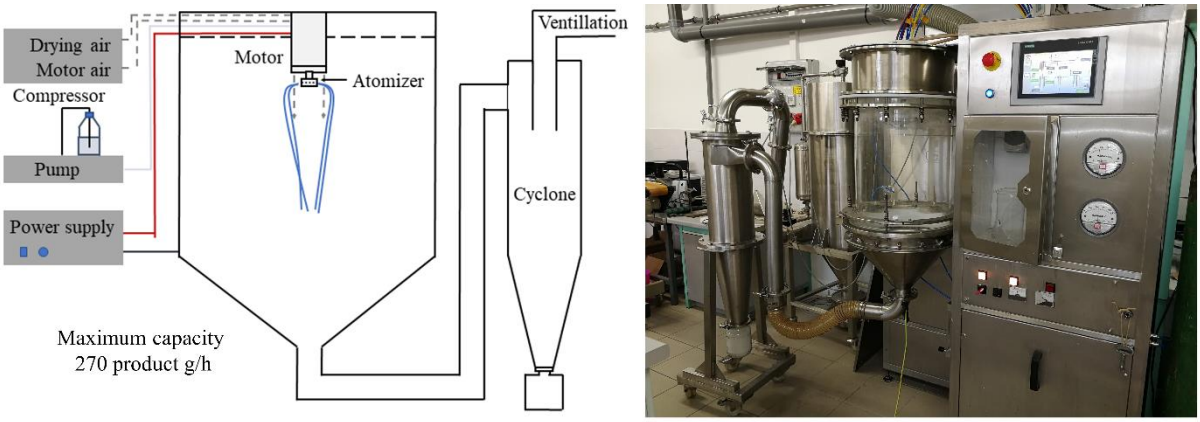

Figure 11 Schematic drawing and photo of the pilot-scale high-speed electrospinning device with a continuous cyclone sample collector

3.4.3 Grinding/milling of the electrospun fibers

The electrospun material was ground to make it suitable for blending with excipients. β-Galactosidase-containing PVA, PEO, and mannitol fibers were pushed through a sieve with 0.8 mm hole size. This kind of milling is similar to oscillating or conical milling with respect to achieved powder properties. A hammer mill (IKA MF10, IKA-WERKE GmbH & Co. KG, Staufen, Germany) was used with a 1.0 mm sieve at 3000 rpm for the VOR-containing SBE-β-CD and the β-galactosidase-containing HP-β-CD samples. An oscillating mill (Quick 2000 Kft., Tiszavasvári, Hungary) was used with a 1.0 mm sieve at 100 1/min for the bacteria-containing HP-β-CD samples.

3.4.4 Tablet preparation

Standard convex-shaped tablets were prepared on a CPR-6 eccentric tablet press (Dott Bonapace, Limbiate, Italy) equipped with 14 mm concave punches.

3.4.5 Storage stability test

For storage stability testing of the formulations containing β-galactosidase, the reference enzyme formulation, and the prepared enzyme-loaded tablets were kept in locked glass vials at 4°C and at room temperature. The prepared bacteria-containing fibers were kept in locked glass vials at -20 °C, 4 °C, and room temperature aerobically and anaerobically.

3.5 Analytical methods

3.5.1 Viscosity measurement

The viscosity of the solutions was determined using an AR 2000 rotational rheometer (TA Instruments, New Castle, DE, USA) in parallel plate configuration. The upper moving plate of 40 mm diameter and the lower Peltier plate, which adjusted the temperature of the solutions to 25 °C, were made of stainless steel. Viscosity was measured at shear rates linearly increased from 20 to 100 s^{-1}. The reported viscosities are the overall averages of values measured at 5 different shear rates using 2 independent samples (replicates). There were no practically relevant changes in the measured viscosities as a function of shear rate.

3.5.2 Scanning electron microscopy (SEM)

Morphology of the electrospun samples was examined by a JEOL 6380LVa (JEOL, Tokyo, Japan) type scanning electron microscope in high vacuum. Samples were fixed by conductive double-sided carbon adhesive tape and sputtered by gold using ion sputter (JEOL 1200, JEOL, Tokyo, Japan). The applied accelerating voltage was set to 15 kV and the working distance was 10 mm.

3.5.3 Energy dispersive spectroscopy (EDS)

Energy dispersive spectrometry (EDS) was used in conjunction with SEM for the mapping of fluorine and sulfur in the samples. (The detection and calculation were based on the peaks identified at 0.677 and 2.307 keV). The detected X-ray radiation was between 4000 and 5000 counts/s, and 10 scans were accumulated.

3.5.4 Moisture balance measurement

The residual water content of the PVA, PEO, and mannitol fibers containing β-galactosidase was measured right after the electrospinning process using a Sartorius MA40 moisture balance (Göttingen, Germany). The residual water content was determined based on the moisture loss of approximately 0.1 g sample after 10 min at 105 °C.

3.5.5 Thermogravimetric measurement

The residual water content of all the other samples was determined by thermogravimetric examination, carried out with a Q5000 TGA instrument (TA Instruments, New Castle, DE, USA) under nitrogen atmosphere (n = 3). The sample was heated up from 25 to 105 °C at 10 °C/min, and it was kept at 105 °C for 10 minutes. The applied nitrogen flush was 50 mL/min during the measurement.

3.5.6 Modulated differential scanning calorimetry (DSC)

Modulated differential scanning calorimetry measurements were carried out using a DSC3+ (Mettler Toledo AG, Switzerland) DSC instrument in TOPEM® mode (sample weight: ~5-15 mg, pierced pan, nitrogen flush, 50 mL/min). The equipment uses a stochastic temperature modulation superimposed on the underlying heating rate. The overall heating rate was 1 °C/min, while the pulse height was set to 1 °C (which means that the temperature was modulated by ±0.5 °C). The pulse width – the frequency of the modulation – was varying randomly between 15 and 30 s. The temperature was increased from 0 °C to 200 °C.

3.5.7 X-ray powder diffraction (XRPD)

X-ray powder diffraction patterns were recorded with a PANalytical X'Pert Pro MDP X-ray diffractometer (Almelo, The Netherlands) using Cu-Ka radiation (1.542 Å) and Ni filter. Measurements were conducted in a range of 2Θ=4-44° to determine the crystalline structure of the electrospun samples and the other materials. XRPD measurements were carried out in reflection mode with a step size of 0.0167°.

3.5.8 FTIR measurement

Fourier-transform infrared (FTIR) spectra were collected using a Bruker Tensor 37 type FTIR spectrometer equipped with DTGS detector (Bruker Corporation, Billerica, MA, USA). The samples were ground with KBr and cold-pressed (200 bars) into discs. The measurement was carried out in transmission mode, at a scanning range of 400–4000 cm^{-1} with a resolution of 4 cm^{-1}.

3.5.9 Raman mapping

The Labram-type Raman instrument of Horiba Jobin–Yvon (Kyoto, Japan) coupled with external 532 nm Nd:YAG laser source and Olympus BX-40 optical microscope was employed for spectrum collection. Objectives of 50x and 100x (laser spot size: ~2 μm) were used in the high-resolution measurements for the samples containing VOR and β-galactosidase, respectively. A 950 groove/mm grating monochromator dispersed the Raman photons, directing them to the CCD detector. The spectral ranges of 460–1680 cm^{-1} with 3 cm^{-1} resolution (samples containing VOR) and 390–1500 cm^{-1} with 1 cm^{-1} resolution (samples containing β-galactosidase) were measured. The maps were collected with 5 μm (samples containing VOR) and 1 μm (samples containing β-galactosidase) step size in both directions and consisted of 31 x 31 points. One spectrum acquisition took 30 s and accumulated 2 times in each mapping point. In each case, acquisition, spectrum preprocessing (baseline correction and normalization), visualization and evaluation of the obtained maps were performed using

LabSpec 5.41 software (Horiba Jobin-Yvon, Kyoto, Japan). The evaluation was carried out by the classical least squares (CLS) method using the spectra of the reference substances.

3.5.10 Reconstitution test and concentration measurement

A dissolution test (reconstitution) of the electrospun sample containing VOR and Vfend® was carried out following the instructions in the Vfend® package insert [118]. 3400 mg ground sample (containing 200 mg VOR) and a physical mixture of 200 mg VOR and 3200 mg SBE-β-CD were weighed into glass vials. 19 mL purified water was added into the vials, which were then shaken vigorously to dissolve powder stuck on the walls as well. In order to monitor the dissolution, pictures were taken at predetermined time intervals using a digital camera.

For the concentration measurements, 1 mL of the solution was filtered through a regenerated cellulose filter with 0.45 μm pores. 40 μL of the filtered solution was filled up to 10 mL. The sampling points were 0.5 and 2 minutes. An Agilent 8453 UV-VIS spectrophotometer (Hewlett-Packard, Palo Alto, USA) was used to measure the absorbance of dissolved VOR at the wavelength of 256 nm. The concentration could be readily calculated based on the calibration curve of VOR in water.

3.5.11 Powder characterization

Bulk and tapped densities of powder mixtures for tableting were examined on an ERWEKA SVM12 (Heusenstamm, Germany) type tapped density tester. After that, the values of Hausner ratio and Carr index were calculated according to Ph. Eur. [119].

3.5.12 Tablet characterization

Tablet breaking force was measured on a Schleuniger 4M hardness tester (Thun, Switzerland) with 3 tablets. Friability was measured on PharmaTest PTF 20E (Hainburg, Germany) friability tester after 100 rounds on 5 tablets.

3.5.13 Enzyme activity measurement

The activity of β-galactosidase was measured with ONPG as the substrate. ONPG is a colorless compound hydrolyzed by β-galactosidase to galactose (colorless) and o-nitrophenol (ONP, yellow if pH ≥ 9) (Figure 12). The amount of this latter compound can be evaluated spectrophotometrically (at 420 nm, based on a previously created calibration). 1.5 mL of a 6 M ONPG solution in 0.1 M acetate buffer (pH = 4.8) was added to 0.1 mL of 10^{-3} g/L preincubated (55°C) aqueous enzyme solution. The reaction was run for 10 min at 55°C and was stopped by adding 1 mL of 1 M Na_2CO_3 solution. After cooling to room temperature, the

absorbance of the reaction mixture was determined using a Pharmacia Ultraspec III UV/Vis spectrophotometer (Cambridge, UK). A stable enzyme formulation (over the course of the experiments) was measured in parallel to each fibrous enzyme-containing sample to serve as a reference. In each time point a single sample was taken from each enzyme-containing fibrous formulation. From each sample, 4 activity reactions were run in parallel. In each time point 3 tablets were measured, and from each tablet 4 activity reactions were run in parallel.

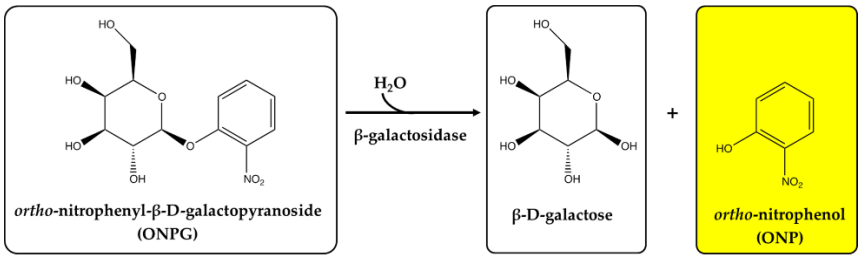

Figure 12 Enzymatic hydrolysis of ONPG by β-galactosidase [120]

3.5.14 Microscopical analysis

A laboratory light microscope (Olympus BH-2, Tokyo, Japan) at 2000x magnification was used to study the bacterial cells and spores. Spore staining using malachite green was applied to differentiate the spores from the vegetative cells [121]. Fibers were dissolved in water and bacteria were centrifuged and washed before spore staining.

3.5.15 Viability test of Clostridium butyricum

The viability of *C. butyricum* was determined by the colony-forming unit (CFU) measurement method. Serial ten-fold dilutions were prepared from the samples in sterile water and 100 µL was plated from each of the dilutions onto Columbia Blood Agar plates. The plates were incubated anaerobically at 37 °C for 48 hours. The plates with the appropriate number of colonies (10 to 200) were counted.

3.5.16 Butyrate production measurement

Butyric acid production capacity of the bacteria in the fibers was tested by inoculating 50 mL CNM with 50 mg bacteria-containing electrospun material. The inoculated medium was incubated anaerobically at 37 °C for 24 hours. Butyric acid content in the samples was measured by reversed-phase high-performance liquid chromatography (RP-HPLC) (Agilent 1200 series LC System). An isocratic elution of water containing 0.5% phosphoric acid and ACN (85:15 V/V ratio) was performed at a flow rate of 1.0 mL min^{-1} and 25 °C for 5 min. The UV detection wavelength was set to 210 nm. A 3 µL of sample volume (after 10x dilution) was injected onto a Phenomenex Luna C18 column (3 µm; 100 × 4.6 mm).

4. Results and discussion

4.1 Scaled-up production of grindable electrospun fibers containing a protein-type drug from an aqueous polymeric matrix

4.1.1 High-speed electrospinning of fibers containing a protein-type drug

The broadly applied single-needle electrospinning is not capable of the mass production of fibers, and therefore, its productivity is far from the needs of commercial pharmaceutical manufacturing. In this research, HSES was used to increase the throughput of the technology. Based on the results of our previous study [102] on placebo systems, a matrix solution composed of 7.65 w/w% PVA, 0.57 w/w% PEO and 15.30 w/w% mannitol was selected for the experiments with β-galactosidase to achieve a grindable fibrous product.

The placebo system was supplemented with β-galactosidase powder so that the enzyme would be 20 w/w% of the solid product (Table 4).

Table 4 Composition of the PVA-based electrospinning solutions of β-galactosidase

	Amount (g)		**Concentration (w/w%)**		**Ratio of components in the solid product (%)**	
	Original	**Optimized**	**Original**	**Optimized**	**Original**	**Optimized**
PVA 130,000	1.000	1.000	7.2	7.6	26.0	32.5
PEO 2M	0.075	0.075	0.5	0.6	2.0	2.4
Mannitol	2.000	1.300	14.4	9.9	52.0	42.3
β-Galactosidase	0.770	0.700	5.6	5.4	20.0	22.8
Water	10.00	10.00	72.2	76.5	-	-

Even though it was possible to obtain enzyme-containing fibers by electrospinning of this solution, the high solid content caused premature drying of the material, which resulted in the blocking of the spinneret and it was needed to be cleaned regularly during the electrospinning process. To address this problem, the amount of mannitol in the system was reduced so that together with β-galactosidase their amount would equal the amount of mannitol in the placebo system (Table 4). Electrospinning could be performed seamlessly using the optimized solution composition, which suggests that decreasing the amount of mannitol in the matrix leads to better processability. However, in our earlier study it's been shown that when the sugar alcohol content in the fibers was decreased below a critical concentration, fiber grindability deteriorated [102]. Due to this, the mannitol amount was not decreased further in the present work.

The feeding rate used in the electrospinning experiment with the optimized composition was 30 mL/h, which is about 30x higher than what is achievable with single-needle electrospinning of aqueous solutions [102]. The obtained fibrous mat was easily removable from the aluminum foil used on the collector (Figure 13). The product was examined by means of SEM. The fibrous nature of the produced β-galactosidase-containing sample can be seen in Figure 14A. Bead-free fibers were obtained with diameters around 1-5 µm, but submicronic fibers were also observable.

4.1.2 Processing of the β-galactosidase-containing fibers

Processability of the formed fibers (e.g. milling, powder properties, etc.) is critical in the development of solid pharmaceutical products. The produced enzyme-containing fibers collected in the form of a fibrous mat were not suitable for conventional tablet production. Therefore, the collected mat needed to be ground to a powder before further processing. Grindability of the fibrous mats from the two matrix compositions containing β-galactosidase was evaluated right after electrospinning by pushing the material through a sieve with a pestle. The friability of the enzyme-containing fibers was sufficient without secondary drying, and the grinding of the mat resulted in a fibrous powder (Figure 13). It was noticed, however, that the fibers with the optimized matrix composition were slightly less friable than the fibers with the original composition. This suggests that less mannitol in the fibers results in decreased grindability, which is in line with our previous findings [102]. Further examinations were carried out only on the fibers with the optimized composition.

Figure 13 Electrospun sample removal from the collector and grinding process

The morphology of the enzyme-loaded fibrous powder was studied with SEM (Figure 14B). It can be seen that the fibrous structure of the electrospun material was preserved during the grinding process and the diameter of the fibers was unchanged. However, grinding reduced the length of the fibers resulting in a powder with improved flowability compared to the original unground material.

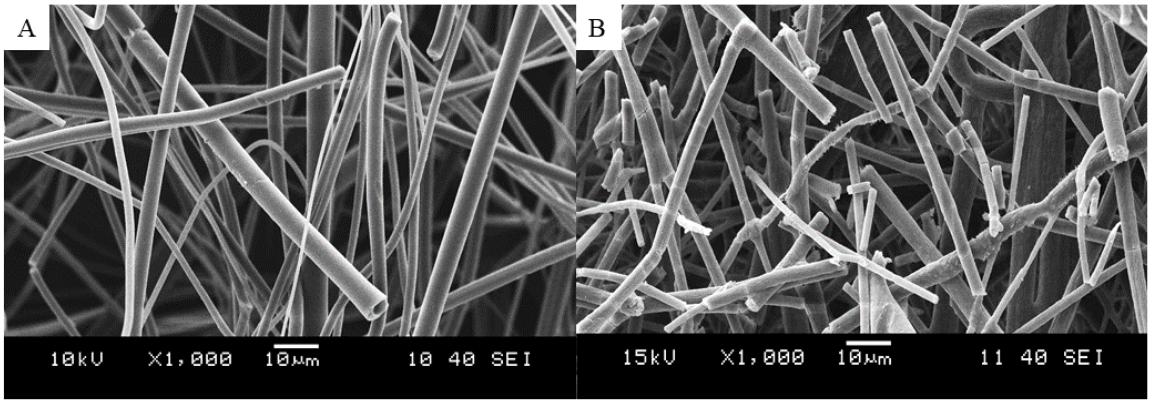

Figure 14 Scanning electron microscope images of β-galactosidase containing PVA-based fibers after electrospinning (A) and grinding (B) (at 1000-fold magnification)

4.1.3 Characterization of the fibers

In order to reveal the physical state of the different materials in the fibers, DSC, XRPD and Raman examinations were carried out. The reference PEO and PVA are semi-crystalline polymers (glass transition temperature of PVA could be detected at 46.1 °C), which was confirmed by this measurement. The reference β-galactosidase powder did not show any significant peak (except for water loss). The reference δ-mannitol had a sharp melting peak at 165.9 °C, even though other researchers detected two peaks (the first belonging to the melting of the δ polymorph, followed by the fast recrystallization to the more stable β polymorph, with a second melting peak) [122,123]. Similarly, the fibrous material had two endothermic peaks at 148.8 °C and 160.8 °C which probably belong to mannitol. During the DSC run, a melting point depression was seen (165.9 °C → 148.8 °C) due to the submicronic mannitol crystals with large specific surface [124], which is probably followed by recrystallization to a more stable form and the melting of it [122,123]. Based on these results, it can be concluded that all fiber components are amorphous except mannitol.

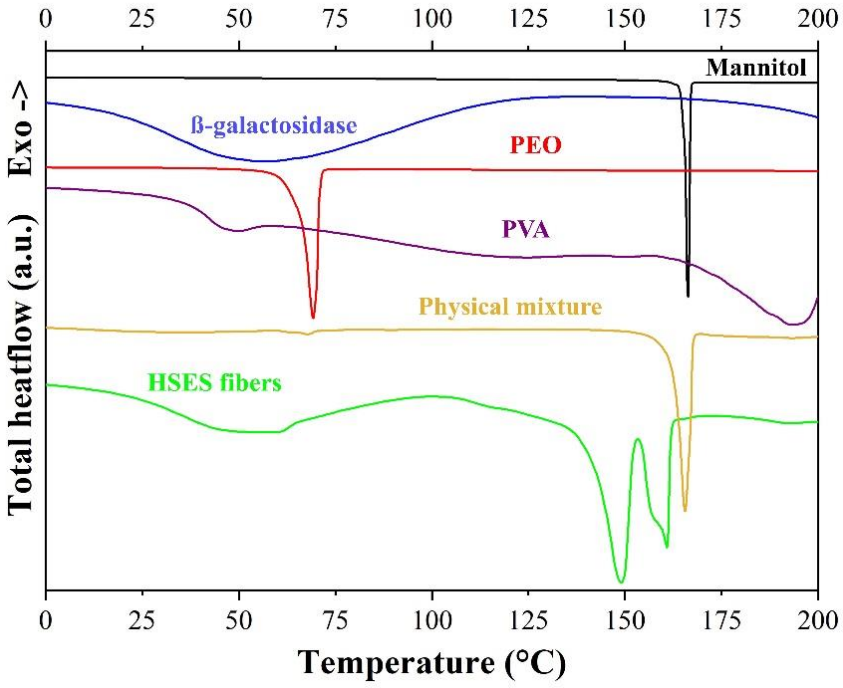

Figure 15 Differential scanning calorimetry (DSC) thermograms of δ-mannitol, β-galactosidase, PEO, PVA, the physical mixture of the fiber components, and the ground electrospun PVA+PEO+mannitol+β-galactosidase (HSES fibers)

In order to confirm the results obtained by DSC, XRPD measurements were performed. According to the diffractograms, only mannitol was crystalline in the fibers, showing the characteristic peaks of the δ-polymorph. This polymorph of mannitol has been shown to be the least stable at ambient conditions [125] and it can transform into the α- or β-polymorph [123], which can be found in the physical mixture of the electrospinning matrix and β-galactosidase (Figure 16). During drying (e.g. spray drying), the formation of α- and β-mannitol is expected [126]. However, in the fibers, δ-mannitol can be found, which might be ascribed to the even faster drying with ES (and therefore, no possibility for rearrangement into a stable form) or to the presence of the other substances.

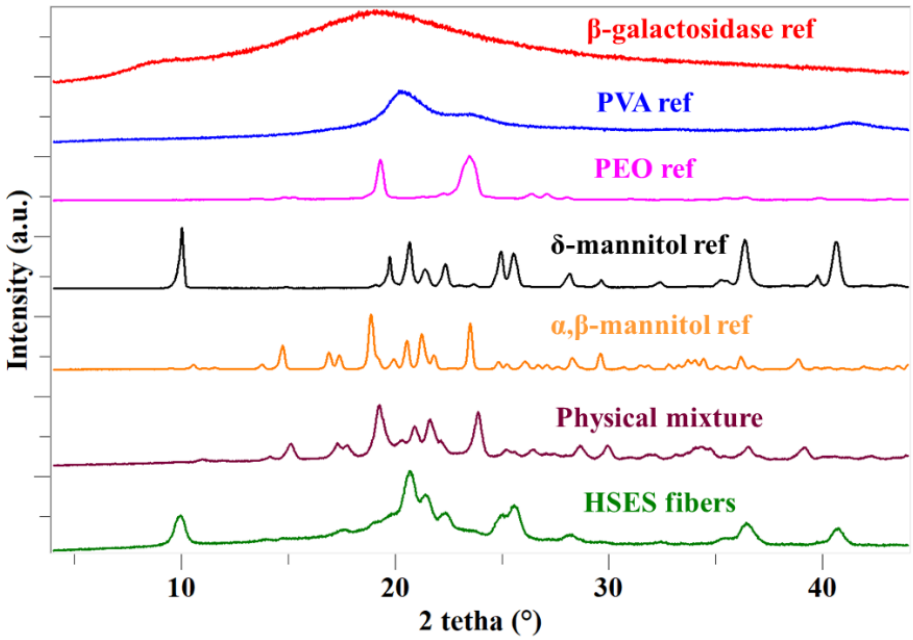

Figure 16 X-ray powder diffraction (XRPD) patterns of β-galactosidase, PVA, PEO, δ-mannitol, α,β-mannitol, the physical mixture of PVA, PEO, α,β-mannitol and β-galactosidase, and the ground electrospun PVA+PEO+mannitol+β-galactosidase

To evaluate the molecular interactions FTIR spectroscopy was applied on the samples. PVA and mannitol molecules contain free hydroxyl groups (which can act as potential proton donors for hydrogen bonding) and β-galactosidase possesses numerous different groups that can act as potential proton donors or receptors. Therefore, hydrogen bonding might occur in the fibers. Characteristic absorption peaks of β-galactosidase are at 3298 cm^{-1} due to OH stretching and at 2939 cm^{-1} due to CH stretching. The absorptions bands at 1651 cm^{-1} indicate the CONH vibration, and 1541 cm^{-1} peak is the NH bending vibration of the β-galactosidase structure [127]. These peaks indicate the protein nature of β-galactosidase. PVA has a broad absorption band from OH at 3319 cm^{-1}, bands from a stretching vibrations of CH_2/CH groups at 2941/2910 cm^{-1} and from C=O at 1736 cm^{-1} (characteristic of the carbonyl group of polyvinyl acetate), together with deformation bands of CH_2/CH at 1437/1375 cm^{-1}, and CO stretching vibrations at 1096 cm^{-1} and 1261 cm^{-1} [128]. Characteristic absorption bands of PEO include the band at 2893 cm^{-1} due to symmetric and antisymmetric CH stretching, bands at 1468 cm^{-1} (asymmetric CH_2 bending) and 846 cm^{-1} (CH_2 rocking). The band in PEO at 1104 cm^{-1} indicate asymmetric COC stretching [129]. Mannitol showed the characteristic peaks of the OH group at 3289 cm^{-1} and the CH stretching at 2936 cm^{-1}. Multiple characteristic absorption bands of δ-mannitol can be observed in the 500-1500 cm^{-1} region, which can also be seen in the spectrum of the electrospun sample, indicating the presence of the crystalline δ polymorph in the fibers [122]. The characteristic bands of β-galactosidase,

PVA, and PEO either disappeared or appeared shifted in the spectrum of the HSES fibers indicating molecular interaction (presumably hydrogen bonding) between the components.

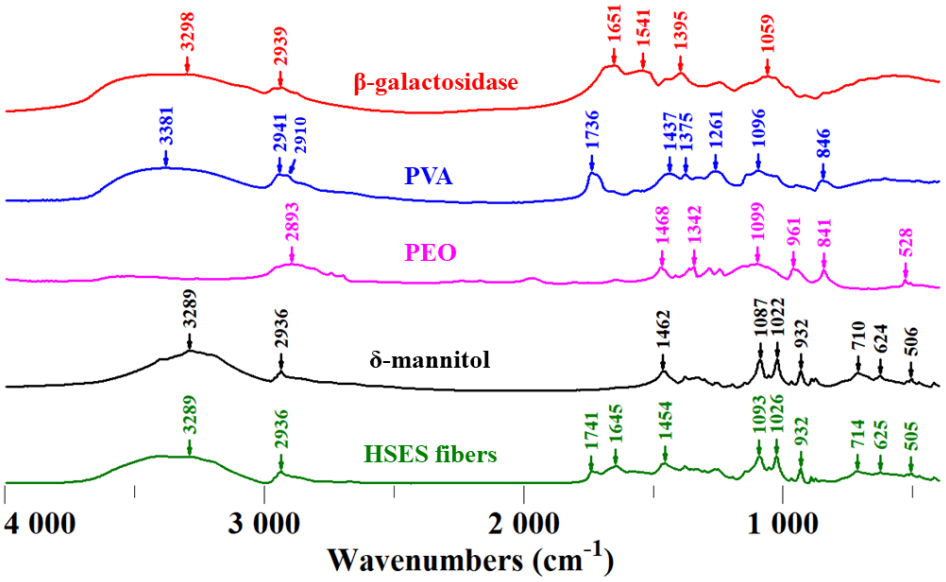

Figure 17 FTIR spectra of β-galactosidase, PVA, PEO, δ-mannitol, and the ground electrospun PVA+PEO+mannitol+β-galactosidase

The local distribution of the components in the ground fibers was analyzed by Raman mapping. For accurate dosing, homogeneity of the enzyme in the formulation is required. According to the Raman chemical map (Figure 18A), β-galactosidase seems to be uniformly distributed in the ground fibers as very small differences in color are seen.

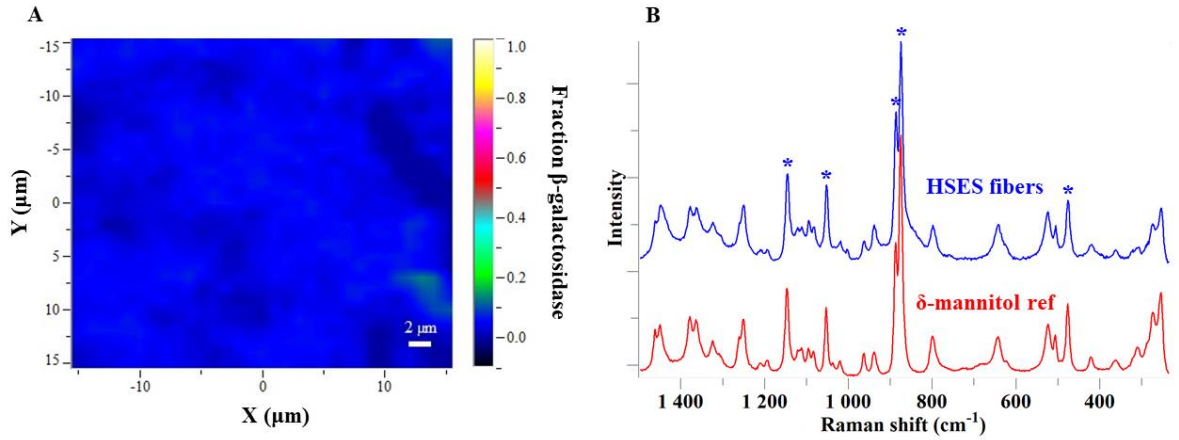

*Figure 18 A) Homogeneity study of β-galactosidase in the electrospun fibers by Raman mapping B) Raman spectra of the ground electrospun fibers and δ-mannitol (characteristic peaks marked with *)*

The Raman mapping results also confirmed that the electrospun fibers mainly contained δ-mannitol. The characteristic peaks of the δ polymorph are shown in Figure 18B and these are in good agreement with data reported by others in the literature [130,131]. The ground

electrospun fibers were reanalyzed by DSC, XRPD and Raman after 1 year of storage at 4 °C. Even though the δ-polymorph is the least stable among the mannitol polymorphs, no recrystallization was observed in the fibers after this extended storage.

It has been previously shown that sugars and sugar alcohols can interact with water vapor and they have different water sorption capacities based on their physical state [132,133]. Amorphous sugars tend to absorb large amounts of water into their bulk structure, whereas crystalline sugars interact with water-based on surface adsorption only. Water can act as a plasticizer in electrospun fibers and consequently, the water content of the electrospun materials influences their grindability significantly. It has been shown that a water content below 8% ensures acceptable grindability of sugar-containing fibers [102]. It was furthermore shown that the physical state of excipients could impact the grindability with crystalline mannitol eliminating the need for post drying. The water content of the β-galactosidase-containing fibrous sample measured by the loss on drying (LOD) method was 6.0%. Presumably, this relatively low water content is due to the crystalline nature of mannitol in the fibers.

4.1.4 Tableting and long-term stability study of the tablets

Table 5 Composition of the produced tablets

Ingredients	Amount (mg)/tablet	Amount (%)/tablet
MCC 200	150	30
Mannitol	150	30
Crospovidone	50	10
Fibrous powder	150	30
∑	500	100

As the marketable final form of a lactase enzyme is preferably tablet, the purpose of this study was not only to investigate the processability of enzyme-containing electrospun fibers but also to produce tablets without losing the achieved advantages (i.e. activity preserved after processing). The fibrous powder was mixed with MCC, mannitol, and crospovidone, and the powder mixture was subsequently tableted. The main compression force was ~8 kN in this experiment. The composition of the produced tablets can be found in Table 5.

Enzyme activity was measured after HSES, grinding, and tableting to assess the effect of the processing steps on β-galactosidase. The activity of a stable enzyme formulation was

measured parallel to each sample to serve as a reference. The results are depicted in Figure 19. No significant difference can be seen between the activity of the reference enzyme and the electrospun and processed β-galactosidase, which suggests that the drying conditions with HSES are so gentle temperature wise that no degradation of this protein-type drug is seen.

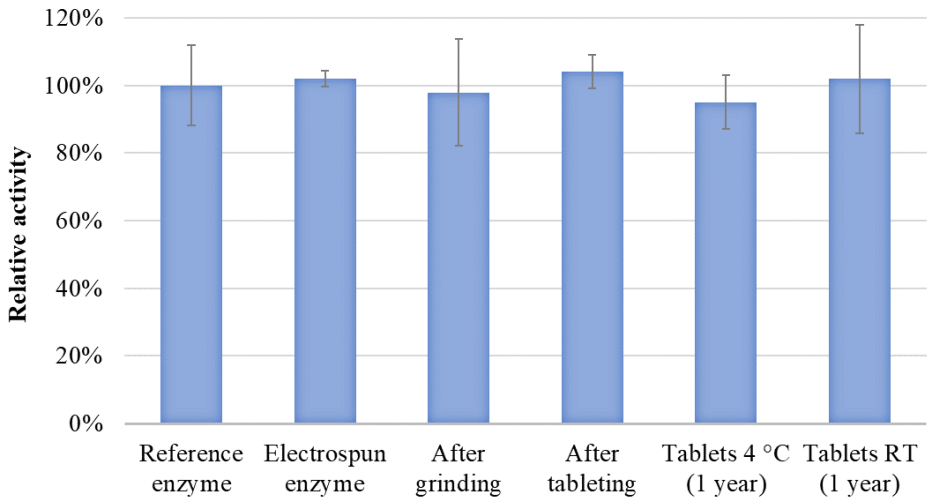

Figure 19 Enzyme activity of β-galactosidase in the fibers after HSES, after grinding, after tableting and one-year stability result of the tablets (stored at 4 °C and room temperature)

Ensuring long-term stability of biopharmaceutical products is one of the main challenges in their pharmaceutical use and therefore new formulations need to stabilize biopharmaceuticals to maintain their activity during storage. The storage stability of the electrospun and tableted β-galactosidase was compared with a reference enzyme formulation. The tablets of electrospun β-galactosidase were kept at 4 °C and room temperature and their activity were measured after 1 month, 3 months, 6 months and 1 year. The periodic activity measurements showed that the enzyme remained stable in the tablets both at 4 °C and 25 °C even after one year of storage (Figure 19). This result shows that the processable matrix containing PVA, PEO, and mannitol is suitable for stabilizing β-galactosidase in the long term as well.

4.1.5 Conclusion regarding fibers containing a protein-type drug

The present work demonstrated that HSES is a feasible technology to produce biopharmaceutical-containing, grindable fibers. A PVA-PEO-mannitol matrix was used to incorporate a model protein-type drug, β-galactosidase. A feeding rate of 30 mL/h was achieved in the experiments, which is 30x higher than what is achievable for aqueous systems using single-needle ES. The produced fibrous mat was easily removable from the collector and it was found to be grindable without the need for a post-drying step, which simplifies downstream processing. All excipients were in amorphous state in the fibers, except

mannitol. The low water content and the crystalline mannitol in the fibrous sample could be the reason for the adequate grindability. The ground fibrous powder was mixed with tableting excipients and was successfully tableted. No decrease in enzyme activity was observed after either of the processing steps (electrospinning, grinding, and tableting). Besides, β-galactosidase remained stable in the tablets after 1 year of storage both at 4 °C and room temperature. In conclusion, the gentle drying by HSES and the processability of the applied matrix enabled the production of a final dosage form for the easy oral administration of this model protein without decreasing its activity.

4.2 Scaled-up production of directly compressible electrospun fibers containing a polymer-free matrix and a protein-type drug from an aqueous solution

In the previous chapter, it was demonstrated that grindable fibers can be produced from aqueous polymeric solutions of a model protein drug. As a continuation, our aim in this work was to evaluate if high-speed electrospinning can be used to produce protein-containing fibers from an aqueous cyclodextrin solution and to process the produced fibers into tablets through direct compression. To the best of our knowledge, this is the first attempt to develop an electrospun formulation of a protein-type drug using a polymer-free matrix. The model protein was β-galactosidase in this part of the work as well.

4.2.1 Optimization of fiber formation of HP-β-CD using high-speed electrospinning

Cyclodextrins form substantial aggregates in their concentrated solutions and the intermolecular interactions make it possible to electrospin cyclodextrin solutions into fibers [134]. First, HP-β-CD solution without β-galactosidase was attempted to be electrospun with the scaled-up technology. Previous studies by Celebioglu and Uyar [110] showed that aqueous HP-β-CD solutions start to form bead-free fibers from 61.5 w/w% when using single-needle electrospinning (SNES). According to our previous experiences with HSES, the concentration of the fiber-forming agent occasionally needs to be increased slightly when transferring a system from SNES to HSES. Presumably, the reason behind this phenomenon is that in SNES there is a free liquid surface (the droplet at the end of the spinneret) and due to this some amount of solvent evaporation takes place. Therefore, jet formation starts from a slightly concentrated solution. As there is no free liquid surface present in HSES, the solvent evaporation cannot take place and this way the original solution needs to have a slightly higher concentration compared to SNES for jet formation to start. Therefore, electrospinning of 61.5, 64.3 and 67.4 w/w% HP-β-CD solutions were attempted with HSES. Morphology of the prepared samples was investigated by SEM (Figure 20). As expected, electrospinning of 61.5 w/w% solution resulted mostly in particle formation instead of fibers (Figure 20A). When the HP-β-CD concentration was increased to 64.3 w/w%, mixed particle and fiber formation was noticed (Figure 20B), and bead-free fibers were only formed at 67.4 w/w% concentration solution (Figure 20C).

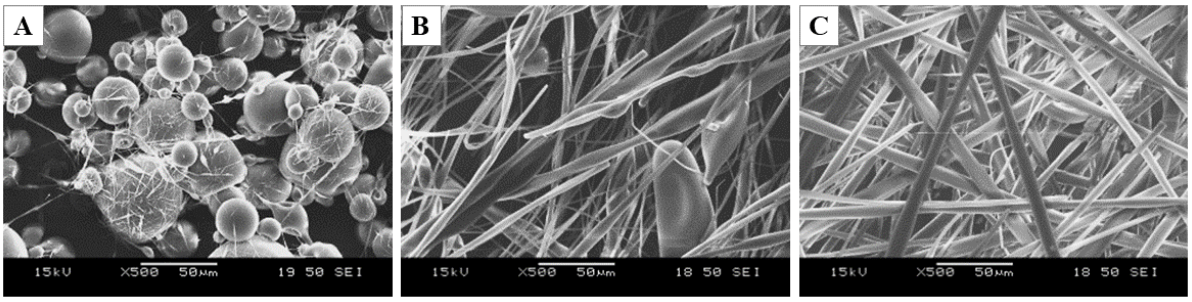

Figure 20 Scanning electron microscopic images of 61.5 (A), 64.3 (B), and 67.4 (C) w/w% concentration HP-β-CD fibers

4.2.2 High-speed electrospinning of drug-loaded cyclodextrin fibers

Dissolving β-galactosidase along with HP-β-CD might increase solution viscosity, thus might also play a role in the fiber formation and slightly shift the boundaries of the feasible concentration range. Therefore, aqueous HP-β-CD solution with β-galactosidase was prepared by substituting HP-β-CD with β-galactosidase so their total concentration in the solution would be 66.7 w/w% (Table 6). This way, drug loading of the electrospun fibers was 20 w/w%.

Table 6 Details of the production of HP-β-CD + β-galactosidase containing fibrous material by HSES

Dissolved HP-β-CD + β-galactosidase in 50 mL water (g)	**Feeding rate (mL/h)**	**Solution density (g/cm^3)**	**Yield (w/w%)**	**Productivity for dried material (g/h)**	**Water content of dried material (wt. %)**
80 + 20 (66.7 w/w% total solids content)	400	1.3	78 ± 6	270	6.8 ± 1.2

Figure 21 shows the fibrous nature of the produced β-galactosidase – HP-β-CD electrospun sample with fiber diameters in the range of approximately 2-10 μm. Some fibers are fragmented in the picture, which could be caused by the circular motion of the solid material in the collector bin of the cyclone.

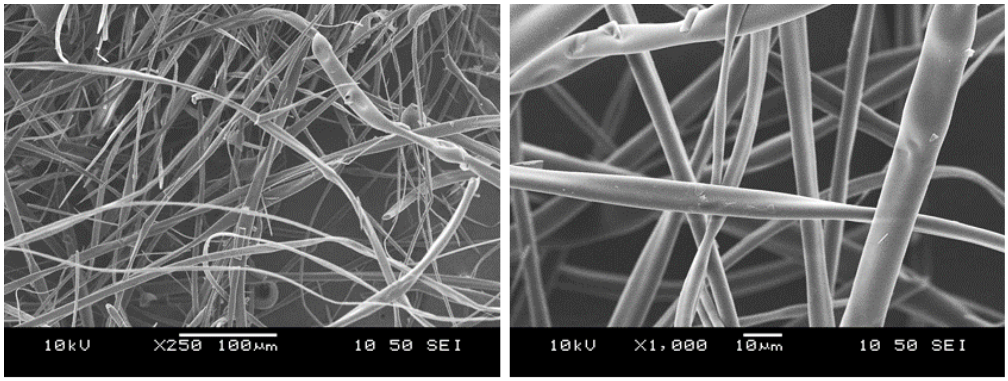

Figure 21 Scanning electron microscope images of β-galactosidase containing HP-β-CD-based fibers after HSES (250x and 1000x magnifications)

The feeding rate applied during the experiments was 400 mL/h. The details of these experiments are summarized in Table 6. An average yield of 78% was achieved with the current settings and machine setup (material loss was noticed on the walls of the drying chamber), which means that the average productivity rate was ~270 g/h. Further process and equipment optimizations would probably result in increased yields. Subsequently, a hypothetical productivity of ~6 kg/day is achievable with the current HSES setup. To determine the residual water content in the electrospun fibers, thermogravimetric measurements were performed (Figure 22). The weight loss of the fibers and the reference HP-β-CD powder was around 6.8 wt.% and 6.5 wt.%, respectively.

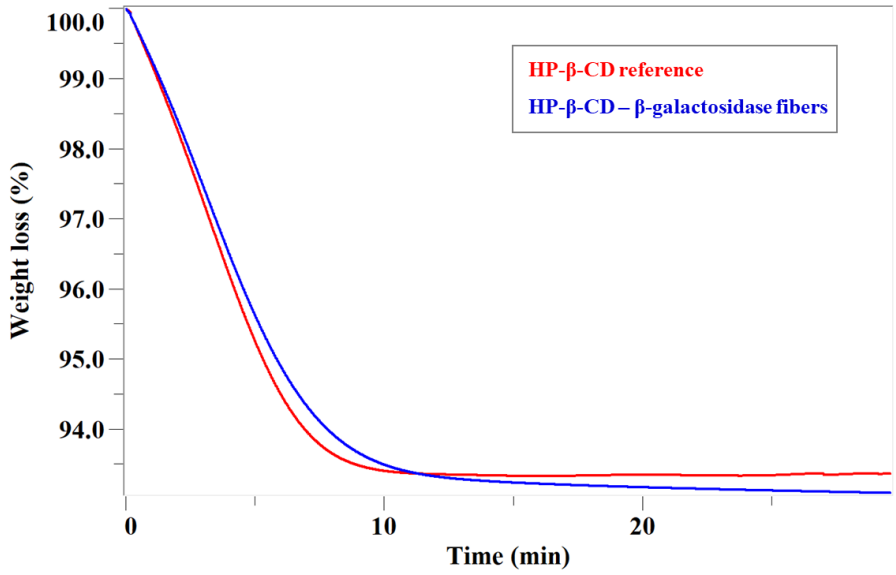

Figure 22 TGA curve of the reference HP-β-CD material and the electrospun HP-β-CD – protein fibers

4.2.3 Milling of the enzyme-containing fibers

Processability of the produced drug-loaded fibers (e.g. milling, powder properties, etc.) is critical in the development of solid pharmaceutical products. Although fragmentation of the

fibers occurred during collection, the flowability of the produced enzyme-loaded fibers was not suitable for conventional tablet production by direct compression. Therefore, the collected fibrous sample needed to be milled to a powder before further processing. Milling of the fibrous mat containing β-galactosidase was carried out right after electrospinning by a hammer mill. The friability of the enzyme-containing fibers was excellent without secondary drying as the milling of the fibrous sample resulted in a powder. The SEM images revealed that the fibers were broken into many smaller fragments, but the fibrous structure remained intact (Figure 23).

Figure 23 Photo and a scanning electron microscope image of β-galactosidase containing HP-β-CD-based fibers after milling

4.2.4 Mixing with excipients and powder characterization

The ground fibrous powder exhibited the properties of a low-density powder with 'poor' flow properties (Hausner ratio: 1.40; Carr index: 28.8%). Therefore, the addition of flowability aiding excipients was necessary. The composition of the prepared blend can be found in Table 8. The powder mixture consisting of the β-galactosidase containing HP-β-CD fibers and the tableting excipients exhibited improved flowability properties (Table 7). The bulk density of this mixture was appropriate for tableting by direct compression.

Table 7 Properties of the prepared powder mixture consisting of the β-galactosidase containing HP-β- fibers and the tableting excipients

Bulk density	0.513 g/mL
Tapped density	0.688 g/mL
Hausner ratio	1.34
Carr index	25.4%

4.2.5 Tableting of the enzyme-containing fibrous powder

Several hundred tablets were prepared by direct compression from the blend discussed in the previous section (Table 8, Figure 24). The applied compression force was around 12 kN (± 1.1 kN). The properties of the prepared tablets can be found in Table 9.

Table 8 Composition of the produced tablets

Ingredients	Amount (mg)/tablet	Amount (%)/tablet
MCC	189	31.5
Mannitol	189	31.5
Croscarmellose sodium	60	10.0
Aerosil	6	1.0
Magnesium stearate	6	1.0
Fibrous powder	150	25.0
∑	600	100.0

Figure 24 Tablets prepared from ground fibrous enzyme-containing powder, MCC, mannitol, croscarmellose sodium, and magnesium stearate

To assess the effect of electrospinning and the processing of the electrospun material on β-galactosidase, enzyme activity was measured after HSES, grinding, and tableting. The activity of a stable enzyme formulation was measured parallel to each sample to serve as a reference. The results of these measurements are shown in Figure 25. No significant difference can be seen between the activity of the reference enzyme and the electrospun and processed β-galactosidase, which suggests that the chosen cyclodextrin is a suitable matrix for the formulation of this protein-type drug. In conclusion, the gentle drying by HSES and the processability of the applied matrix enabled the production of a final dosage form for the easy oral administration of this model protein without decreasing its activity.

Table 9 Properties of the prepared tablets

Compression force	12.0 ± 1.1 kN
Individual Weight	600.3 ± 2.8 mg
Tablet breaking force	65.0 ± 6.4 N
Friability	0.56 %
Thickness	4.100 ± 0.023 mm

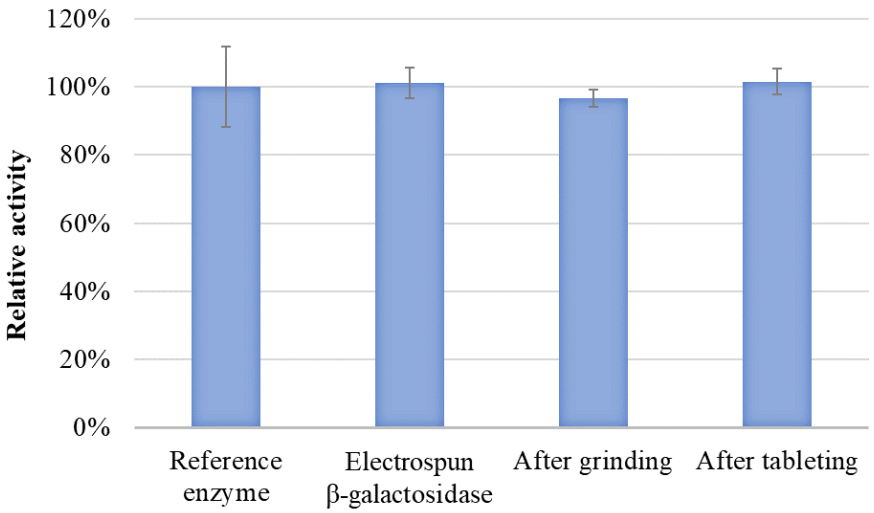

Figure 25 Enzyme activity of β-galactosidase in the HP-β-CD fibers after HSES, after grinding, and after tableting

4.2.6 Enzyme stability in the tablets

Ensuring long-term stability of biopharmaceutical products is one of the main challenges in their pharmaceutical use and therefore new formulations need to stabilize biopharmaceuticals to maintain their activity during storage. The storage stability of the electrospun and tableted β-galactosidase was compared with a reference enzyme formulation. The tablets of electrospun β-galactosidase were kept at 4 °C and room temperature and their activity was measured after 1 month, 3 months and 6 months (Figure 26).

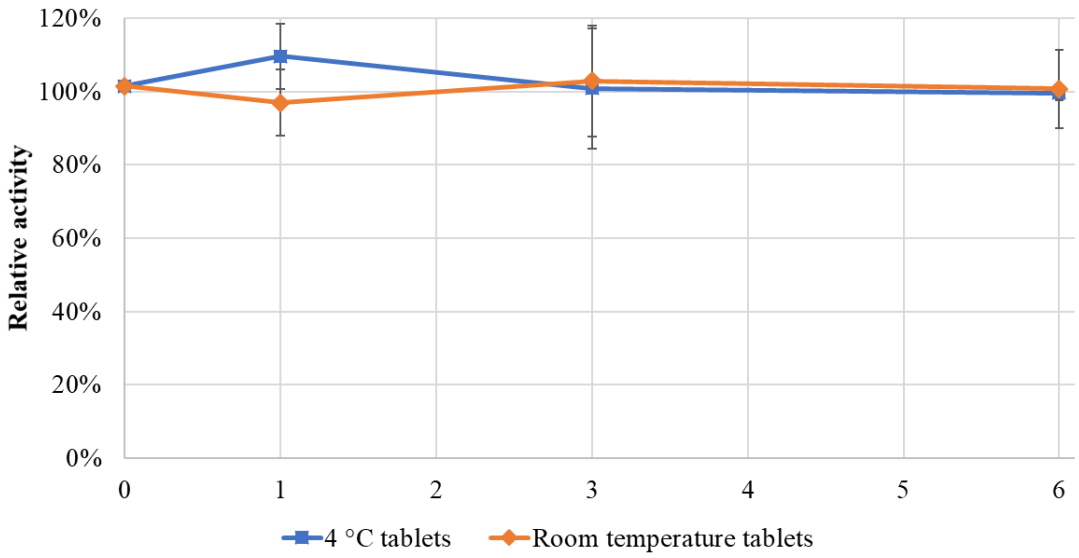

Figure 26 Long-term stability results of the tablets produced from β-galactosidase-containing fibers (stored at 4°C and room temperature)

The periodic activity measurements showed that the enzyme remained stable in the prepared tablets both at 4 °C and room temperature after 6 months of storage. This result shows that the processable HP-β-CD-based matrix is suitable for stabilizing β-galactosidase in the long term as well.

4.2.7 Conclusion regarding drug-loaded cyclodextrin fibers

In the present work HSES was proven to be a feasible technology to gently and continuously produce stable protein-containing, processable fibers. A water-soluble cyclodextrin, HP-β-CD was used to incorporate a model protein-type drug, β-galactosidase. The feeding rate of 400 mL/h used gives ~270 g solid product per hour. Therefore, a ~6 kg/day production rate is hypothetically possible with the HSES technology. This scalable, continuous and flexible manufacturing process appears to be capable of fulfilling the requirements of the pharmaceutical industry. The enzyme-containing cyclodextrin fibers were found to be grindable without the need for a secondary drying step. The ground fibrous powder was mixed with tableting excipients and was successfully tableted using direct compression. No decrease in enzyme activity was observed after either of the processing steps (electrospinning, grinding, and tableting). Besides, β-galactosidase remained stable in the tablets after 6 months of storage both at 4 °C and room temperature. Even though in this work the final dosage form of the protein drug was the tablet, CDs are injectable and therefore electrospun formulations of CDs with other sensitive proteins (e.g. monoclonal antibodies) have the potential to be used in reconstitution dosage forms as well.

4.3 Production of cyclodextrin-based reconstitution powder from an aqueous solution using scaled-up electrospinning

The previous chapters demonstrated that aqueous high-speed electrospinning can be used to prepare processable biopharmaceutical-loaded 2-hydroxypropyl-β-cyclodextrin fibers, which can be converted into tablets by direct compression.

In this part of the work, scaled-up electrospinning of another cyclodextrin, sulfobutylether-β-cyclodextrin sodium (SBE-β-CD) was attempted with an aim to prepare a parenteral drug dosage form. The model active pharmaceutical ingredient was voriconazole (VOR), an antifungal drug from the azole family, which is used for the treatment of severe fungal infections (e.g. invasive aspergillosis) occurring in immunocompromised patients [135]. VOR has low aqueous solubility (0.2 mg/mL at pH 3 and 0.6 mg/mL at pH 7), which classifies it to the class II of the Biopharmaceutics Classification System (BCS) [136]. In the marketed, freeze-dried powder for reconstitution of VOR (Vfend®), molecular encapsulation with sulfobutylether-β-cyclodextrin sodium (SBE-β-CD) is applied to increase the VOR solubility in water [136,137]. The freeze drying of VOR with SBE-β-CD results in the amorphization of the drug [138]. A single dose of the marketed product contains 200 mg VOR and 3200 mg SBE-β-CD, and it is intended for reconstitution with 19 mL water to produce a solution containing 10 mg/mL of VOR [118].

4.3.1 Optimization of fiber formation by drop electrospinning

Challenges in process development were anticipated because SBE-β-CD is not an obvious fiber-forming material due to its small molecular mass (2163 Da) and the possible ionic repulsions among its molecules. To determine the suitable SBE-β-CD concentration for fiber formation, a small-scale screening process was carried out using DES. The amount of dissolved SBE-β-CD in the aqueous solution was gradually increased from ~33 w/w% to ~75 w/w% since the concentration of the fiber-forming agent is considered to be one of the most critical parameters for ES due to the impact on viscosity and fiber formation [139,140]. Morphology of the prepared samples was investigated by visual inspection and SEM (Figure 27). Below 67 w/w% concentration, no fiber formation was observed, only particles of the SBE-β-CD solution were collected (presumably, the entanglement of CD molecules is not adequate for forming fibers). Starting from 67 w/w%, particle and fiber formation was noticed, although bead-free fibers were only formed at 71 and 75 w/w% concentration solutions. The presence of beads in the fibrous material is detrimental to the specific surface area and the dissolution rate. Therefore, it is important to select a solution concentration from

which bead-free fibers can be produced. As the results show, a wide enough concentration region where stable and robust fiber formation was possible could be identified, and thus, SBE-β-CD acted as a 'quasi-polymer' at high concentrations. Keeping in mind that VOR might also play a role in the fiber formation and may slightly shift the boundaries of the feasible concentration range, 68.8 w/w% aqueous SBE-β-CD solution was chosen for the experiments with VOR.

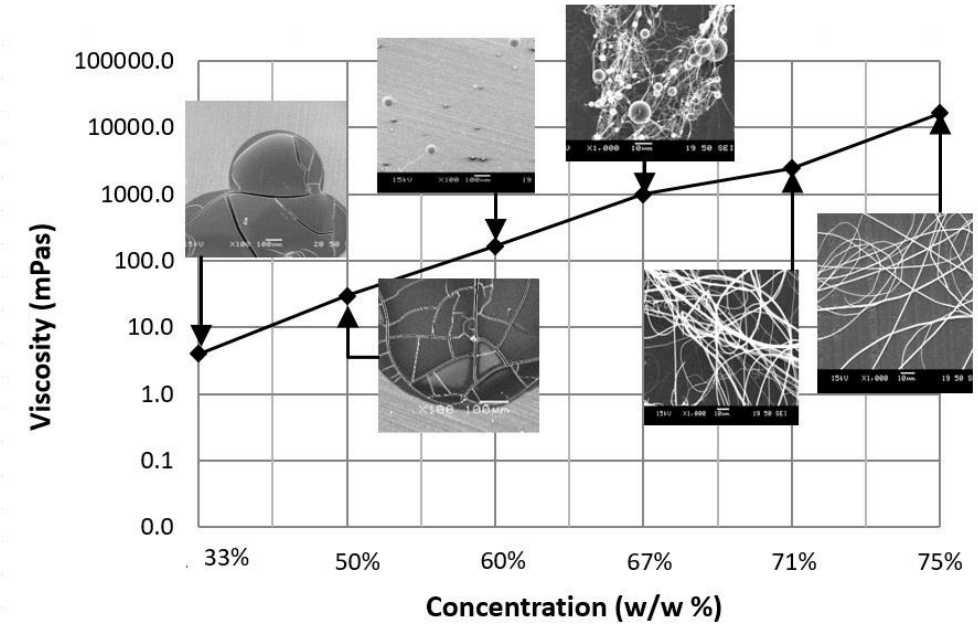

Figure 27 Optimization of fiber formation

4.3.2 High-speed electrospinning for forming cyclodextrin-based reconstitution powder

Laboratory scaled electrospinning (single needle electrospinning) is incapable of mass production of fibrous material, and therefore, its throughput is far from the needs of commercial pharmaceutical manufacturing. In our experiments, HSES was applied to increase the productivity of the technology.

HSES experiments were carried out using aqueous SBE-β-CD and VOR–SBE-β-CD solutions. When electrospinning from SBE-β-CD without VOR (but keeping the dissolved SBE-β-CD amount the same) particles were formed beside fibers (Figure 28 a). Figure 28 b shows the fibrous nature of the produced VOR–SBE-β-CD electrospun material with fiber diameters in the range of approx. 0.5-2 μm. Among the fibers, fewer particles were observable compared to the placebo SBE-β-CD sample. This might suggest that VOR enhances the association (i.e. the entanglement) among the SBE-β-CD molecules and aids the fiber formation. Fragmentation of the fibers is also noticeable, which could be caused by the centrifugal force inside the cyclone resulting in a circular motion of the solid material in the

collector bin. It is important to note that all experiments were conducted at room temperature, which makes electrospinning a platform technology that can be employed in the case of biopharmaceuticals as well.

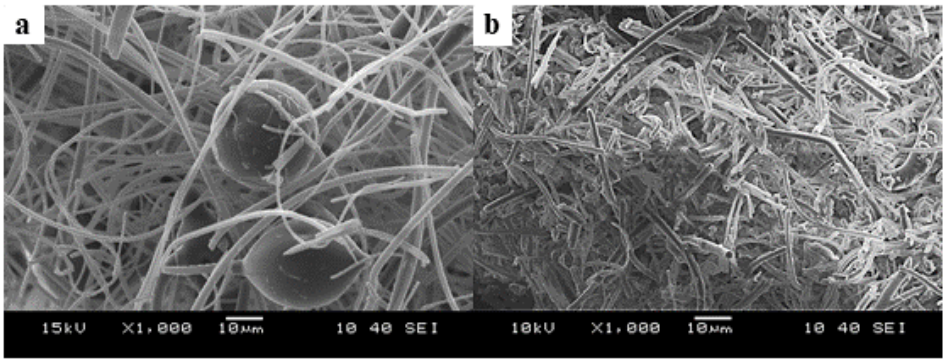

Figure 28 Scanning electron microscopic images of a) placebo SBE-β-CD fibers; b) VOR–SBE-β-CD complex based fibers

The highest feeding rate applied during the experiments was 300 mL/h. Details of this experiment are summarized in Table 6. The total solids concentration in the aqueous solution was 70 w/w% with a mass ratio of 1:16 for VOR:S BE-β-CD. A yield of 88% was achieved with the current settings (material loss was noticed on the walls of the drying chamber), which means that the productivity rate was ~240 g/h. With further process and equipment optimizations (e.g. with additional air knives in the chamber), and during extended productions, it is estimated that the yield of the process could be further increased. Consequently, theoretically, a productivity of ~5 kg/day is achievable with the current HSES setup. This equals an output rate of more than 1600 doses/day, which can be further increased by increasing the drying temperature and scaling the spinneret up similarly to rotary atomizers in spray drying [35]. This productivity rate is more than 12x higher than the highest aqueous electrospinning production rate reported so far for pharmaceutical applications [66]. According to Harrington *et al.*, 2990 people were hospitalized with a primary diagnosis of invasive aspergillosis in 2013 in the USA. If these patients are treated with intravenous Vfend® for 20 days with an average of 3 doses per day, 179400 doses are required. With our HSES setup (which can still be increased), this amount can be manufactured in less than 4 months. Besides this, obviously, downscaling is also possible in order to produce for smaller markets. Therefore, this scaled-up, continuous and flexible manufacturing process seems to be capable of fulfilling the capacity requirements of the pharmaceutical industry.

Table 10 Details of the production of SBE-β-CD+VOR containing fibrous material by HSES

Dissolved SBE-β-CD + VOR in 100 ml water (g)	Feeding rate (mL/h)	Solution density (g/cm^3)	Yield	Productivity for dried material (g/h)	Productivity for dried VOR (doses/day)	Water content of dried material
220 + 13.75 (70 w/w% total solids content)	300	1.29	88%	240	1600	6.9%

4.3.3 Results of differential scanning calorimetry (DSC) and X-ray powder diffraction (XRPD) measurements

To investigate the physical state of VOR in the fibrous sample and in Vfend®, DSC and XRPD examinations were carried out. The pure crystalline VOR served as the reference. The DSC thermograms (Figure 29) of Vfend® and the VOR-SBE-β-CD fibrous material did not show the endothermic melting peak of crystalline VOR around 130 °C, which suggests that VOR is amorphous in both solid formulations. The wide endothermic activity that can be detected in the thermogram of the electrospun sample is related to the water loss of the matrix (in a second heating cycle, this peak does not appear, data not shown). The reversing heat flow did not contain any noticeable glass transition or melting peak (data not shown). No glass transition temperature of the fibrous material (and Vfend®) could be detected by further DSC investigations. This has also been observed previously by other researchers, as Zhang *et al.* could not detect any glass transition temperature of a lyophilized complex of VOR and SBE-β-CD [138]. Possibly, SBE-β-CD and VOR molecules form strong structures that do not show α-relaxation upon heating, while the material decomposes from 245 °C based on our experiment. Glass transition temperatures of actual polymeric derivatives of β-CDs cannot be determined either by conventional methods as they are above the degradation point [141]. The lack of peaks on the XRPD diffractograms (Figure 30) of Vfend® and the electrospun sample also confirmed the amorphous state of VOR in the two formulations.

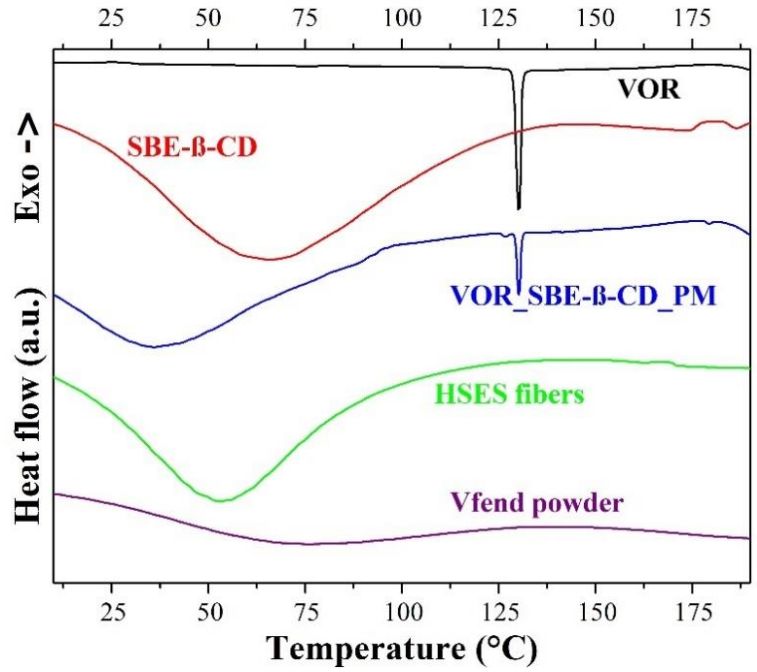

Figure 29 Differential scanning calorimetry (DSC) thermograms of crystalline VOR, SBE-β-CD, the physical mixture (PM) of VOR and SBE-β-CD, the electrospun VOR–SBE-β-CD complex, and the Vfend® powder

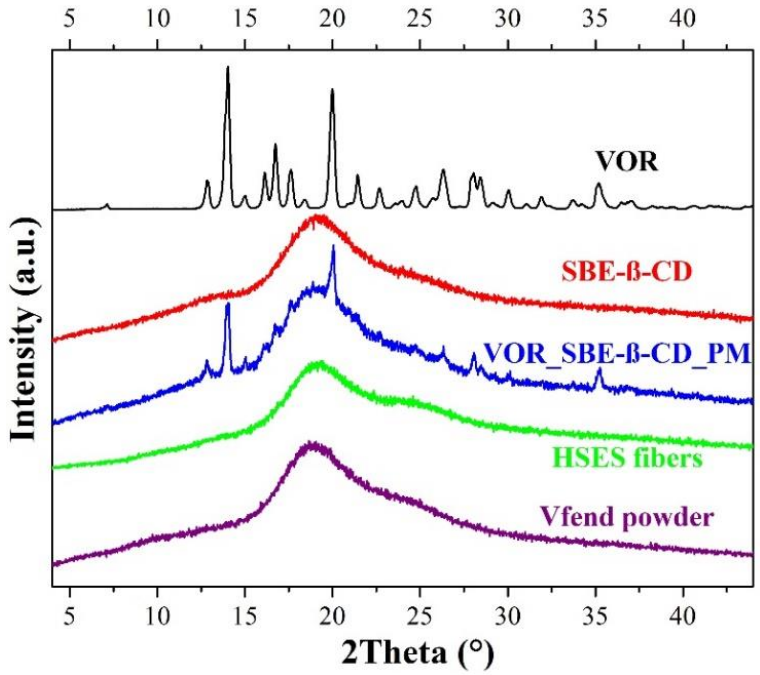

Figure 30 X-ray powder diffraction (XRPD) patterns of crystalline VOR, SBE-β-CD, the physical mixture (PM) of VOR and SBE-β-CD, the electrospun VOR–SBE-β-CD complex, and the Vfend® powder

4.3.4 Results of the Raman mapping and EDS of the voriconazole-containing powders

DSC and XRPD only tell us about the state of the VOR but do not provide exact information about the local concentration of the incorporated drug. Distribution of the amorphous VOR in the fibrous samples was evaluated by EDS and Raman mapping. For accurate dosing, homogeneity of the VOR in a drug formulation is required. The fibrous material produced by HSES was compared to Vfend® and to the physical mixture of SBE-β-CD and VOR (Figure 31).

As expected, the Raman chemical map (Figure 31 b) of the reference physical mixture shows definite areas with high VOR concentrations indicating the uneven distribution of VOR in the mixture on a microscopic level. In contrast, VOR seems to be uniformly distributed in the HSES fibers, as well as in the Vfend® powder according to the maps (Figure 31 d and f, respectively). However, the modeling error of the CLS evaluation was increased due to the fact that the analysis was performed using the reference spectrum of crystalline VOR, (and not the amorphous). Therefore, the chemical mapping was performed with EDS as well. Figure 31 a, c, and e show colored elemental maps of the physical mixture, the electrospun material, and the Vfend® powder, respectively. Fluorine and sulfur can be used to differentiate VOR and SBE-β-CD from each other (VOR contains fluorine but not sulfur and SBE-β-CD contains sulfur but not fluorine). The coloring of the EDS maps was performed by following the fluorine (red) and the sulfur (green) signals. It can be seen that the physical mixture contains separate SBE-β-CD and VOR particles whereas the electrospun sample and the Vfend® powder contain SBE-β-CD and VOR evenly distributed. Heterogeneity of VOR cannot be seen either in the fibrous sample or in the Vfend® powder. These examinations imply that the VOR is molecularly dispersed both in the electrospun fibers and the Vfend® powder as well.

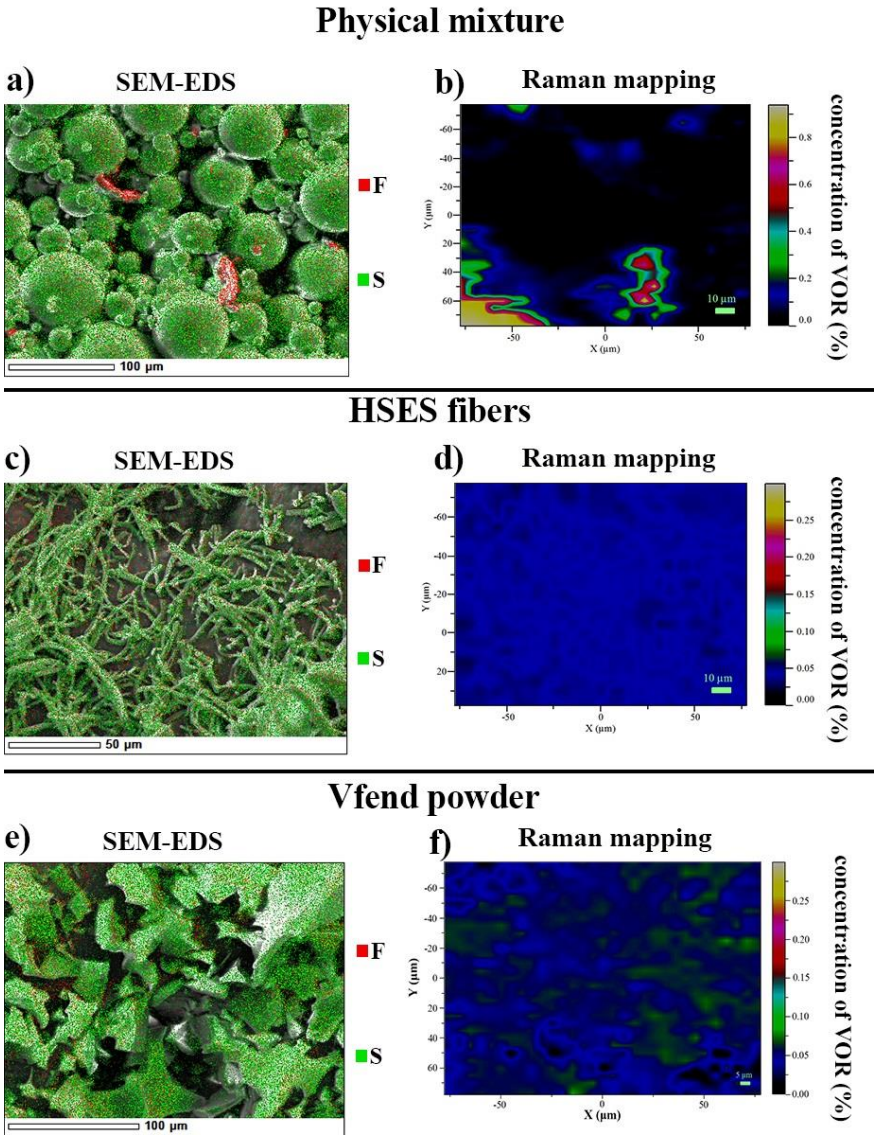

Figure 31 Homogeneity study of the physical mixture of VOR and SBE-β-CD, the electrospun VOR–SBE-β-CD complex, and the Vfend® powder by SEM-EDS (a, c, e, respectively) and Raman mapping (b, d, f, respectively).

4.3.5 Reconstitution test on the voriconazole-containing powders

Following the procedure described on the Vfend® package, the dissolution properties of the prepared electrospun complex were evaluated by adding 19 mL of water to a vial containing 3400 mg of electrospun material (comprising of 3200 mg SBE-β-CD and 200 mg voriconazole). The resulting concentration in the final solution was 10 mg/mL for VOR [118]. Vfend® and the physical mixture of SBE-β-CD and VOR were tested the same way as well to ensure a fair comparison of the different formulations.

The electrospun material could be ground easily by a hammer mill, which increased the previously low bulk density. As it is visible on the recorded images (the vials used in the experiment had the same dimensions), the milled fibers take up significantly less volume than

the freeze-dried cake (Figure 32). After the addition of water, the vials were shaken vigorously to dissolve parts stuck on the wall. The fibrous sample and Vfend® dissolved completely within 30 s (Figure 32 and Table 11). SBE-β-CD in the physical mixture dissolved nearly instantly due to the good solubility of the cyclodextrin but the crystalline drug (marked with arrows in Figure 32) persisted for a longer time. The difference between the dissolution rates of the electrospun sample and the physical mixture was confirmed by UV measurements after 30 s and 2 minutes of dissolution (Table 11). This proves that the enhanced specific surface area of the amorphous fibrous material provides fast dissolution, which makes electrospinning a feasible technology for the preparation of reconstitution injection dosage form.

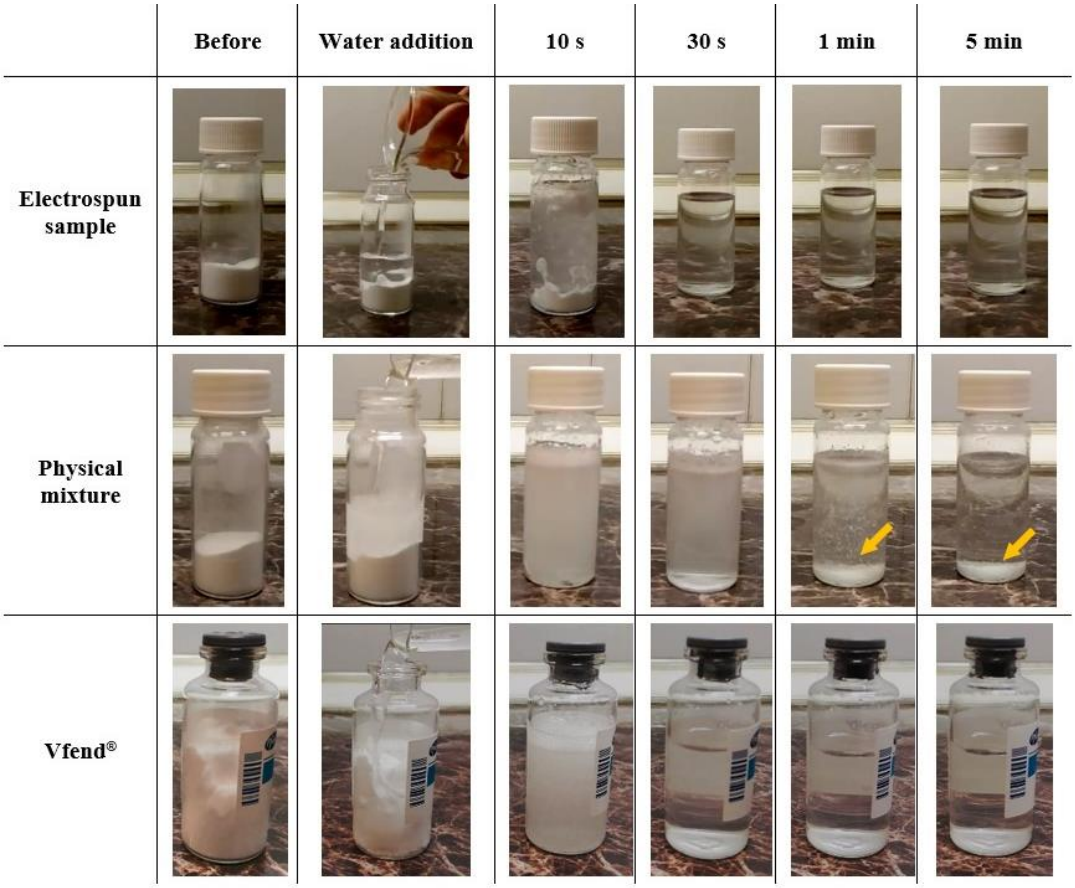

Figure 32 Images of dissolution test of electrospun VOR–SBE-β-CD complex, the physical mixture, and Vfend®

Table 11 Results of dissolution rate measurements (n=3, except for Vfend®, where only 1 sample was measured). 100% equals the VOR concentration of 10 mg/mL.

	30 s	2 min
Electrospun sample	(100.9 ± 2.2)%	(102.4 ± 4.1)%
Physical mixture	(39.1 ± 1.0)%	(53.7 ± 3.0)%
Vfend®	103%	102%

4.3.6 Conclusions regarding the cyclodextrin-based fibrous reconstitution powder

Scaled-up electrospinning was performed from aqueous solutions of VOR–SBE-β-CD complex to demonstrate the feasibility of HSES to produce a fast dissolving reconstitution injection dosage form, which allowed comparison to the marketed freeze-dried VOR formulation (Vfend®). Our experiments showed that the incorporated VOR was amorphous and homogeneously dispersed in the produced fibers. The reconstitution test of the fibers confirmed the expected fast dissolution characteristics as a clear solution was obtained within 30 seconds.

The feeding rate of 300 mL/h used gives ~240 g solid product per hour, which is more than 12x higher than the maximum reported productivity rate of ES for pharmaceutical application up to now. The fibers were collected by a cyclone, which is a novel fiber collection method. This scaled-up, continuous and flexible manufacturing process seems to be capable of fulfilling the requirements of the pharmaceutical industry. Our experiments prove that HSES has the potential to replace freeze drying since it is a continuous, high-throughput process of very low energy consumption providing an economically viable production alternative. Furthermore, HSES was performed under ambient conditions, and therefore, it can become a platform technology as biopharmaceuticals could be dried this way as well.

4.4 Large-scale production and tableting of electrospun HP-β-CD fibers incorporating anaerobic bacteria from the gut microbiome

The human gut microbiome has been shown to play a significant role in the induction, training, and function of the immune system [142]. Dysbiosis of the microbiome has been associated with various inflammatory diseases and numerous other diseases and therefore the development of microbiome-based therapeutics has surged in the recent years [143,144]. In the case of therapeutic microbes, parenteral delivery is not an option, and thus the development of solid formulations is imperative. Electrospinning has been used for the encapsulation of bacterial cells into fibers for more than 15 years [145,146]. Studies related to electrospinning of single [48] and multiple strains [147-149] of aerobic and facultative anaerobic strains can be found in the literature. However, so far there has not been any published work about electrospinning carried out with anaerobic bacteria. Therefore, in this part of the work, it was investigated if scaled-up electrospinning can be used as a gentle drying method for a strictly anaerobic bacterium from the gut microbiome.

4.4.1 High-speed electrospinning of fibers containing anaerobic bacteria

To study the effect of growth conditions of bacteria on survival after electrospinning, cells grown using two different culture conditions were used in the experiments. One of the culture conditions resulted in samples with mixed populations of spores and vegetative cells and the other culture condition yielded exclusively vegetative cells.

Cyclodextrins form strong aggregates in their concentrated solutions and the intermolecular interactions make it possible to electrospin cyclodextrin solutions into fibers [134]. Electrospinning of hydroxypropyl-β-cyclodextrin solutions containing spores and vegetative cells and purely vegetative cells was attempted using the high-speed electrospinning device and the fiber formation could be performed seamlessly. The feeding rate applied during the experiments was 300 mL/h. The details of these experiments are summarized in Table 12. The electrospinning process yields were ~84% and ~48% for the samples incorporating both spores and vegetative cells and only vegetative bacteria, respectively. Material loss was noticed on the wall of the drying chamber and in the pipes of the machine. Supposedly, in the case of longer production, the material loss would not increase significantly and therefore higher process yields (>95%) could be achieved.

Table 12 Production data of the scaled-up high-speed electrospinning of mixture of sporulated and vegetative and vegetative C. butyricum

	Mixed sample	**Vegetative sample**
Cell state composition	30% spores 70% vegetative cells	100% vegetative cells
Feeding rate (mL/h)	300	300
Solution density (g/cm^3)	1.197	1.194
Solid content of the solution (w/w%)	68.4	66.7
Yield (%)	83.8 ± 4.3	48.3 ± 9.5
Water content of the fibers (wt.%)	7.3 ± 0.6	6.3 ± 0.2

Figure 33 shows the fibrous nature of both samples with fiber diameters in the range of approximately 1-10 μm. Fiber diameter of the mixed and vegetative bacteria-containing fibers did not differ significantly. No vegetative cells or spores were visible on the outer surface of the fibers, which suggests that the bacteria were incorporated into the cyclodextrin fibers. Figure 33 shows some fragmentation of the fibers, which could be caused by the circular motion of the solid material in the collector bin of the cyclone.

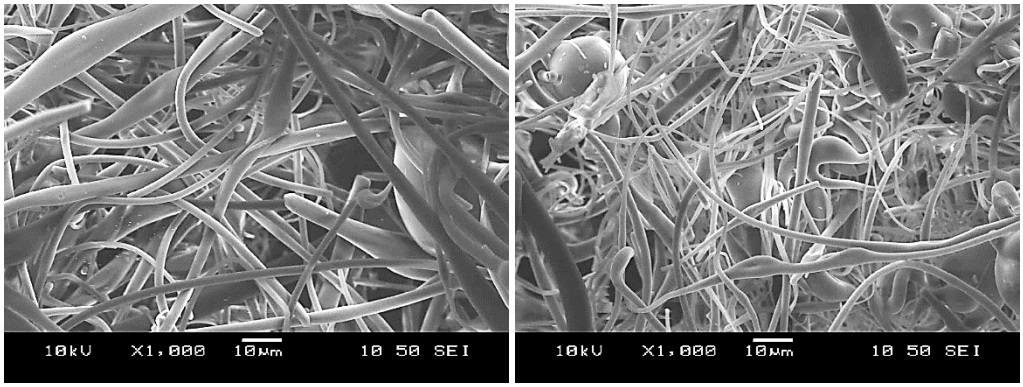

Figure 33 Scanning electron microscope images of the fibers containing both spores and vegetative cells and only vegetative cells produced by high-speed electrospinning

To determine the residual water content in the electrospun fibers, thermogravimetric measurements were performed. The weight loss of the fibers containing mixture of spores and vegetative cells and only vegetative cells was ~7.3 wt.% and ~6.3 wt.%, respectively. The weight loss of the reference HP-β-CD powder was around 6.8 wt.%, which means that rapid and continuous drying of the fibers to the equilibrium moisture content of the matrix was possible at room temperature by HSES. The productivity of the technology with the applied feeding rate was around 150 g/h, attesting that more than 3.5 kg bacteria-containing electrospun material can be produced in a day by using high-speed electrospinning.

4.4.2 Viability of bacteria in the cyclodextrin solution and in the fibers after electrospinning

CFU measurements were carried out to evaluate the effect of the cyclodextrin solution and the electrospinning process on *Clostridium butyricum*. Survival of mixed state and vegetative bacteria compared to the starting cell culture viability can be seen in Figure 34. The number of viable cells or spores were reduced by a maximum of 0.16 log unit in the cyclodextrin solution and by a maximum of 0.33 log unit in the electrospun fibers. Cells and spores are exposed to changes in the osmotic environment when introduced into the cyclodextrin solution and high voltage and ultrafast solvent evaporation during the electrospinning process, which could presumably cause the observed slightly decreased viability.

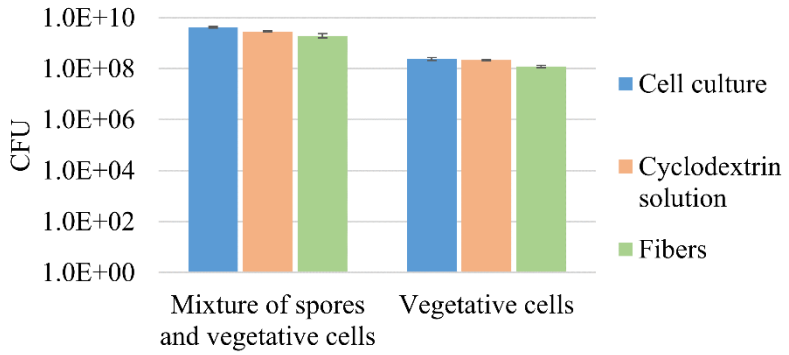

Figure 34 Survival of mixture of sporulated and vegetative and vegetative Clostridium butyricum in the cyclodextrin solution and in the electrospun fibers compared to the original cell culture viability

Butyrate, produced by *C. butyricum* has been shown to have anti-inflammatory effects and therefore it is important to investigate if the butyrate production capacity of the bacteria is retained after electrospinning. Medium was inoculated with bacteria-containing fibers and the sample was checked for the presence of butyrate after 24 hours of anaerobic incubation. The HPLC measurement showed the presence of butyrate in the samples (~ 1 µg/mL), besides the other medium components. The measurement confirmed that the ability of *C. butyricum* to produce this anti-inflammatory molecule was preserved in the fibers proving that this innovative solid form of the bacteria has a real therapeutic potential.

4.4.3 Long term stability of the bacteria in the fibers

Long term viability of bacteria in the fibers is crucial for the application in solid dosage forms. The viability of the fibrous samples containing sporulated and vegetative and vegetative *Clostridium butyricum* stored at different temperatures aerobically and anaerobically can be seen in Figure 35. Generally, it can be concluded that the samples stored anaerobically had higher viability compared to the samples stored in the presence of oxygen

at the same storage temperature. The lowest survival rates belonged to the samples stored at room temperature aerobically – the number of viable cells in the vegetative sample was reduced to 0. However, high viability of this strictly anaerobic bacterial strain could be preserved at room temperature in the presence of oxygen, as the viability loss of the sample containing both spores and vegetative cells was less than 1 log unit after 1 year. The outstanding stability at room temperature, aerobic storage (the preferred storage conditions from a practical perspective), suggests that the growth conditions used to prepare the sample containing both spores and vegetative cells were favorable for the application compared to the growth conditions used to culture exclusively vegetative cells.

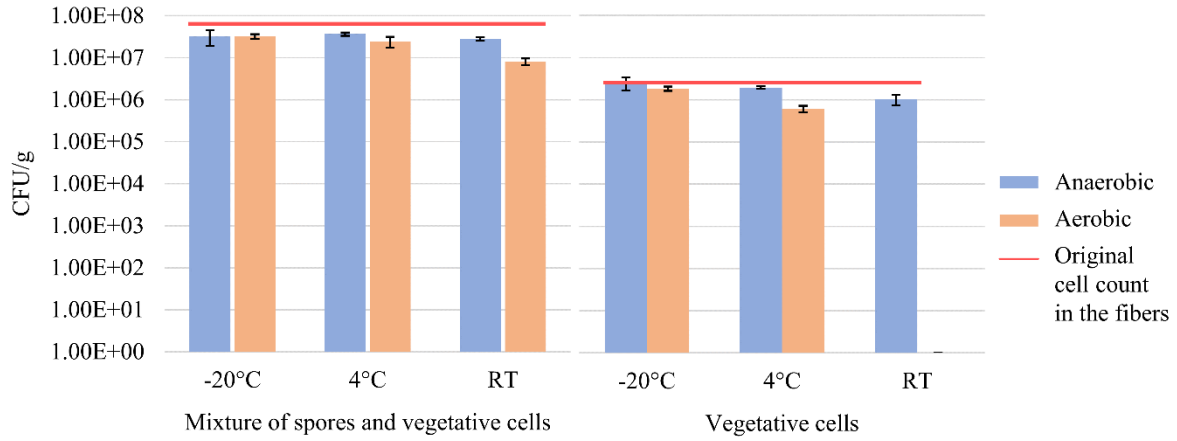

Figure 35 Stability of the mixture of sporulated and vegetative and vegetative Clostridium butyricum in the electrospun HP-β-CD fibers after 1 year of storage anaerobically and aerobically at -20 °C, 4 °C, and room temperature

The homogeneity of bacteria in the fibers was assessed after 1 year by taking 3 samples from different locations of the fibrous mass. No significant differences were found in cell count between the different samples and therefore it can be concluded that living bacteria is homogeneously distributed in the fibrous mass.

The state of bacteria in the fibers was evaluated to see if drying by electrospinning induces sporulation of *C. butyricum*. Bacteria were spore stained before electrospinning and after 3 months and 1 year of storage of the fibers. The spore stained samples were observed under the microscope. The ratio of spores and cells was approximately the same before electrospinning, after electrospinning, and after storage (at all the different storage conditions), which suggests that drying by electrospinning and being encapsulated in HP-β-CD fibers for an extended period of time do not induce sporulation of *C. butyricum*.

4.4.4 Milling of the bacteria-containing fibers

The processability of the electrospun bacteria-loaded fibers (grinding, powder properties, etc.) is crucial in the development of solid pharmaceutical products. Even though fiber fragmentation was observed after the cyclone collection, the flowability of the fragmented bacteria-loaded fibers was not suitable for conventional tableting by direct compression. Therefore, the collected fibers had to be milled to a powder for further processing. Milling of the bacteria-loaded fibrous material was performed right after electrospinning by the use of an oscillating mill. Bacteria-containing fibers exhibited excellent friability without secondary drying as the milling of the fibers resulted in a powder. The SEM image of the ground fibers shows that the fibers were broken into many smaller fragments, but the fibrous structure was preserved (Figure 36). The yield of the small-scale grinding was ~86%. The material that remained in the oscillating mill was not sticky, lumped or molten.

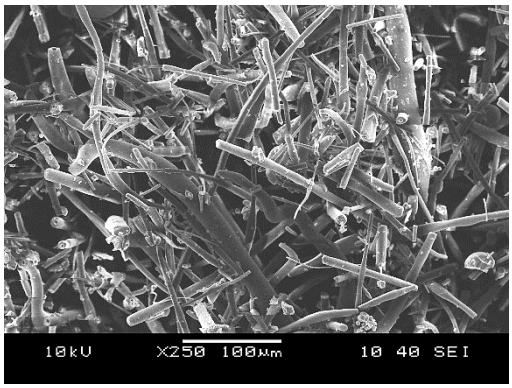

Figure 36 Scanning electron microscope image of the ground fibers containing mixture of spores and vegetative bacteria

4.4.5 Tableting of the ground bacteria-containing fibers

The ground fibers showed the properties of a low-density powder (bulk density: ~0.15 g/mL, tapped density: ~0.24 g/mL) with poor flow properties. Therefore, the addition of flowability aiding excipients was required to gain a powder appropriate for tableting. The composition of the prepared blend can be found in Table 8.

Table 13 Composition of the produced tablets

Ingredients	Amount (mg)/tablet	Amount (%)/tablet
MCC	189	31.5
Mannitol	189	31.5
Croscarmellose sodium	60	10.0
Aerosil	6	1.0
Magnesium stearate	6	1.0
Fibrous powder	150	25.0
∑	600	100.0

The powder mixture consisting of the milled bacteria-containing HP-β-CD fibers and the tableting excipients exhibited improved flowability (Table 14). The obtained powder mixture was suitable for tableting by direct compression.

Table 14 Properties of the prepared powder mixture consisting of the bacteria-containing HP-β-fibers and the tableting excipients

	Ground fibers	Ground fibers mixed with excipients
Bulk density	0.150 g/mL	0.450 g/mL
Tapped density	0.240 g/mL	0.628 g/mL
Hausner ratio	1.60	1.40
Carr index	33.3%	28.3%

Characteristics of the produced tablets were evaluated (Table 15). The tablets were found to be free from capping, chipping, and sticking.

Table 15 Properties of the prepared tablets

Compression force	0.77 ± 0.18 kN
Individual Weight	606.2 ± 12.6 mg
Tablet breaking force	89.2 ± 11.6 N
Friability	0.9 %

4.4.6 Bacteria survival after milling and tableting of the electrospun fibers

To evaluate if the processing of the electrospun fibers (milling and tableting) had an effect on the viability of *C. butyricum*, CFU measurements were carried out after milling and

tableting. Figure 37 shows that the viability of the bacteria in the fibers was preserved after the processing steps. This suggests that the chosen cyclodextrin is a suitable matrix for the formulation of this anaerobic bacteria strain by electrospinning.

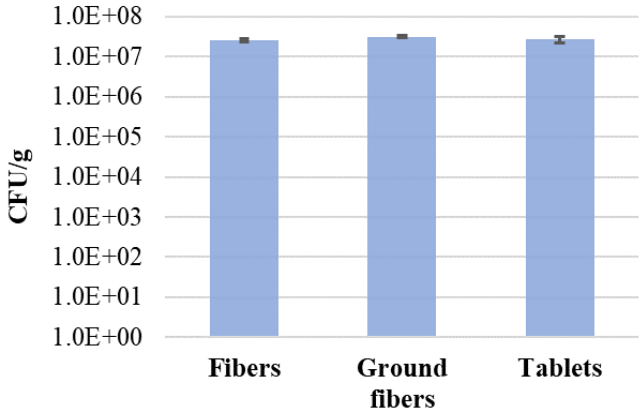

Figure 37 Bacteria survival after oscillating milling and tableting of the electrospun fibers

4.4.7 Conclusion regarding anaerobic bacteria-containing fibers

This part of the work demonstrated that high-speed electrospinning is capable to gently and continuously produce processable fibers incorporating anaerobic bacteria from the gut microbiome. Bacteria-containing fibers were produced using a water-soluble cyclodextrin matrix (HP-β-CD) with 300 mL/h feeding rate, which equals to ~150 g/h solid product per hour. High viability of the fibrous sample containing both sporulated and vegetative anaerobic bacteria was preserved after 12 months of storage at room temperature in the presence of oxygen, which makes drug storage possible in a flexible way. The bacteria-containing fibers were grindable by an oscillating mill without the need for a secondary drying step enabling a very economic downstream processing. The ground fibrous powder with bacteria was mixed with tableting excipients and was successfully tableted using direct compression. No significant decrease in bacterial viability was observed after either of the processing steps (electrospinning, grinding, and tableting). In summary, the gentle drying by HSES and the processability of the applied matrix enabled the production of a final dosage form for the easy oral administration of the anaerobic gut bacteria strain, *Clostridium butyricum*.

5. Summary

In this work, developments related to aqueous electrospinning were discussed. Two model biopharmaceuticals, a protein (β-galactosidase) and an anaerobic bacterium (*Clostridium butyricum*), and a small molecule drug (voriconazole) were dried/formulated using high-speed electrospinning (HSES) starting from aqueous solutions. Downstream processing of the drug-loaded fibers to generate oral or parenteral dosage forms was performed as well.

β-Galactosidase was electrospun with aqueous solutions of a polymeric and a polymer-free matrix. The first matrix consisted of polyvinyl alcohol, polyethylene oxide, and mannitol, and it was optimized to be electrospinnable with β-galactosidase. A 30-fold higher feeding rate could be achieved by the laboratory-scaled HSES technique compared to the single-needle electrospinning of aqueous solutions. Bead-free fibers were obtained, which were found to be grindable without a secondary drying step. According to the differential scanning calorimetry (DSC) and X-ray powder diffraction measurements (XRPD), all components of the fibers were in amorphous state, except mannitol. The low water content and the crystalline mannitol in the fibrous sample could be the reason for the adequate grindability. The ground powder was successfully tableted. The effect of the different processing steps (electrospinning, grinding, tableting) on β-galactosidase was evaluated, but no decrease in enzyme activity was observed. Besides, β-galactosidase remained stable in the tablets after 1 year of storage both at 4 °C and room temperature.

Another polymer-free matrix was also used for the electrospinning of β-galactosidase. An aqueous solution of 2-hydroxypropyl-β-cyclodextrin (HP-β-CD) and the protein was dried by the pilot-scale HSES technology with ~270 g/h productivity. The fibers could be easily ground by a hammer mill, due to the high friability of the cyclodextrin fibers. The ground fibrous powder was mixed with tableting excipients, and the flowability of the blend was suitable for tableting by direct compression. The enzyme remained stable after the processing steps (electrospinning, grinding, and tableting), and in the tablets after 6 months of storage both at 4 °C and room temperature.

To demonstrate the feasibility of HSES to produce a fast-dissolving reconstitution injection dosage form, pilot-scale HSES was utilized to produce fibers from aqueous solutions of VOR–SBE-β-CD complex with a ~240 g/h productivity. The fibers were collected by a cyclone with a 78% yield. The fibers were characterized and compared to both

the physical mixture of VOR-SBE-β-CD and the marketed freeze-dried VOR formulation (Vfend®). According to the DSC and XRPD measurements, VOR was fully amorphous in the fibers, similarly to Vfend®. Raman mapping and energy dispersive spectrometry showed that VOR was homogenously distributed in the fibers and in Vfend® as well. The reconstitution test of the fibers confirmed the expected fast dissolution characteristics as a clear solution was obtained within 30 seconds. These experiments demonstrated that HSES can be a viable alternative to freeze drying since it is a continuous, high-throughput process of very low energy consumption providing an economically viable production alternative.

Sporulated and vegetative *Clostridium butyricum* was also incorporated into HP-β-CD fibers using the pilot-scale HSES technique, allowing the comparison of the growth conditions on survival. The effect of storage temperature and the presence of oxygen on the viability of bacteria was also investigated in the long-term stability study. High viability of the sample containing both spores and vegetative bacteria was preserved at room temperature in the presence of oxygen. Tablet dosage form was prepared from the bacteria-containing fibers after milling by an oscillating mill. The fibrous powder together with the tableting excipients showed acceptable flowability for tableting by direct compression.

Acknowledgments

This work was performed in the frame of FIEK_16-1-2016-0007 project, implemented with the support provided from the National Research, Development and Innovation Fund of Hungary, financed under the FIEK_16 funding scheme.

Publications

Publications on which thesis findings are based:

I. I. Wagner, Z.K. Nagy, **P. Vass**, C. Fehér, Z. Barta, T. Vigh, P.L. Sóti, A.H. Harasztos, H. Pataki, A. Balogh, G. Verreck, I.V. Assche, G. Marosi, Stable formulation of protein-type drug in electrospun polymeric fiber followed by tableting and scaling-up experiments, Polymers for Advanced Technologies, 26 (2015) 1461-1467, doi: 10.1002/pat.3569.

IF: 1.823 IC: 7

II. **P. Vass**, B. Démuth, E. Hirsch, B. Nagy, S.K. Andersen, T. Vigh, G. Verreck, I. Csontos, Z.K. Nagy, G. Marosi, Drying technology strategies for colon-targeted oral delivery of biopharmaceuticals, Journal of Controlled Release, 296 (2019) 162-178, doi: 10.1016/j.jconrel.2019.01.023.

IF: 7.877 IC: 18

III. **P. Vass**, B. Démuth, A. Farkas, E. Hirsch, E. Szabó, B. Nagy, S.K. Andersen, T. Vigh, G. Verreck, I. Csontos, G. Marosi, Z.K. Nagy, Continuous alternative to freeze drying: Manufacturing of cyclodextrin-based reconstitution powder from aqueous solution using scaled-up electrospinning, Journal of Controlled Release, 298 (2019) 120-127, doi: 10.1016/j.jconrel.2019.02.019.

IF: 7.877 IC: 15

IV. E. Hirsch, **P. Vass**, B. Demuth, Z. Petho, E. Bitay, S.K. Andersen, T. Vigh, G. Verreck, K. Molnar, Z.K. Nagy, G. Marosi, Electrospinning scale-up and formulation development of PVA nanofibers aiming oral delivery of biopharmaceuticals, Express Polymer Letters, 13 (2019) 590-603, doi: 10.3144/expresspolymlett.2019.50.

IF: 2.875 IC: 4

V. **P. Vass**, E. Hirsch, R. Kóczián, B. Démuth, A. Farkas, C. Fehér, E. Szabó, Á. Németh, S.K. Andersen, T. Vigh, G. Verreck, I. Csontos, G. Marosi, Z.K. Nagy, Scaled-up production and tableting of grindable electrospun fibers containing a protein-type drug, Pharmaceutics, 11 (2019) 329, doi: 10.3390/pharmaceutics11070329.

IF: 4.773 IC: 2

VI. **P. Vass**, Z.K. Nagy, R. Kóczián, C. Fehér, B. Démuth, E. Szabó, S.K. Andersen, T. Vigh, G. Verreck, I. Csontos, G. Marosi, E. Hirsch, Continuous drying of a protein-type drug

using scaled-up fiber formation with HP-β-CD matrix resulting in a directly compressible powder for tableting, European Journal of Pharmaceutical Sciences, 141 (2020) 105089, doi: 10.1016/j.ejps.2019.105089.

IF: 3.532 IC: 0

VII. E. Szabó, B. Démuth, D.L. Galata, **P. Vass**, E. Hirsch, I. Csontos, G. Marosi, Z.K. Nagy, Continuous formulation approaches of amorphous solid dispersions: Significance of powder flow properties and feeding performance, Pharmaceutics, 11 (2019) 654, doi: 10.3390/pharmaceutics11120654.

IF: 4.773 IC: 1

VIII. **P. Vass**, E. Szabó, A. Domokos, E. Hirsch, D. Galata, B. Farkas, B. Démuth, S.K. Andersen, T. Vigh, G. Verreck, G. Marosi, Z.K. Nagy, Scale-up of electrospinning technology: Applications in the pharmaceutical industry, WIREs Nanomedicine and Nanobiotechnology, (2019) e1611, doi: 10.1002/wnan.1611.

IF: 6.140 IC: 7

IX. **P. Vass**, E. Pantea, A. Domokos, E. Hirsch, J. Domján, Á. Németh, M. Molnár, Cs. Fehér, S.K. Andersen, T. Vigh, G. Verreck, I. Csontos, G. Marosi, Z.K. Nagy, Electrospun solid formulation of anaerobic gut microbiome bacteria, AAPS PharmSciTech, 21 (2020) 214, doi: 10.1208/s12249-020-01769-y.

IF: 2.401 IC: 0

Further, related publications:

X. E. Hirsch, H. Pataki, A. Farkas, H. Bata, **P. Vass**, C. Fehér, Z. Barta, L. Párta, I. Csontos, A. Ballagi, Z.K. Nagy, G.J. Marosi, Raman-based feedback control of the enzymatic hydrolysis of lactose, Organic Process Research & Development, 20 (2016) 1721-1727, doi: 10.1021/acs.oprd.6b00212.

IF: 2.857 IC: 3

XI. B. Nagy, A. Farkas, E. Borbás, **P. Vass**, Z.K. Nagy, G. Marosi, Raman spectroscopy for process analytical technologies of pharmaceutical secondary manufacturing, AAPS PharmSciTech, 20 (2018) 1, doi: 10.1208/s12249-018-1201-2.

IF: 2.608 IC: 7

XII. E. Hirsch, H. Patak, J. Domján, A. Farkas, **P. Vass**, C. Fehér, Z. Barta, Z.K. Nagy, G.J. Marosi, I. Csontos, Inline noninvasive Raman monitoring and feedback control of glucose concentration during ethanol fermentation, Biotechnology Progress, (2019) e2848, doi: 10.1002/btpr.2848.

IF: 2.406 IC: 3

XIII. K. Kiss, **P. Vass**, A. Farkas, E. Hirsch, E. Szabó, G. Mező, Z.K. Nagy, G. Marosi, A solid doxycycline HP-β-CD formulation for reconstitution (i.v. bolus) prepared by scaled-up electrospinning, International Journal of Pharmaceutics, 586 (2020) 119539, doi: 10.1016/j.ijpharm.2020.119539.

IF: 4.845 IC: 0

Further, unrelated publications:

XIV. K. Ilyés, A. Balogh, T. Casian, T. Igricz, E. Borbás, B. Démuth, **P. Vass**, L. Menyhárt, N.K. Kovács, G. Marosi, I. Tomuta, Z.K. Nagy, 3D Floating tablets: appropriate 3d design from the perspective of different in vitro dissolution testing methodologies, International Journal of Pharmaceutics, (2019) 118433, doi: 10.1016/j.ijpharm.2019.06.024.

IF: 4.213 IC: 0

Oral presentations (in English):

XV. **P. Vass**, I. Wagner, Cs. Fehér, Z.K. Nagy, G. Marosi, Solid formulation of biopharmaceuticals by electrospinning, International Conference on Bio-friendly Polymers and Polymer Additives, Budapest, Hungary, 2014. 05. 19-21.

XVI. **P. Vass**, E. Hirsch, B. Démuth, S.K. Andersen, T. Vigh, G. Verreck, I. Csontos, Z.K. Nagy, G. Marosi, Solid formulation of β-galactosidase by electrospinning, 11th PBP World meeting, Granada, Spain, 2018. 03.19-22.

XVII. **P. Vass**, E. Hirsch, S.K. Andersen, G. Verreck, T. Vigh, Á. Németh, G. Marosi, Z.K. Nagy, Solid formulation of living *Clostridium butyricum* by electrospinning, 12th CESPT conference, Szeged, Hungary, 2018. 09.20-22.

XVIII. **P. Vass**, E. Haraszti, E. Hirsch, B. Démuth, Á. Németh, M. Molnár, S.K. Andersen, G. Verreck, T. Vigh, G. Marosi, Z.K. Nagy, Scaled up solid formulation of living anaerobic bacteria for oral delivery using electrospinning, 3rd Conference on Pharmaceutics, Bologna, Italy, 2019. 03.25-26.

Poster presentations:

XIX. **P. Vass**, E. Hirsch, N. Elvegyi, S.K. Andersen, T. Vigh, G. Verreck, I. Csontos, Z.K. Nagy, G. Marosi, Solid formulation of biopharmaceuticals for oral delivery by electrospinning, 11th PBP World meeting, Granada, Spain, 2018. 03.19-22.

XX. **P. Vass**, B. Démuth, A. Farkas, E. Hirsch, E. Szabó, S.K. Andersen, T. Vigh, G. Verreck, I. Csontos, Z.K. Nagy, G. Marosi, Continuous low-cost alternative to freeze drying: Scaled-up aqueous electrospinning, 1st APV Continuous Manufacturing Conference, Antwerpen, Belgium, 2019. 02. 19-20.

XXI. **P. Vass**, B. Démuth, A. Farkas, E. Hirsch, E. Szabó, S.K. Andersen, T. Vigh, G. Verreck, I. Csontos, Z.K. Nagy, G. Marosi, Continuous low-cost alternative to freeze drying: Scaled-up aqueous electrospinning for cyclodextrin based reconstitution injection, 3rd Conference on Pharmaceutics, Bologna, Italy, 2019. 03.25-26.

XXII. **P. Vass**, B. Démuth, A. Farkas, E. Hirsch, E. Szabó, S.K. Andersen, T. Vigh, G. Verreck, I. Csontos, Z.K. Nagy, G. Marosi, Continuous low-cost alternative to freeze drying: Scaled-up aqueous electrospinning, 2nd Global Janssen Post Doc and PhD Student Scientific Symposium, Beerse, Belgium, 2019. 10. 23.

References

[1] Walsh, G. Biopharmaceutical benchmarks 2018. *Nature Biotechnology*, **2018**, *36:12*, 1136-1145, doi:10.1038/nbt.4305.

[2] Biotech products accounted for 35% of all new FDA approvals in 2000-16. *Tufts CSDD Impact Reports,* **2017**, *19:3*.

[3] Mitragotri, S.; Burke, P.A.; Langer, R. Overcoming the challenges in administering biopharmaceuticals: formulation and delivery strategies. *Nature Reviews: Drug Discovery,* **2014**, *13:9*, 655-672, doi:10.1038/nrd4363.

[4] Leader, B.; Baca, Q.J.; Golan, D.E. Protein therapeutics: a summary and pharmacological classification. *Nature Reviews Drug Discovery,* **2008**, *7:1*, 21-39, doi:10.1038/nrd2399.

[5] Blumberg, R.; Powrie, F. Microbiota, Disease, and Back to Health: A Metastable Journey. *Science Translational Medicine,* **2012**, *4:137*, 137rv137, doi:10.1126/scitranslmed.3004184.

[6] Cho, I.; Blaser, M.J. The human microbiome: at the interface of health and disease. *Nature Reviews Genetics,* **2012**, *13:4*, 260-270, doi:10.1038/nrg3182.

[7] Reardon, S. Microbiome therapy gains market traction. *Nature,* **2014**, *509:7500*, 269-270, doi:10.1038/509269a.

[8] van der Lelie, D.; Taghavi, S.; Henry, C.; Gilbert, J.A. The microbiome as a source of new enterprises and job creation: Considering clinical faecal and synthetic microbiome transplants and therapeutic regulation. *Microbial Biotechnology,* **2017**, *10:1*, 4-5, doi:10.1111/1751-7915.12597.

[9] Moodley, T.; Mistry, E. *Could the Gut Microbiome Revolutionize Medical Care?*; 2019.

[10] Jameel, F.; Hershenson, S. *Formulation and process development strategies for manufacturing biopharmaceuticals*; John Wiley & Sons: 2010.

[11] Langford, A.; Bhatnagar, B.; Walters, R.; Tchessalov, S.; Ohtake, S. Drying technologies for biopharmaceutical applications: Recent developments and future direction. *Drying Technology,* **2017**, *36:6*, 1-8, doi:10.1080/07373937.2017.1355318.

[12] Abdul-Fattah, A.M.; Kalonia, D.S.; Pikal, M.J. The challenge of drying method selection for protein pharmaceuticals: product quality implications. *Journal of Pharmaceutical Sciences,* **2007**, *96:8*, 1886-1916, doi:10.1002/jps.20842.

[13] Tang, X.; Pikal, M.J. Design of freeze-drying processes for pharmaceuticals: practical advice. *Pharmaceutical Research,* **2004**, *21:2*, 191-200.

[14] Kasper, J.C.; Friess, W. The freezing step in lyophilization: physico-chemical fundamentals, freezing methods and consequences on process performance and quality attributes of biopharmaceuticals. *European Journal of Pharmaceutics and Biopharmaceutics,* **2011**, *78:2*, 248-263, doi:10.1016/j.ejpb.2011.03.010.

[15] Costantino, H.R.; Pikal, M.J. *Lyophilization of biopharmaceuticals*; American Association of Pharmaceutical Scientists: 2004.

[16] Cameron, P. *Good pharmaceutical freeze-drying practice*; CRC Press: 1997.

[17] Oetje, G.-W.; Haseley, P. *Freeze-drying*, 2nd ed.; Wiley-VCH: 2004.

[18] Rambhatla, S.; Pikal, M.J. Heat and mass transfer scale-up issues during freeze-drying, I: Atypical radiation and the edge vial effect. *AAPS PharmSciTech*, **2003**, *4:2*, 22-31, doi:10.1208/pt040214.

[19] Gan, K.H.; Bruttini, R.; Crosser, O.K.; Liapis, A.I. Freeze-drying of pharmaceuticals in vials on trays: effects of drying chamber wall temperature and tray side on lyophilization performance. *International Journal of Heat and Mass Transfer,* **2005**, *48:9*, 1675-1687, doi:10.1016/j.ijheatmasstransfer.2004.12.004.

[20] Van Bockstal, P.-J.; De Meyer, L.; Corver, J.; Vervaet, C.; De Beer, T. Noncontact infrared-mediated heat transfer during continuous freeze-drying of unit doses. *Journal of Pharmaceutical Sciences,* **2017**, *106:1*, 71-82, doi:10.1016/j.xphs.2016.05.003.

[21] Ratti, C. Hot air and freeze-drying of high-value foods: a review. *Journal of Food Engineering,* **2001**, *49:4*, 311-319, doi:10.1016/s0260-8774(00)00228-4.

[22] Pisano, R.; Capozzi, L.C.; Trout, B. Continuous freeze-drying and its relevance to the pharma/biotech industry. In Proceedings of Integrated Continuous Manufacturing III, Cascais, Portugal.

[23] De Meyer, L.; Van Bockstal, P.J.; Corver, J.; Vervaet, C.; Remon, J.P.; De Beer, T. Evaluation of spin freezing versus conventional freezing as part of a continuous pharmaceutical freeze-drying concept for unit doses. *International Journal of Pharmaceutics,* **2015**, *496:1*, 75-85, doi:10.1016/j.ijpharm.2015.05.025.

[24] Wang, W. Lyophilization and development of solid protein pharmaceuticals. *International Journal of Pharmaceutics,* **2000**, *203:1-2*, 1-60, doi:10.1016/s0378-5173(00)00423-3.

[25] Taborsky, G. Protein alterations at low temperatures: an overview. In *Proteins at Low Temperatures,* American Chemical Society: 1979; Vol. 180, pp. 1-26.

[26] Izutsu, K.-i.; Yoshioka, S.; Terao, T. Effect of mannitol crystallinity on the stabilization of enzymes during freeze-drying. *Chemical & Pharmaceutical Bulletin,* **1994**, *42:1*, 5-8, doi:10.1248/cpb.42.5.

[27] Angkawinitwong, U.; Sharma, G.; Khaw, P.T.; Brocchini, S.; Williams, G.R. Solid-state protein formulations. *Therapeutic Delivery,* **2015**, *6:1*, 59-82, doi:10.4155/tde.14.98.

[28] Xie, Y.; Ma, Y.; Xu, J.; Liu, Y.; Yue, P.; Zheng, Q.; Hu, P.; Yang, M. Panax notoginseng saponins as a novel nature stabilizer for poorly soluble drug nanocrystals: a case study with baicalein. *Molecules,* **2016**, *21:9*, 1149, doi:10.3390/molecules21091149.

[29] Thybo, P.; Pedersen, B.L.; Hovgaard, L.; Holm, R.; Müllertz, A. Characterization and physical stability of spray dried solid dispersions of probucol and PVP-K30. *Pharmaceutical Development and Technology,* **2008**, *13:5*, 375-386, doi:10.1080/10837450802244843.

[30] Maltesen, M.J.; van de Weert, M. Drying methods for protein pharmaceuticals. *Drug Discovery Today: Technologies,* **2008**, *5:2-3*, 81-88, doi:10.1016/j.ddtec.2008.11.001.

[31] McAdams, D.; Chen, D.; Kristensen, D. Spray drying and vaccine stabilization. *Expert Review of Vaccines,* **2014**, *11:10*, 1211-1219, doi:10.1586/erv.12.101.

[32] Ameri, M.; Maa, Y.-F. Spray drying of biopharmaceuticals: stability and process considerations. *Drying Technology*, **2006**, *24:6*, 763-768, doi:10.1080/03602550600685275.

[33] Zamora, L.M.; Carretero, C.; Parés, D. Comparative survival rates of lactic acid bacteria isolated from blood, following spray-drying and freeze-drying. *Food Science and Technology International*, **2016**, *12:1*, 77-84, doi:10.1177/1082013206062443.

[34] Chávez, B.E.; Ledeboer, A.M. Drying of probiotics: Optimization of formulation and process to enhance storage survival. *Drying Technology*, **2007**, *25:7-8*, 1193-1201, doi:10.1080/07373930701438576.

[35] Masters, K. *Spray drying handbook*; Longman Scientific & Technical: 1991.

[36] Mensink, M.A.; Frijlink, H.W.; van der Voort Maarschalk, K.; Hinrichs, W.L.J. How sugars protect proteins in the solid state and during drying (review): Mechanisms of stabilization in relation to stress conditions. *European Journal of Pharmaceutics and Biopharmaceutics*, **2017**, *114*, 288-295, doi:10.1016/j.ejpb.2017.01.024.

[37] Varshney, D.; Singh, M. *Lyophilized biologics and vaccines: modality-based approaches*; Springer New York: 2015.

[38] Bowen, M.; Turok, R.; Maa, Y.-F. Spray drying of monoclonal antibodies: Investigating powder-based biologic drug substance bulk storage. *Drying Technology*, **2013**, *31:13-14*, 1441-1450, doi:10.1080/07373937.2013.796968.

[39] Ziaee, A.; Albadarin, A.B.; Padrela, L.; Femmer, T.; O'Reilly, E.; Walker, G. Spray drying of pharmaceuticals and biopharmaceuticals: Critical parameters and experimental process optimization approaches. *European Journal of Pharmaceutical Sciences*, **2019**, *127*, 300-318, doi:10.1016/j.ejps.2018.10.026.

[40] Batens, M.; Massant, J.; Teodorescu, B.; Van den Mooter, G. Formulating monoclonal antibodies as powders for reconstitution at high concentration using spray drying: Models and pitfalls. *European Journal of Pharmaceutics and Biopharmaceutics*, **2018**, *127*, 407-422, doi:10.1016/j.ejpb.2018.02.002.

[41] Hulse, W.L.; Forbes, R.T.; Bonner, M.C.; Getrost, M. Influence of protein on mannitol polymorphic form produced during co-spray drying. *International Journal of Pharmaceutics*, **2009**, *382:1-2*, 67-72, doi:10.1016/j.ijpharm.2009.08.007.

[42] Lee, G. Spray-Drying of Proteins. In *Rational design of stable protein formulations*, Springer: 2002; Vol. 13, pp. 135-158.

[43] Sollohub, K.; Cal, K. Spray drying technique: II. Current applications in pharmaceutical technology. *Journal of Pharmaceutical Sciences*, **2010**, *99:2*, 587-597, doi:10.1002/jps.21963.

[44] Al-Khattawi, A.; Bayly, A.; Phillips, A.; Wilson, D. The design and scale-up of spray dried particle delivery systems. *Expert Opinion on Drug Delivery*, **2017**, *15:1*, 47-63, doi:10.1080/17425247.2017.1321634.

[45] April 30, 2015 Approval Letter - RAPLIXA Availabe online: https://www.fda.gov/downloads/BiologicsBloodVaccines/BloodBloodProducts/ApprovedProducts/LicensedProductsBLAs/FractionatedPlasmaProducts/UCM445351.pdf (accessed on 2019.01.12.).

[46] Huang, S.; Vignolles, M.-L.; Chen, X.D.; Le Loir, Y.; Jan, G.; Schuck, P.; Jeantet, R. Spray drying of probiotics and other food-grade bacteria: A review. *Trends in Food Science & Technology*, **2017**, *63*, 1-17, doi:10.1016/j.tifs.2017.02.007.

[47] Gayakwad, S.G.; Bejugam, N.K.; Akhavein, N.; Uddin, N.A.; Oettinger, C.E.; D'Souza, M.J. Formulation and in vitro characterization of spray-dried antisense oligonucleotide to NF-κB encapsulated albumin microspheres. *Journal of Microencapsulation*, **2009**, *26:8*, 692-700, doi:10.3109/02652040802666910.

[48] Nagy, Z.K.; Wagner, I.; Suhajda, A.; Tobak, T.; Harasztos, A.H.; Vigh, T.; Soti, P.L.; Pataki, H.; Molnar, K.; Marosi, G. Nanofibrous solid dosage form of living bacteria prepared by electrospinning. *Express Polymer Letters,* **2014**, *8:5*, 352-361, doi:10.3144/expresspolymlett.2014.39.

[49] Mehta, P.; Haj-Ahmad, R.; Rasekh, M.; Arshad, M.S.; Smith, A.; van der Merwe, S.M.; Li, X.; Chang, M.-W.; Ahmad, Z. Pharmaceutical and biomaterial engineering via electrohydrodynamic atomization technologies. *Drug Discovery Today,* **2017**, *22:1*, 157-165, doi:10.1016/j.drudis.2016.09.021.

[50] Zeng, J.; Aigner, A.; Czubayko, F.; Kissel, T.; Wendorff, J.H.; Greiner, A. Poly(vinyl alcohol) Nanofibers by Electrospinning as a Protein Delivery System and the Retardation of Enzyme Release by Additional Polymer Coatings. *Biomacromolecules,* **2005**, *6:3*, 1484-1488, doi:10.1021/bm0492576.

[51] Tran, D.N.; Balkus, K.J. Enzyme immobilization via electrospinning. *Topics in Catalysis,* **2012**, *55:16-18*, 1057-1069, doi:10.1007/s11244-012-9901-4.

[52] Zussman, E. Encapsulation of cells within electrospun fibers. *Polymers for Advanced Technologies,* **2011**, *22:3*, 366-371, doi:10.1002/pat.1812.

[53] Cooley, J.F. Apparatus for electrically dispersing fluids - US692631A. **1902**.

[54] Morton, W.J. Method of dispersing fluids - US705691A. **1902**.

[55] Coffee, R.A. A dispensing device and method for forming material - WO1998003267A1. **1998**.

[56] Scardino, F.L.; Balonis, R.J. Fibrous structures containing nanofibrils and other textile fibers - US6106913A. **2000**.

[57] Smith, D.; Reneker, D.; Mcmanus, A.; Schreuder-Gibson, H.; Mello, C.; Sennett, M.; Gibson, P. Electrospun fibers and an apparatus therefor - WO2001027365A1. **2001**.

[58] Cramariuc, B.; Cramariuc, R.; Scarlet, R.; Manea, L.R.; Lupu, I.G.; Cramariuc, O. Fiber diameter in electrospinning process. *Journal of Electrostatics,* **2013**, *71:3*, 189-198, doi:10.1016/j.elstat.2012.12.018.

[59] Taylor, G. Disintegration of water drops in an electric field. *Proceedings of the Royal Society A: Mathematical, Physical and Engineering Sciences,* **1964**, *280:1382*, 383-397, doi:10.1098/rspa.1964.0151.

[60] Huang, C.; Soenen, S.J.; Rejman, J.; Lucas, B.; Braeckmans, K.; Demeester, J.; De Smedt, S.C. Stimuli-responsive electrospun fibers and their applications. *Chemical Society Reviews,* **2011**, *40:5*, 2417-2434, doi:10.1039/c0cs00181c.

[61] Castro-Mayorga, J.L.; Fabra, M.J.; Cabedo, L.; Lagaron, J.M. On the use of the electrospinning coating technique to produce antimicrobial polyhydroxyalkanoate materials containing in situ-stabilized silver nanoparticles. *Nanomaterials (Basel),* **2016**, *7:1*, doi:10.3390/nano7010004.

[62] Démuth, B.; Farkas, A.; Szabó, B.; Balogh, A.; Nagy, B.; Vágó, E.; Vigh, T.; Tinke, A.P.; Kazsu, Z.; Demeter, Á.; Bertels, J.; Mensch, J.; Van Dijck, A.; Verreck, G.; Van Assche, I.; Marosi, G.; Nagy, Z.K. Development and tableting of directly compressible powder from electrospun nanofibrous amorphous solid dispersion. *Advanced Powder Technology,* **2017**, *28:6*, 1554-1563, doi:10.1016/j.apt.2017.03.026.

[63] Nagy, Z.K.; Balogh, A.; Vajna, B.; Farkas, A.; Patyi, G.; Kramarics, Á.; Marosi, G. Comparison of electrospun and extruded Soluplus®-based solid dosage forms of improved

dissolution. *Journal of Pharmaceutical Sciences,* **2012**, *101:1,* 322-332, doi:10.1002/jps.22731.

[64] Phaneuf, M.; Brown, P.; Bide, M. Nanofibrous materials as drug, protein, or genetic release vehicles - US20060200232A1. **2006**.

[65] Sóti, P.L.; Weiser, D.; Vigh, T.; Nagy, Z.K.; Poppe, L.; Marosi, G. Electrospun polylactic acid and polyvinyl alcohol fibers as efficient and stable nanomaterials for immobilization of lipases. *Bioprocess and Biosystems Engineering,* **2016**, *39:3,* 449-459, doi:10.1007/s00449-015-1528-y.

[66] Wagner, I.; Nagy, Z.K.; Vass, P.; Fehér, C.; Barta, Z.; Vigh, T.; Sóti, P.L.; Harasztos, A.H.; Pataki, H.; Balogh, A.; Verreck, G.; Assche, I.V.; Marosi, G. Stable formulation of protein-type drug in electrospun polymeric fiber followed by tableting and scaling-up experiments. *Polymers for Advanced Technologies,* **2015**, *26:12,* 1461-1467, doi:10.1002/pat.3569.

[67] Smith, D.J.; Kataphinan, W.; Reneker, D.H.; Dabney, S. Preservation of biological materials using fiber-forming techniques - US6821479B1. **2004**.

[68] Lancina, M.G.; Shankar, R.K.; Yang, H. Chitosan nanofibers for transbuccal insulin delivery. *Journal of Biomedical Materials Research Part A,* **2017**, *105:5,* 1252-1259, doi:10.1002/jbm.a.35984.

[69] Choi, J.S.; Han, S.-H.; Hyun, C.; Yoo, H.S. Buccal adhesive nanofibers containing human growth hormone for oral mucositis. *Journal of Biomedical Materials Research Part B: Applied Biomaterials,* **2016**, *104:7,* 1396-1406, doi:10.1002/jbm.b.33487.

[70] Angkawinitwong, U.; Awwad, S.; Khaw, P.T.; Brocchini, S.; Williams, G.R. Electrospun formulations of bevacizumab for sustained release in the eye. *Acta Biomaterialia,* **2017**, *64,* 126-136, doi:10.1016/j.actbio.2017.10.015.

[71] Škrlec, K.; Zupančič, Š.; Prpar Mihevc, S.; Kocbek, P.; Kristl, J.; Berlec, A. Development of electrospun nanofibers that enable high loading and long-term viability of probiotics. *European Journal of Pharmaceutics and Biopharmaceutics,* **2019**, *136,* 108-119, doi:10.1016/j.ejpb.2019.01.013.

[72] Knockenhauer, K.E.; Sawicka, K.M.; Roemer, E.J.; Simon, S.R. Protective antigen composite nanofibers as a transdermal anthrax vaccine. **2008**, 10.1109/iembs.2008.4649337, 1040-1043, doi:10.1109/iembs.2008.4649337.

[73] Cabello, J.M.L.; Sandoval, W.R.C.; Rovira, M.J.F.; Rubio, A.L. Nozzle with multiple outlets. EP3225722B1, **2017**.

[74] Lee, W.S.; Jo, S.M.; Go, S.G.; Chun, S.W. Apparatus of polymer web by electrospinning process. US6616435B2, **2003**.

[75] Wang, X.; Niu, H.; Wang, X.; Lin, T. Needleless Electrospinning of Uniform Nanofibers Using Spiral Coil Spinnerets. *Journal of Nanomaterials,* **2012**, *2012,* 1-9, doi:10.1155/2012/785920.

[76] Lin, T.; Wang, X.; Wang, X.; Niu, H. Electrostatic spinning assembly. US8747093B2, **2014**.

[77] Smit, A.E.; Sanderson, R.D. Method and apparatus for the production of fine fibres. US9205453B2, **2015**.

[78] Yang, R.; He, J.; Xu, L.; Yu, J. Bubble-electrospinning for fabricating nanofibers. *Polymer,* **2009**, *50:24,* 5846-5850, doi:10.1016/j.polymer.2009.10.021.

[79] Smit, A.E.; Sanderson, R.D. Process for the production of fibers. US8916086B2, **2014**.

[80] Andrady, A.L.; Ensor, D.S.; Newsome, R.J. Electrospinning of fibers using a rotatable spray head. US7134857B2, **2006**.

[81] Takahashi, M.; Takezawa, M.; Tominaga, Y.; Kurokawa, T.; Ishikawa, K.; Sumida, H. Method and apparatus for producing nanofibers and polymer web. US8110136B2, **2012**.

[82] Bioinicia. Availabe online: https://bioinicia.com/ (accessed on 2019.10.11.).

[83] Um, I.C.; Fang, D.; Hsiao, B.S.; Okamoto, A.; Chu, B. Electro-spinning and electro-blowing of hyaluronic acid. *Biomacromolecules,* **2004**, *5:4*, 1428-1436, doi:10.1021/bm034539b.

[84] Balogh, A.; Horváthová, T.; Fülöp, Z.; Loftsson, T.; Harasztos, A.H.; Marosi, G.; Nagy, Z.K. Electroblowing and electrospinning of fibrous diclofenac sodium-cyclodextrin complex-based reconstitution injection. *Journal of Drug Delivery Science and Technology,* **2015**, *26*, 28-34, doi:10.1016/j.jddst.2015.02.003.

[85] Sóti, P.L.; Bocz, K.; Pataki, H.; Eke, Z.; Farkas, A.; Verreck, G.; Kiss, É.; Fekete, P.; Vigh, T.; Wagner, I.; Nagy, Z.K.; Marosi, G. Comparison of spray drying, electroblowing and electrospinning for preparation of Eudragit E and itraconazole solid dispersions. *International Journal of Pharmaceutics,* **2015**, *494:1*, 23-30, doi:10.1016/j.ijpharm.2015.07.076.

[86] El-Newehy, M.H.; Al-Deyab, S.S.; Kenawy, E.-R.; Abdel-Megeed, A. Fabrication of electrospun antimicrobial nanofibers containing metronidazole using nanospider technology. *Fibers and Polymers,* **2012**, *13:6*, 709-717, doi:10.1007/s12221-012-0709-4.

[87] Krogstad, E.A.; Woodrow, K.A. Manufacturing scale-up of electrospun poly (vinyl alcohol) fibers containing tenofovir for vaginal drug delivery. *International Journal of Pharmaceutics,* **2014**, *475:1-2*, 282-291, doi:10.1016/j.ijpharm.2014.08.039.

[88] Molnar, K.; Nagy, Z.K. Corona-electrospinning: needleless method for high-throughput continuous nanofiber production. *European Polymer Journal,* **2016**, *74*, 279-286, doi:10.1016/j.eurpolymj.2015.11.028.

[89] Molnár, K.; Nagy, Z.K.; Marosi, G.; Mészáros, L. Electrospinning spinneret and modified electrospinning method for producing nanofibers in productive ways. P1200677, **2012**.

[90] Lukas, D.; Sarkar, A.; Pokorny, P. Self-organization of jets in electrospinning from free liquid surface: A generalized approach. *Journal of Applied Physics,* **2008**, *103:8*, 084309, doi:10.1063/1.2907967.

[91] Sebe, I.; Szabó, B.; Nagy, Z.K.; Szabó, D.; Zsidai, L.; Kocsis, B.; Zelkó, R. Polymer structure and antimicrobial activity of polyvinylpyrrolidone-based iodine nanofibers prepared with high-speed rotary spinning technique. *International Journal of Pharmaceutics,* **2013**, *458:1*, 99-103, doi:10.1016/j.ijpharm.2013.10.011.

[92] Nagy, Z.K.; Balogh, A.; Demuth, B.; Pataki, H.; Vigh, T.; Szabo, B.; Molnar, K.; Schmidt, B.T.; Horak, P.; Marosi, G.; Verreck, G.; Van Assche, I.; Brewster, M.E. High speed electrospinning for scaled-up production of amorphous solid dispersion of itraconazole. *International Journal of Pharmaceutics,* **2015**, *480:1-2*, 137-142, doi:10.1016/j.ijpharm.2015.01.025.

[93] Démuth, B.; Farkas, A.; Pataki, H.; Balogh, A.; Szabó, B.; Borbás, E.; Sóti, P.L.; Vigh, T.; Kiserdei, É.; Farkas, B. Detailed stability investigation of amorphous solid dispersions

prepared by single-needle and high speed electrospinning. *International Journal of Pharmaceutics,* **2016**, *498:1-2*, 234-244, doi:10.1016/j.ijpharm.2015.12.029.

[94] Vigh, T.; Démuth, B.; Balogh, A.; Galata, D.L.; Van Assche, I.; Mackie, C.; Vialpando, M.; Van Hove, B.; Psathas, P.; Borbás, E.; Pataki, H.; Boeykens, P.; Marosi, G.; Verreck, G.; Nagy, Z.K. Oral bioavailability enhancement of flubendazole by developing nanofibrous solid dosage forms. *Drug development and industrial pharmacy*, **2017**, *43:7*, 1126-1133, doi:10.1080/03639045.2017.1298121.

[95] Wang, L.; Zhang, C.; Gao, F.; Pan, G. Needleless electrospinning for scaled-up production of ultrafine chitosan hybrid nanofibers used for air filtration. *RSC Advances,* **2016**, *6:107*, 105988-105995, doi:10.1039/c6ra24557a.

[96] Sousa, A.M.M.; Souza, H.K.S.; Uknalis, J.; Liu, S.-C.; Gonçalves, M.P.; Liu, L. Electrospinning of agar/PVA aqueous solutions and its relation with rheological properties. *Carbohydrate Polymers*, **2015**, *115*, 348-355, doi:10.1016/j.carbpol.2014.08.074.

[97] Szabó, E.; Démuth, B.; Nagy, B.; Molnár, K.; Farkas, A.; Szabó, B.; Balogh, A.; Hirsch, E.; Nagy, B.; Marosi, G.; Nagy, Z. Scaled-up preparation of drug-loaded electrospun polymer fibres and investigation of their continuous processing to tablet form. *Express Polymer Letters*, **2018**, *12:5*, 436-451, doi:10.3144/expresspolymlett.2018.37.

[98] Balogh, A.; Domokos, A.; Farkas, B.; Farkas, A.; Rapi, Z.; Kiss, D.; Nyiri, Z.; Eke, Z.; Szarka, G.; Örkényi, R.; Mátravölgyi, B.; Faigl, F.; Marosi, G.; Nagy, Z.K. Continuous end-to-end production of solid drug dosage forms: Coupling flow synthesis and formulation by electrospinning. *Chemical Engineering Journal*, **2018**, *350*, 290-299, doi:10.1016/j.cej.2018.05.188.

[99] Domokos, A.; Balogh, A.; Dénes, D.; Nyerges, G.; Ződi, L.; Farkas, B.; Marosi, G.; Nagy, Z.K. Continuous manufacturing of orally dissolving webs containing a poorly soluble drug via electrospinning. *European Journal of Pharmaceutical Sciences,* **2019**, *130*, 91-99, doi:10.1016/j.ejps.2019.01.026.

[100] Sebe, I.; Bodai, Z.; Eke, Z.; Kállai-Szabó, B.; Szabó, P.; Zelkó, R. Comparison of directly compressed vitamin B12 tablets prepared from micronized rotary-spun microfibers and cast films. *Drug development and industrial pharmacy,* **2015**, *41:9*, 1438-1442, doi:10.3109/03639045.2014.956112.

[101] Szabó, P.; Kállai-Szabó, B.; Sebe, I.; Zelkó, R. Preformulation study of fiber formation and formulation of drug-loaded microfiber based orodispersible tablets for in vitro dissolution enhancement. *International Journal of Pharmaceutics,* **2014**, *477:1*, 643-649, doi:10.1016/j.ijpharm.2014.11.011.

[102] Hirsch, E.; Vass, P.; Demuth, B.; Petho, Z.; Bitay, E.; Andersen, S.K.; Vigh, T.; Verreck, G.; Molnar, K.; Nagy, Z.K.; Marosi, G. Electrospinning scale-up and formulation development of PVA nanofibers aiming oral delivery of biopharmaceuticals. *Express Polymer Letters*, **2019**, *13:7*, 590-603, doi:10.3144/expresspolymlett.2019.50.

[103] Jivraj, M.; Martini, L.G.; Thomson, C.M. An overview of the different excipients useful for the direct compression of tablets. *Pharmaceutical Science & Technology Today,* **2000**, *3:2*, 58-63, doi:10.1016/s1461-5347(99)00237-0.

[104] Démuth, B.; Farkas, A.; Balogh, A.; Bartosiewicz, K.; Kállai-Szabó, B.; Bertels, J.; Vigh, T.; Mensch, J.; Verreck, G.; Van Assche, I.; Marosi, G.; Nagy, Z.K. Lubricant-Induced Crystallization of Itraconazole From Tablets Made of Electrospun Amorphous Solid

Dispersion. *Journal of Pharmaceutical Sciences,* **2016**, *105:9*, 2982-2988, doi:10.1016/j.xphs.2016.04.032.

[105] Bardal, S.; Waechter, J.; Martin, D. Pharmacokinetics. In *Applied pharmacology*, Saunders: St. Louis, Missouri, 2011; pp. 17-34.

[106] Truong-Le, V.; Lovalenti, P.M.; Abdul-Fattah, A.M. Stabilization Challenges and Formulation Strategies Associated with Oral Biologic Drug Delivery Systems. *Advanced Drug Delivery Reviews,* **2015**, *93*, 95-108, doi:10.1016/j.addr.2015.08.001.

[107] Crini, G.; Fourmentin, S.; Fenyvesi, É.; Torri, G.; Fourmentin, M.; Morin-Crini, N. Fundamentals and Applications of Cyclodextrins. **2018**, *16*, 1-55, doi:10.1007/978-3-319-76159-6_1.

[108] Denadai, Â.M.L.; Santoro, M.M.; Lopes, M.T.P.; Chenna, A.l.; de Sousa, F.B.; Avelar, G.M.; Gomes, T.M.R.; Guzman, F.; Salas, C.E.; Sinisterra, R.D. A supramolecular complex between proteinases and beta-cyclodextrin that preserves enzymatic activity: Physicochemical characterization. *Biodrugs,* **2006**, *20:5*, 283-291, doi:10.2165/00063030-200620050-00004.

[109] Serno, T.; Geidobler, R.; Winter, G. Protein stabilization by cyclodextrins in the liquid and dried state. *Advanced Drug Delivery Reviews,* **2011**, *63:13*, 1086-1106, doi:10.1016/j.addr.2011.08.003.

[110] Celebioglu, A.; Uyar, T. Electrospinning of nanofibers from non-polymeric systems: polymer-free nanofibers from cyclodextrin derivatives. *Nanoscale,* **2012**, *4:2*, 621-631, doi:10.1039/c1nr11364j.

[111] Topuz, F.; Uyar, T. Electrospinning of Cyclodextrin Functional Nanofibers for Drug Delivery Applications. *Pharmaceutics,* **2018**, *11:1*, 6, doi:10.3390/pharmaceutics11010006.

[112] Vigh, T.; Horváthová, T.; Balogh, A.; Sóti, P.L.; Drávavölgyi, G.; Nagy, Z.K.; Marosi, G. Polymer-free and polyvinylpirrolidone-based electrospun solid dosage forms for drug dissolution enhancement. *European Journal of Pharmaceutical Sciences,* **2013**, *49:4*, 595-602, doi:10.1016/j.ejps.2013.04.034.

[113] Yildiz, Z.I.; Celebioglu, A.; Uyar, T. Polymer-free electrospun nanofibers from sulfobutyl ether7-beta-cyclodextrin (SBE7-β-CD) inclusion complex with sulfisoxazole: Fast-dissolving and enhanced water-solubility of sulfisoxazole. *International Journal of Pharmaceutics,* **2017**, *531:2*, 550-558, doi:10.1016/j.ijpharm.2017.04.047.

[114] Ugidos-Rodríguez, S.; Matallana-González, M.C.; Sánchez-Mata, M.C. Lactose malabsorption and intolerance: a review. *Food & Function,* **2018**, *9:8*, 4056-4068, doi:10.1039/c8fo00555a.

[115] National Center for Biotechnology Information. PubChem Database. Voriconazole, CID=71616. Availabe online: https://pubchem.ncbi.nlm.nih.gov/compound/Voriconazole (accessed on 2019.12.30.).

[116] Sun, Y.-Y.; Li, M.; Li, Y.-Y.; Li, L.-X.; Zhai, W.-Z.; Wang, P.; Yang, X.-X.; Gu, X.; Song, L.-J.; Li, Z.; Zuo, X.-L.; Li, Y.-Q. The effect of Clostridium butyricum on symptoms and fecal microbiota in diarrhea-dominant irritable bowel syndrome: a randomized, double-blind, placebo-controlled trial. *Scientific Reports,* **2018**, *8:1*, doi:10.1038/s41598-018-21241-z.

[117] Kanai, T.; Mikami, Y.; Hayashi, A. A breakthrough in probiotics: Clostridium butyricum regulates gut homeostasis and anti-inflammatory response in inflammatory bowel disease. *Journal of Gastroenterology,* **2015**, *50:9*, 928-939, doi:10.1007/s00535-015-1084-x.

[118] Pfizer. VFEND® (voriconazole) for injection, for intravenous use [package insert].

[119] European Pharmacopoeia, 8th ed. Council of Europe: Strasbourg, 2013.

[120] Xu, B.; Labus, K. Effective detection of biocatalysts with specified activity by using a hydrogel-based colourimetric assay – β-galactosidase case study. *PloS One,* **2018**, *13:10*, e0205532, doi:10.1371/journal.pone.0205532.

[121] Bartholomew, J.W.; Mittwer, T. A Simplified Bacterial Spore Stain. *Stain Technology,* **1950**, *25:3*, 153-156, doi:10.3109/10520295009110979.

[122] Burger, A.; Henck, J.-O.; Hetz, S.; Rollinger, J.M.; Weissnicht, A.A.; Stöttner, H. Energy/Temperature Diagram and Compression Behavior of the Polymorphs of d-Mannitol. *Journal of Pharmaceutical Sciences,* **2000**, *89:4*, 457-468, doi:10.1002/(sici)1520-6017(200004)89:4<457::aid-jps3>3.0.co;2-g.

[123] Hao, H.; Su, W.; Barrett, M.; Caron, V.; Healy, A.-M.; Glennon, B. A Calibration-Free Application of Raman Spectroscopy to the Monitoring of Mannitol Crystallization and Its Polymorphic Transformation. *Organic Process Research & Development,* **2010**, *14:5*, 1209-1214, doi:10.1021/op100142k.

[124] Sun, C.Q.; Wang, Y.; Tay, B.K.; Li, S.; Huang, H.; Zhang, Y.B. Correlation between the Melting Point of a Nanosolid and the Cohesive Energy of a Surface Atom. *The Journal of Physical Chemistry B,* **2002**, *106:41*, 10701-10705, doi:10.1021/jp025868l.

[125] Cares-Pacheco, M.G.; Vaca-Medina, G.; Calvet, R.; Espitalier, F.; Letourneau, J.J.; Rouilly, A.; Rodier, E. Physicochemical characterization of d-mannitol polymorphs: The challenging surface energy determination by inverse gas chromatography in the infinite dilution region. *International Journal of Pharmaceutics,* **2014**, *475:1-2*, 69-81, doi:10.1016/j.ijpharm.2014.08.029.

[126] Lee, Y.-Y.; Wu, J.X.; Yang, M.; Young, P.M.; van den Berg, F.; Rantanen, J. Particle size dependence of polymorphism in spray-dried mannitol. *European Journal of Pharmaceutical Sciences,* **2011**, *44:1-2*, 41-48, doi:10.1016/j.ejps.2011.06.002.

[127] Barth, A. Infrared spectroscopy of proteins. *Biochimica et Biophysica Acta (BBA) - Bioenergetics,* **2007**, *1767:9*, 1073-1101, doi:10.1016/j.bbabio.2007.06.004.

[128] Sun, X.-Z.; Williams, G.R.; Hou, X.-X.; Zhu, L.-M. Electrospun curcumin-loaded fibers with potential biomedical applications. *Carbohydrate Polymers,* **2013**, *94:1*, 147-153, doi:10.1016/j.carbpol.2012.12.064.

[129] Wen, S.J.; Richardson, T.J.; Ghantous, D.I.; Striebel, K.A.; Ross, P.N.; Cairns, E.J. FTIR characterization of PEO + LiN(CF3SO2)2 electrolytes. *Journal of Electroanalytical Chemistry,* **1996**, *408:1-2*, 113-118, doi:10.1016/0022-0728(96)04536-6.

[130] Cornel, J.; Kidambi, P.; Mazzotti, M. Precipitation and Transformation of the Three Polymorphs ofd-Mannitol. *Industrial & Engineering Chemistry Research,* **2010**, *49:12*, 5854-5862, doi:10.1021/ie9019616.

[131] De Beer, T.R.M.; Allesø, M.; Goethals, F.; Coppens, A.; Vander Heyden, Y.; Lopez De Diego, H.; Rantanen, J.; Verpoort, F.; Vervaet, C.; Remon, J.P.; Baeyens, W.R.G. Implementation of a Process Analytical Technology System in a Freeze-Drying Process

Using Raman Spectroscopy for In-Line Process Monitoring. *Analytical Chemistry*, **2007**, *79:21*, 7992-8003, doi:10.1021/ac070549h.

[132] Hancock, B.C.; Shamblin, S.L. Water vapour sorption by pharmaceutical sugars. *Pharmaceutical Science & Technology Today*, **1998**, *1:8*, 345-351, doi:10.1016/s1461-5347(98)00088-1.

[133] Burnett, D.J.; Thielmann, F.; Booth, J. Determining the critical relative humidity for moisture-induced phase transitions. *International Journal of Pharmaceutics*, **2004**, *287:1-2*, 123-133, doi:10.1016/j.ijpharm.2004.09.009.

[134] Celebioglu, A.; Uyar, T. Cyclodextrin nanofibers by electrospinning. *Chemical Communications*, **2010**, *46:37*, 6903, doi:10.1039/c0cc01484b.

[135] Denning, D.W.; Ribaud, P.; Milpied, N.; Caillot, D.; Herbrecht, R.; Thiel, E.; Haas, A.; Ruhnke, M.; Lode, H. Efficacy and safety of voriconazole in the treatment of acute invasive aspergillosis. *Clinical Infectious Diseases*, **2002**, *34:5*, 563-571, doi:10.1086/324620.

[136] Harding, V.D. Pharmaceutical formulations containing voriconazole, WO1998058677A1. **1997**.

[137] Humphrey, M.J.; Payne-Cook, T.A. Pharmaceutical formulations comprising voriconazole, WO2005051353A2. **2003**.

[138] Zhang, J.; Zhu, C.; Hu, L.; Liu, H.; Pan, H.-C. Effect of freeze-drying process on the physical stability and properties of Voriconazole complex system. *Drying Technology*, **2018**, *36:7*, 871-878, doi:10.1080/07373937.2017.1362648.

[139] Tiwari, S.K.; Venkatraman, S.S. Importance of viscosity parameters in electrospinning: Of monolithic and core–shell fibers. *Materials Science and Engineering: C*, **2012**, *32:5*, 1037-1042, doi:10.1016/j.msec.2012.02.019.

[140] Gupta, P.; Elkins, C.; Long, T.E.; Wilkes, G.L. Electrospinning of linear homopolymers of poly(methyl methacrylate): exploring relationships between fiber formation, viscosity, molecular weight and concentration in a good solvent. *Polymer*, **2005**, *46:13*, 4799-4810, doi:10.1016/j.polymer.2005.04.021.

[141] Tabary, N.; Garcia-Fernandez, M.J.; Danède, F.; Descamps, M.; Martel, B.; Willart, J.-F. Determination of the glass transition temperature of cyclodextrin polymers. *Carbohydrate Polymers*, **2016**, *148*, 172-180, doi:10.1016/j.carbpol.2016.04.032.

[142] Belkaid, Y.; Hand, T.W. Role of the microbiota in immunity and inflammation. *Cell*, **2014**, *157:1*, 121-141, doi:10.1016/j.cell.2014.03.011.

[143] Bien, J.; Palagani, V.; Bozko, P. The intestinal microbiota dysbiosis and Clostridium difficile infection: is there a relationship with inflammatory bowel disease? *Therapeutic Advances in Gastroenterology*, **2012**, *6:1*, 53-68, doi:10.1177/1756283x12454590.

[144] Mimee, M.; Citorik, R.J.; Lu, T.K. Microbiome therapeutics — Advances and challenges. *Advanced Drug Delivery Reviews*, **2016**, *105*, 44-54, doi:10.1016/j.addr.2016.04.032.

[145] Wnek, G.; Simpson, D.; Bowlin, G.; Yao, L.; Kenawy, E.-R.; Layman, J.; Sanders, E.; Fenn, J. Electroprocessing of materials useful in drug delivery and cell encapsulation - US20040018226A1. **2004**.

[146] Brandis-Heep, A.; Gensheimer, M.; Greiner, A.; Thauer, R.; Wendorff, J.H. Polymer fibres containing bacteria - WO2008014755A3. **2008**.

[147] Salalha, W.; Kuhn, J.; Dror, Y.; Zussman, E. Encapsulation of bacteria and viruses in electrospun nanofibres. *Nanotechnology*, **2006**, *17:18*, 4675-4681, doi:10.1088/0957-4484/17/18/025.

[148] Gensheimer, M.; Brandis-Heep, A.; Agarwal, S.; Thauer, R.K.; Greiner, A. Polymer/Bacteria Composite Nanofiber Nonwovens by Electrospinning of Living Bacteria Protected by Hydrogel Microparticles. *Macromolecular Bioscience*, **2011**, *11:3*, 333-337, doi:10.1002/mabi.201000310.

[149] Chidambaram, D.; Liu, Y.; Rafailovich, M.H. Microbes encapsulated within crosslinkable polymers - US20090258051A1. **2009**.

NYILATKOZAT

Alulírott **Vass Panna** kijelentem, hogy ezt a doktori értekezést magam készítettem és abban csak a megadott forrásokat használtam fel. Minden olyan részt, amelyet szó szerint, vagy azonos tartalomban, de átfogalmazva más forrásból átvettem, egyértelműen, a forrás megadásával megjelöltem.

Budapest, 2020. 08. 20.

.....